THE DEVELOPMENT OF A CRYOGENIC OVER-PRESSURE PUMP

BY

MATTHEW L. ALVAREZ

Submitted in partial fulfillment of the
requirements for the degree of
Master of Science in Mechanical and Aerospace Engineering
in the Graduate College of the
Illinois Institute of Technology

Approved _____
Advisor

Chicago, Illinois
July 2012

ACKNOWLEDGMENT

I would like to dedicate my work to my immediate family. I thank my mother, father, grandmother (1928-2006), and my two sisters for showing me to take pride in the work that I do. Their support and love has allowed me to tackle obstacles that I once thought were insurmountable. My mother and father, Norma and Luis Alvarez, have shown me the value of education. I truly appreciate the time and effort they have put into raising me. My grandmother, Constancia Tinio, has shown me to be kind and loving to all. My sisters, Marylou and Kimberly, have helped steer me in the right direction.

I would like to thank those at Fermi National Accelerator Laboratory. I especially appreciate the help, guidance, and patience of Herman Cease. Also, I thank Andrew Lathrop and Rolando Flores, for helping me setup and assemble the experiment. Moreover, I would like to thank Kurt Krempetz and Brenna Flaugher for allocating funds for this research project.

Thank you to those at the Illinois Institute of Technology. Special thanks to Professor Francisco Ruiz, my advisor, who has provided me with very helpful feedback during the countless meetings in 2011-2012 university calender year. I thank Professors Kevin Cassel and Ganesh Raman for partaking in evaluating my thesis. Also, I would like to thank them for their quality feedback. Lastly, I would like to thank Dr. Jose Garcia for his assistance in identifying and classifying other positive displacement pumps.

TABLE OF CONTENTS

LIST OF TABLES

LIST OF FIGURES

LIST OF SYMBOLS

Symbol	Definition
	Acronyms
ACS	Advanced Camera for Surveys
CCD	Charge Coupled Device
CLV	Cryogenic Liquid Vessel
CV	Control Volume
CFP	Compact Field Point
$CRIO$	CompactRIO
$DECam$	Dark Energy Camera
DES	Dark Energy Survey
EES	Engineering Equation Solver
$FNAL$	Fermi National Accelerator Laboratory
FT	Flow Transmitter
$GN2$	Nitrogen Gas
HP	Heat Pipe
HRC	High Resolution Channel
LLP	Liquid Level Probe
$LN2$	Liquid Nitrogen
$MCCD$	Multi-Charge Coupled Device
$MTBF$	Mean Time Between Failures
$MTFM$	Mean Time For Maintenance
MV	Manual Valve

OPP	Over-Pressure Pump
PC	Process Cylinder
PD	Positive Displacement
PT	Pressure Transducer
RTD	Resistance Temperature Detector
SI	International System of Units
SOV	Solenoid Operated Valve
SV	Solenoid Valve
TI	Temperature Indicator
WFC	Wide Field Channel

Variables

A_{dr}	Area of Piston on the Drive End of a Direct-Acting PD Pump
A_L	Area of Piston on the Liquid End of a Direct-Acting PD Pump
C	Flow Rate of the Suction End of a Reciprocating PD Pump
C_p	Specific Heat
D	Flow Rate of Displaced Fluid in a Reciprocating PD Pump
ΔP_{column}	Pressure due to Potential Energy per Unit Volume
$\Delta P_{discharge}$	Differential Pressure of Process Cylinder
ΔP_{dr}	Drive End Differential Pressure of Direct-Acting PD Pump
$\Delta P_{friction}$	Pressure due to Friction Losses
$\Delta P_{injection}$	Differential Pressure of the GN2 Injection Line
ΔP_L	Liquid End Differential Pressure of Direct-Acting PD Pump
$\Delta P_{minor+major}$	Pressure due to Major and Minor Losses

$\Delta V_{discharge,PC}$	Volume of LN2 discharged from the PC
$\Delta V_{fill,PC}$	Volume of LN2 that Fills the PC during a Refill
$\Delta V_{LN2,Loss}$	Volume of LN2 Lost During Each Cycle
η_I	First Law Efficiency
η_{pump}	Overall OPP Efficiency
η_v	Volumetric Efficiency of a Reciprocating PD Pump
h_f	Enthalpy of LN2
h_g	Enthalpy of GN2
h_{fg}	Difference Between Enthalpy of GN2 and LN2
I	Current Measured from GN2 Generator Heater
L	Stroke Length in meters
$\dot{m}_{discharge}$	Mass LN2 Flow Rate Exiting the PC towards the MCCD Test Vessel
$\dot{m}_{GN2,injection}$	Mass Flow Rate Associated with the GN2 Injection Line
$\dot{m}_{LN2,condense}$	Mass LN2 Flow Rate/Production of Condensation via Cryocooler
N	Reciprocating Pump Cycle Rate in cycles per minute
$P_{160L,CLV}$	Pressure of the 160L Low Pressure Cryogenic Liquid Vessel (CLV)
$P_{200L,CLV}$	Pressure of the 200L Cryogenic Liquid Vessel (CLV)
p_{acc}	Acceleration Head
p_{atm}	Atmospheric Pressure
p_s	Absolute Suction Pressure
p_{sg}	Gage Suction Pressure

p_{vel}	Velocity Head Pressure
$\dot{Q}_{in}$	Heat Input into System via Vaporizer
ρ_{GN2}	GN2 Density
ρ_{LN2}	LN2 Density
S_p	Reciprocating Pump Plunger Speed
$T_{160L,CLV}$	Temperature of the 160L Low Pressure Cryogenic Liquid Vessel (CLV)
t_f	Refill Time in Seconds
$T_{GN2,injection}$	GN2 Injection Line Temperature Indicator (TI-001)
$T_{GN2,injection,flange}$	GN2 Injection Line Flange Temperature Indicator (TI-002)
V	Voltage Applied to GN2 Generator Heater
$V_{discharge}$	Volume of LN2 that returns to the 200L CLV from the PC
V_{fluid}	Fluid that Enters the Pumping Chamber
V_{refill}	Volume of LN2 that enters the PC from the 200L CLV
$V(0)$	Volume of LN2 at t=0s
$V(40)$	Volume of LN2 at t=40s
$V(15+t_f)$	Refill Time in Seconds
$V(55+t_f)$	Volume of LN2 at the End of a Cycle
$\dot{V}_{discharge}$	Volumetric Flow Rate from PC to MCCD Heat Exchanger
$\dot{V}_{injection}$	Volumetric Flow Rate of GN2 that is Injected into the Process Cylinder
$\dot{W}_{electrical}$	Work due to Electrical Power Input
$\dot{W}_{GN2}$	Work Associated with the Flowing GN2 in the GN2 Injection Line

$\dot{W}_{pump}$	Over-Pressure Pump Power
$\dot{Q}_{cryo}$	Heat Removed by Cryogenic Refrigerator

ABSTRACT

The Dark Energy Survey (DES) project will study the accelerated expansion of the universe. In order to further study this phenomenon, scientists have devised a method of creating an array of charged couple devices (CCD) to capture images that will be studied. These CCDs must be cooled and remain at 173K to eliminate thermal gradients and dark current. Therefore, a two-phase CCD liquid nitrogen (LN2) cooling system was designed to maintain the array of CCDs at a constant temperature. However, the centrifugal pump used to supply LN2 has a mean time between failure (MTBF) of approximately two thousand-eight hundred hours (116 days). Because of the low MTBF of the centrifugal pump, a new pump is being considered to replace the existing one. This positive displacement pump is a simpler design that is expected to have a MTBF that will exceed 116 days (2800hrs). This positive displacement reciprocating pump, also known as, the cryogenic over-pressure pump (OPP), was tested in February 2012 and successfully cooled the CCD array to 173K. Though unfit for service for DES CCD cooling system, the overall concept of this pump has been proven. Typical flow rates, pressures, and temperatures trends have been captured via instrumentation and are specific to the operation of future over-pressure pumps.

CHAPTER 1

INTRODUCTION

1.1 Dark Energy Survey Project

The Dark Energy Survey (DES) Project involves the study of the accelerating expansion of the universe. The expansion is a result of a hypothetical energy called dark energy, which opposes the force of gravity on a cosmological scale. Based on general theory of relativity, all celestial objects attract each other via gravity. Therefore, all celestial bodies should eventually, via gravity, slow the expansion of the universe. However, astronomers, in 1998, determined that the universe is expanding as a result of some unknown force that exceeds the gravitational force, which is given the name dark energy. Currently, a model predicts that it will encompass 70% of the known universe. The remaining 30% consists of 25% dark matter and 5% visible matter. [13] [23].

A collaboration of scientists and engineers from various organization and universities from across the world seek to answer questions of the expanding universe. Therefore, the project partners sought out to design a 570 megapixel imager, which is the dark energy camera (DECam). The camera will be mounted on the Blanco 4-meter telescope at Cerro Tololo Inter-American Observatory (CTIO) in the Andes mountains in Chile. The resolution of the camera is a result of the 70 CCDs, where each CCD contains roughly 8 million pixels. Each CCD is held at a constant surface temperature to eliminate and reduce thermal gradients, signal noise, and dark current. Dark current contributes to signal noise, which is a result of a CCD randomly generating a signal when photons are not present. Additionally, the low constant temperature of 173K is associated with recording images in the visible and near infrared spectrum of light. This constant temperature is a result of boiling liquid nitrogen

(LN2) in a closed-loop cooling system.

This two-phase closed loop nitrogen cooling systems (CCD cooling system) consist of slightly sub-cooled LN2, which is supplied to the imager telescope. On the return line, a two-phase flow (liquid-gas) exists and the fluid returns to the 200L cryogenic liquid vessel (CLV), where the generated nitrogen gas (GN2) is condensed back to liquid nitrogen (LN2). Because the boiling of the LN2 at the telescope imager, the focal plate, which holds the CCDs, remains at a constant temperature of 173K. To further regulate this temperature, electrical heaters between the CCD focal plate and the heat exchanger are used. The original process pump, a centrifugal pump (BNLNG-01B-100), supplies the LN2 coolant to the CCDs. However, previous tests of this pump in the LN2 system indicate that the mean time between failures (MTBF) is 2800 hrs for the centrifugal pump, which is inappropriate for a remote site like CTIO. In order to remedy this issue, a new pump is under consideration so that the mean time to failure equals or exceeds the mean time for maintenance (MTFM) of approximately 8000 hrs of the Cryomech AL-300 cryogenic refrigerator.

The CCD cooling system is a two-phase flow of LN2 and GN2, which maintains the focal plate at a constant temperature [8]. The heat generated by the CCDs is conducted away via copper braids through a vacuum space to a copper LN2 tube heat exchanger. The process and instrumentation diagram of the system can be seen in Figures 1.1 and 1.2.

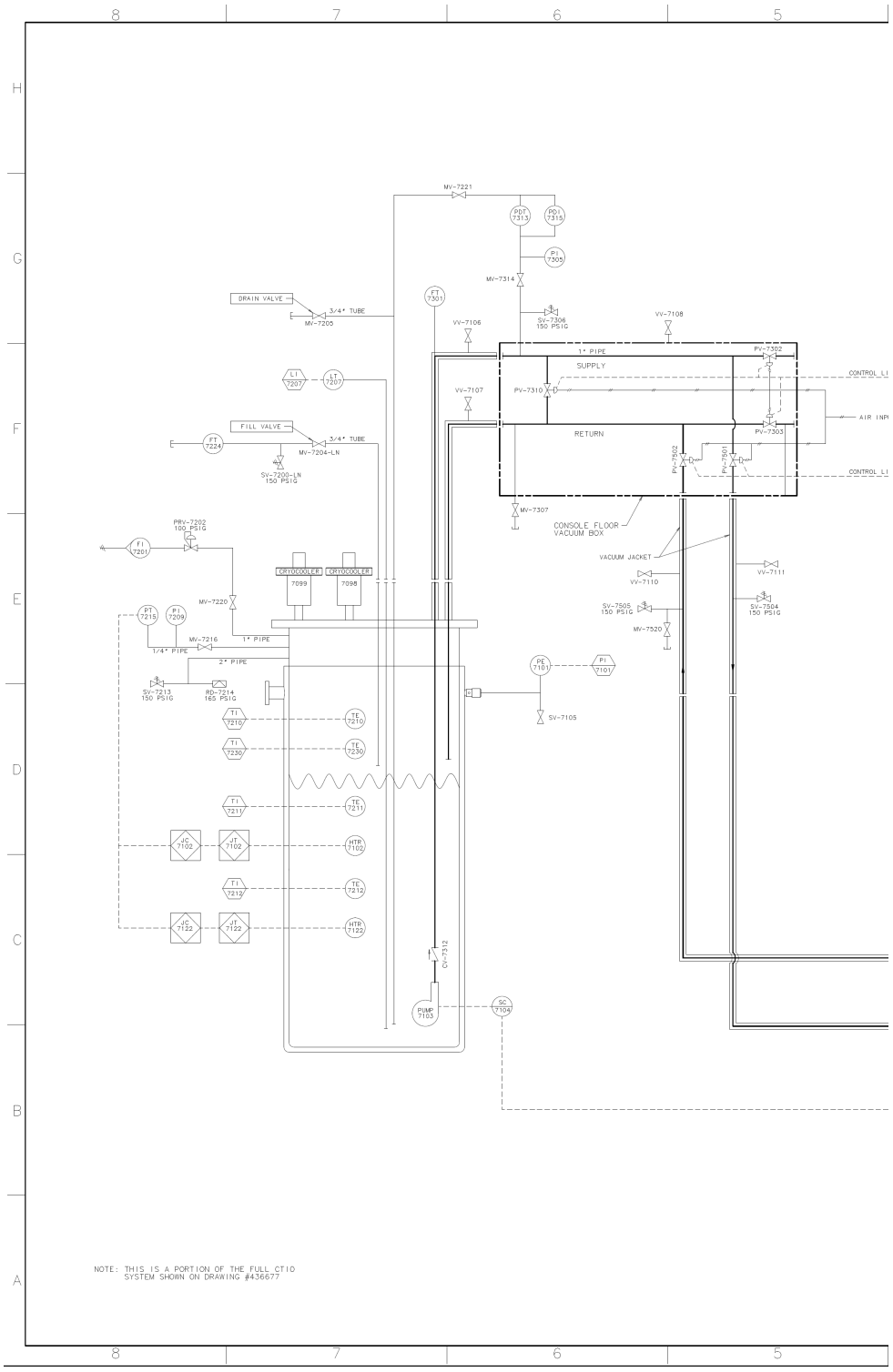

Figure 1.1. Process and Instrumentation Diagram for Cerro Tololo Interamerican Observatory Blanco Telescope Part 1

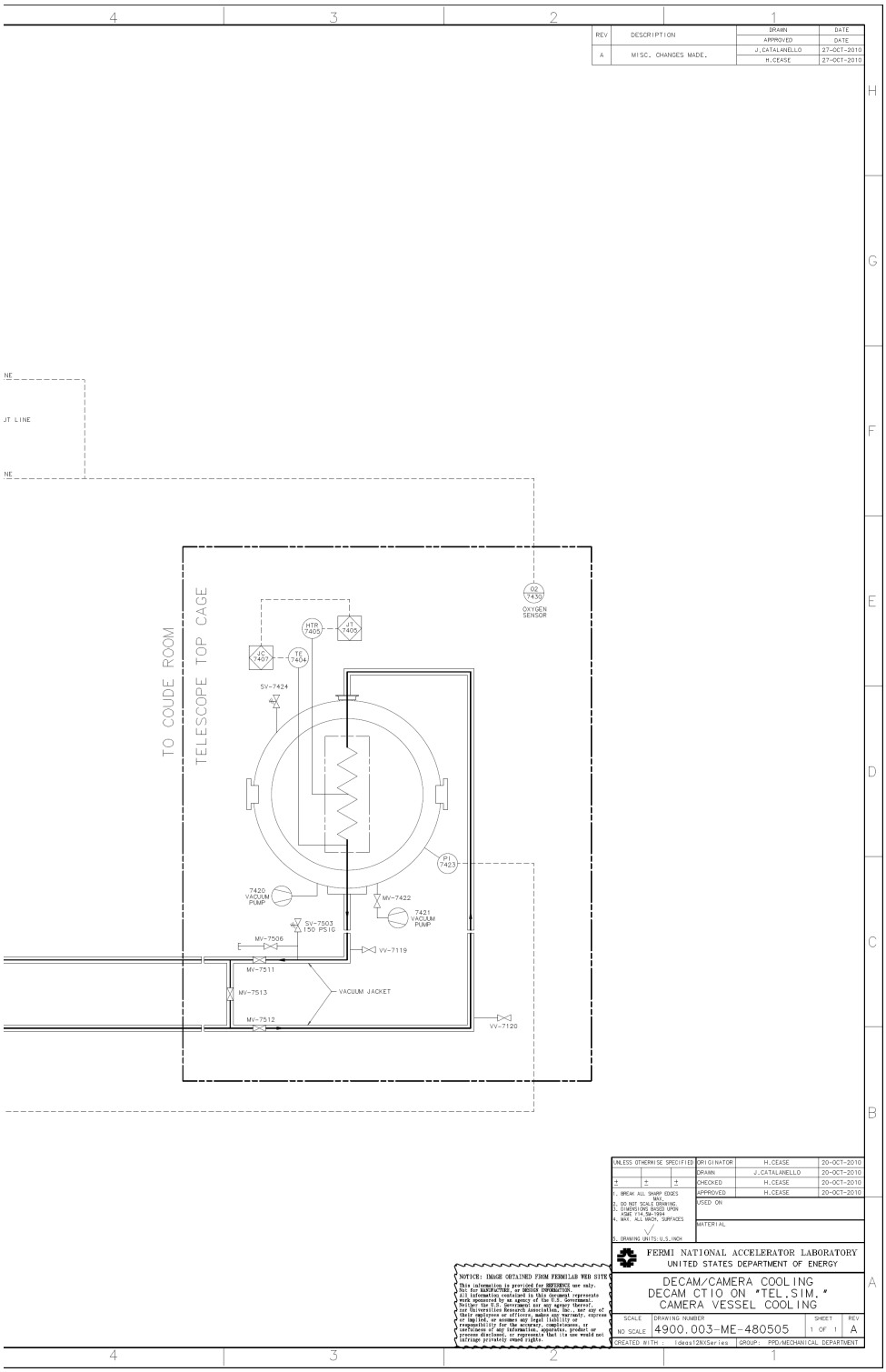

Figure 1.2. Process and Instrumentation Diagram for Cerro Tololo Interamerican Observatory Blanco Telescope Part 2

Initially, a 200L cryogenic liquid vessel (CLV) is filled with liquid nitrogen (LN2). The LN2 is pumped from the 200L CLV (see Fig. 1.1) to a tube heat exchanger, which is attached to the CCD focal plate seen in Figure 1.2. A Barber-Nichols centrifugal pump (BNLNG-01B-100) is used to provide coolant to the telescope. Other components of the system consist of a valve box and two AL-300 cryogenic refrigerators. These cryogenic refrigerators condense the GN2 generated from the CCD heaters, heat leaks, and centrifugal pump. The capacity of these cryocoolers ranges between 200-360W. These coolers place a major constraint on the system as they are both capable of condensing at 360W each for a total of 720W.

The required design parameters for the CCD cooling system at CTIO Blanco telescope are given in Table 2.1.

Table 1.1. Design Specifications for CCD Cooling System [8]

Operating Pressure:	0.76 [MPa]
Required Focal Plate Temperature:	173 [K]
Minimum Flow Rate:	7.5 [LPM]
Height to Top of Telescope:	12.2 [m]
Maximum CCD Heat Load:	200 [W]
Heat Load on System:	415 [W]

The minimum flow rate for the system was chosen to be 7.5 LPM to eliminate stratified flow and other detrimental two-phase flow regimes. Stratified flow is a result of the horizontal orientation of two-phase flow, where the gas and liquid separate due to density differences between the gas and liquid. Furthermore, the maximum CCD heat load is governed by the control heaters on the copper braids that are used to conduct excess heat away from the focal plate. Moreover, the parasitic heat inputs into the system was determined based upon the manufacturers heat loss per unit length of flex tubing, heat loss per valve, and heat loss due to metering. Finally, the focal plate temperature must remain constant at 173K to eliminate thermal gradients

and dark current that will distort the scientific data.

Based on the system description at CTIO, the alternate pump design must abide by the specification in Table 2.1. In other words, it must be capable of supplying at least 7.5 Liters/min to cool the focal plate to 173K. It must have maintenance schedule equal to that of the Cryomech AL-300 cryorefrigerators. This pump must operate closed loop, which implies that any heat added via the pump must be removed by the cryorefrigerators. Moreover, the pumping system must not obstruct the imager field of view of the night sky. Also, it must not impede the overall motion of the telescope along the equatorial and polar axes.

1.2 Current Telescope Cooling Systems

There are various telescopes world wide that require special cooling to capture specific wavelengths of light. Each type of CCD examines different spectra of light. Thus, it requires a special means of cooling. For instance, space telescopes capable of viewing scenes in the infrared (IR) spectrum of light allow scientists to study the atmosphere of various planets and distant galaxies and stars [24]. Similarly, DES will examine small patches of sky to discover and study supernova, which are studied in the visible spectrum of light. Table 1.2 shows the correlation between the material of the CCD, required cooling temperature, and spectrum of light that is being captured.

Table 1.2. CCD Selection Chart: Radiation Type, Wavelength, Blackbody Temperature, Detector Technology, and Detector Temperature[24]

Radiation Type	Wavelength (microns)	Blackbody Temp. [K]	Detector	
			Technology	Temp. [K]
γ-rays	10^(-5)	3x10^8	Ge Diodes	80
γ-rays	10^(-4)	3x10^7	Ge Diodes	80
x-rays	10^(-3)	3x10^6	micro	0.05
x-rays	10^(-2)	3x10^5	calorimeters	0.05
UV	0.1	30000	CCD/CMOS	200-300
Visible	1	3000	CCD/CMOS	200-300
IR	2	1500	HgCdTe	80-130
IR	5	600	HgCdTe	80-120
LWIR	10	300	HgCdTe	35-80
LWIR	15	200	HgCdTe	35-60
LWIR	20	150	Si;As	7-10
LWIR	50	60	Ge;Ga	2
LWIR/μwaves	100	30	Ge;Ga	1.5
μwaves	200	15	Bolometers	0.1
μwaves	500	6	Bolometers	0.1

Knowing the above, DES will examine supernovas to understand the accelerating expansion of the known universe; the visible spectrum of light will be examined. According to Table 1.2, the required temperature for capturing the visible spectrum of light is in the ideal range of 200K-300K. With the current CCDs installed in DECam, the engineering specified temperature is 173K, which is more than enough cooling required to capture light in the visible spectrum. Additional information of the CCD operation and details can be found in *Dark Energy Physics Expectations at DES* [23]. Therefore, current telescope cooling methods will be explored. A couple of the common types of cooling systems include modular cryostats and flexible heat pipes.

A modular cryostat for large format and mosaic CCDs have a similar cooling requirement as DES telescope imager. That is, both must cool the CCDs to 173K and do so effectively. This modular cryostat uses an open loop cooling method. The heat from the CCDs and control heaters boil LN2 and vent GN2 to atmosphere. This saturated mixture allows the CCDs to be maintained at a constant temperature of 173K. The primary components consist of a 2.4L LN2 dewar, LN2 fill port, GN2 vent port, vacuum insulation, activated charcoal plate, and a cold connector [18]. The LN2 fill port allows LN2 to be resupplied to the 2.4L dewar. Additionally, the GN2 vent allows the boiled GN2 to be vented to atmosphere. The vacuum insulation prevents heat transfer losses from conduction and free and forced convection. The inner walls of the vacuum chamber are polished to have high reflectivity to reduce radiation heat transfer. Moreover, the outer wall of the 2.4L LN2 dewar is polished for a similar reason. Lastly, the heat generated via the CCDs is conducted via the cold connector seen in Figure 1.2.

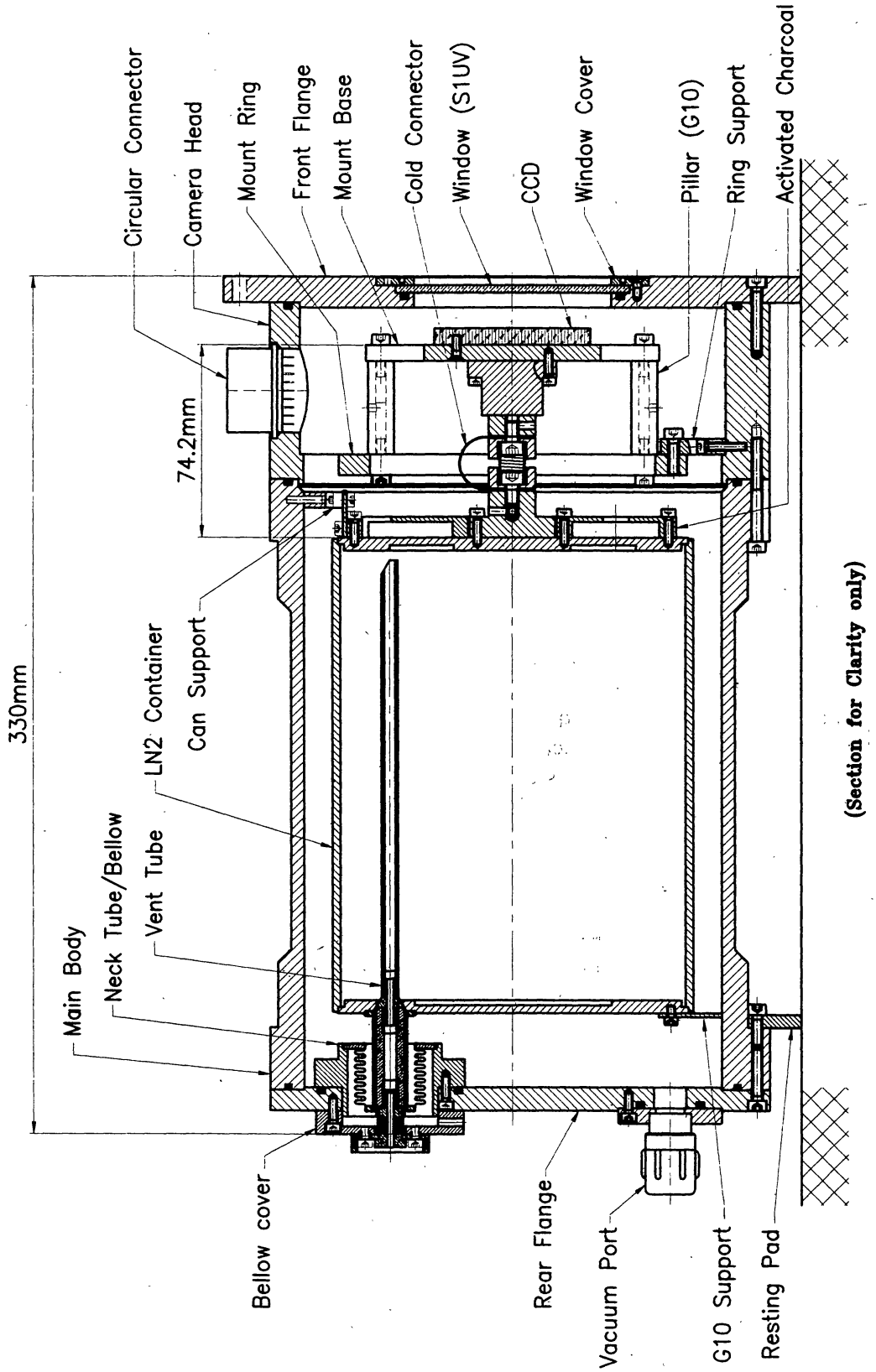

Figure 1.3. Modular CCD Cryostat[18]

In a small scale test of this cryostat, it was determined that in the inverted orientation the hold time of the 2.4L of LN2 was reduced. This was a result of conduction losses from the GN2 vent tube as see in Figure 1.2. Moreover, LN2 passes through the GN2 vent tube and spills onto the test floor, which further contributed to the reduced hold time of 34hrs to 24hrs. Also, the LN2 container must be evacuated every two months for optimal performance. In general, this device can hold LN2 for 34hrs before it is required to be refilled. However, this does not meet the specifications, because the system maintenance time must be at least 8000 hrs; the modular cryostat had decreased performance every 1440 hrs. Additionally, the arrangement does not allow scientist to start and stop the system without being concerned with the amount of LN2 in the 2.4L container.

The next device utilizes flexible heat pipes for CCD cooling for outer space telescopes. The heat pipe accepts heat from thermoelectric devices mounted on the CCDs focal plate. Similar to the DES telescope imager, the CCD detector must operate at 193K, which is slightly warmer than the DES specifications. The heat pipe specifications call for removing up to 30W of heat from the CCDs and transferring that heat to space, via radiation heat transfer. The basic components consist of the heat pipes mounted from the High Resolution Channel (HRC) CCD assembly and the Wide Field Channel (WFC) CCD detectors to the enclosure wall, where it is radiated to outer space. A heat pipe is simply a device that utilizes a wicking structure to generate capillary forces that draw liquid into hot regions where vapor is generated. In Figure 1.2, the heat pipes (HP) that attach to the HRC and WFC CCD assemblies are on the evaporator end. Likewise, the HPs attach to the enclosure or the condenser. The working fluid is ammonia and the wicking structure is a rolled metal mesh screen. Also, the overall performance of the heat pipe is governed by the product of the heat transferred by the transported length.

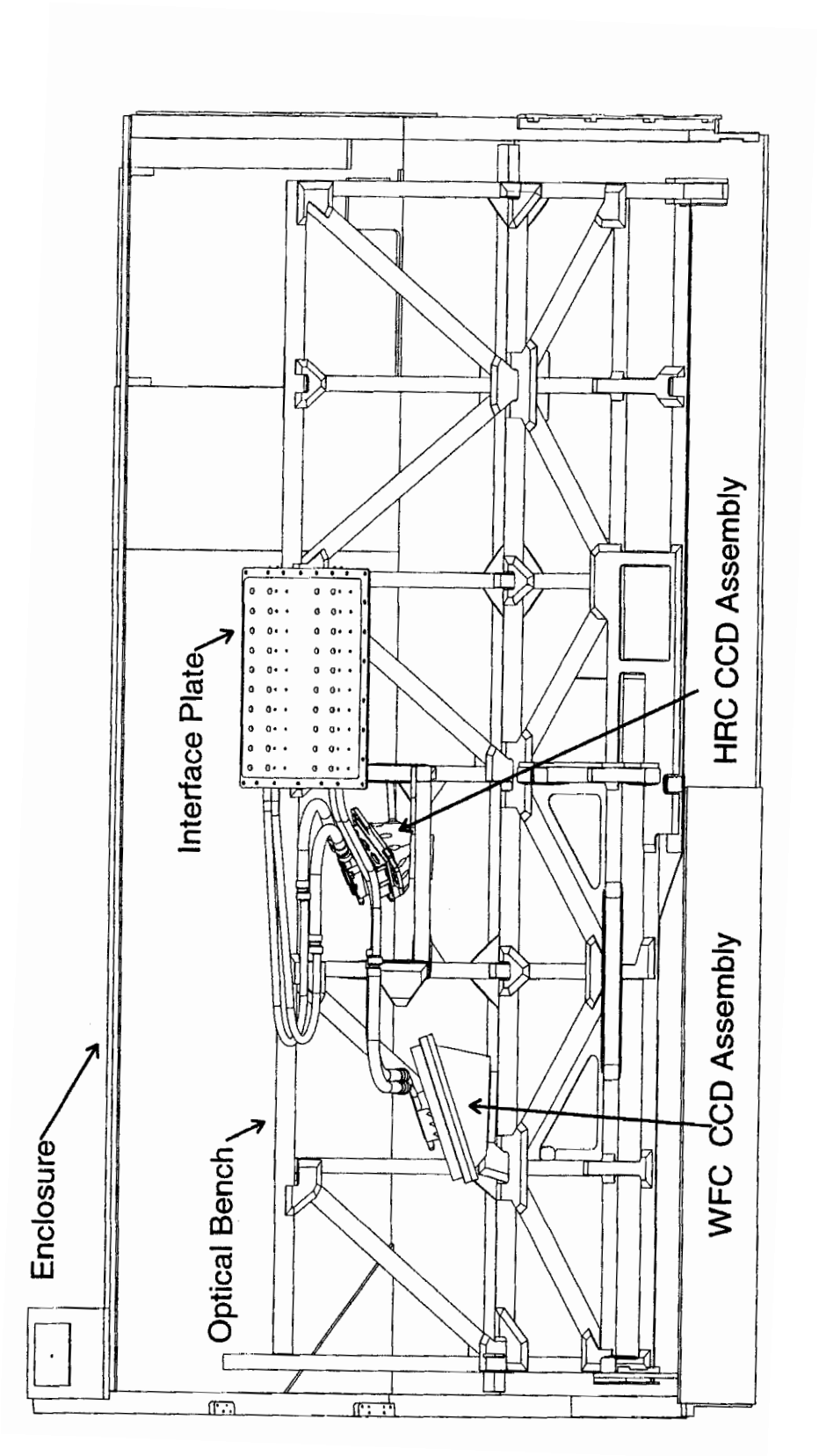

Figure 1.4. Heat Pipe Locations in the ACS [22]

In a small scale test, the HPs were able to achieve the required performance of 3340 Wcm within a temperature range of 249 K to 273K. Despite this success, the heat pipes did not indicate an impending dry out. Typically, axial grooved HPs show a gradual increase in its temperature difference. However, the flexible HPs show an abrupt increase in temperature. A designer typically would be concerned with a dry out indicator as it can damage system components due to the lack of liquid coolant in required areas. All HPs in any vertical position perform poorly due to the effect of gravity. Therefore, they are typically utilized in space where gravity is absent. If the DES telescope imager could be cooled using HPs, the HPs themselves would limit the viewing angle of the telescope. Recall that the telescope imager is mounted at most 12m above the floor, which is the Zenith position. Because the performance of an HP is the product of the heat transferred to the transported length of tubing, a DES telescope imager cooling system utilizing heat pipes would be very inefficient. This would be a result of the length component dominating over the heat transferred from the CCDs as well as the heat load on the tubing. In other words, the shorter the length of tubing given a fixed heat load the better the HP will perform.

In conclusion, many telescopes utilize different methods of cooling the CCDs. Each CCD requires a particular required temperature, which corresponds to the specific wavelength of light being investigated. Table 1.2 shows this correlation between the CCD material, the wavelength being studied, and the required temperature of the CCD. Two telescope cooling methods have been discussed. The first was a modular cryostat that utilized pool boiling to maintain the CCDs at a constant temperature. However, the system requires maintenance every 1440 hrs, which is significantly below the minimum required maintenance schedule of 8,000hrs. Furthermore, HPs are one method of cooling space telescopes where gravity is absent. Creating an HP closed loop cooling system for DECam will be insufficient as a HP operates optimally in the absence of gravity. Recall, that vertical sections of HPs, in the presence of gravity,

degrade their performance. Additionally, the performance is degraded with the length of tubing that is needed to supply the coolant to the top of the telescope. Therefore, further study is required to understand fluid delivery to best select a mechanically simple and innovative design.

1.3 Fundamental Pumping Methods

The motivation in selecting the new pump is governed by the mechanical simplicity for expected high reliability and innovation for telescope cooling systems. Therefore, a fundamental perspective must be used. Several fundamental pumps are identified by the Food and Agriculture Organization of the United Nations [19]. This organization was able to classify hundreds of types of fluid transport devices into five fundamental pumping methods, which can be seen below.

1. Direct Lift (i.e. water wheels, water well and bucket, etc.) Figure 1.5A
2. Displacement (i.e. scroll, gear, peristaltic, etc.) Figure 1.5B
3. Gravity (waterway, Roman aqueduct, etc.) Figure 1.5D
4. Velocity Head Pumps (centrifugal, electrohydrodynamic pump, etc.) Figure 1.5E
5. Using the buoyancy of a gas (coffee maker, espresso maker, etc.) Figure1.5C

Figure 1.5A illustrates a method of lifting the fluid to the cooling process using fixed volumes. Because of the arrangement of the telescope, it is not practical to directly lift the LN2 to the top of it because most direct lift devices are either reciprocating or rotary. This in turn results in mechanical lifts that are required to transport these fixed volume of fluid. A mechanical lift can consist of a conveyor system or pulley system that will have to traverse the telescope structure to the

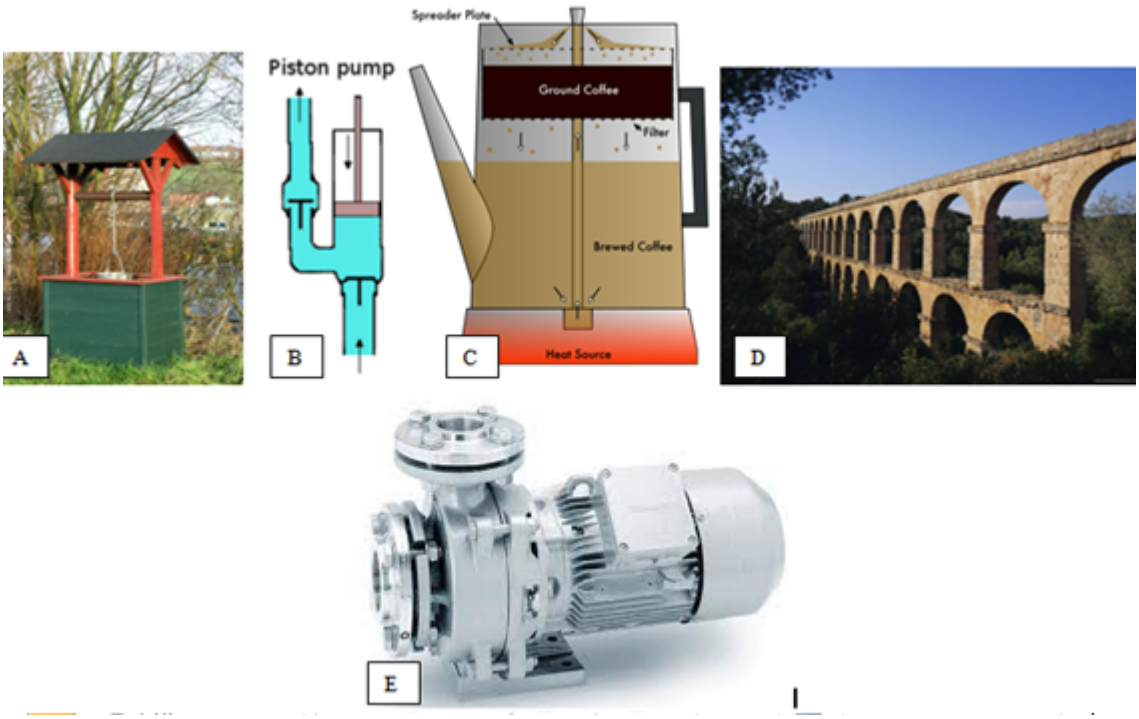

Figure 1.5. Fundamental Pumping Methods

imager. This can be rather complicated journey for mechanical devices. The flexible tubing journey can be seen in the Appendix B. Therefore, it is necessary to only consider using flexible hosing, from the base of the telescope to the imager for fluid delivery. Therefore, a stationary device similar to a centrifugal pump must be used.

Figure 1.5C shows a coffee percolator, which uses the buoyancy of a gas to displace a fluid volume. This two-phase flow has an overall density that is less than the liquid phase of the process fluid, which results in the rise of the liquid and gas of the process coolant. The mechanism behind this method is simply a heat pipe. A heat pipe design is discussed in Section 1.2. Recall, that this device requires a wicking structure to generate the needed capillary forces to pump the liquid. Operating such a system in the presence of gravity and vertical section of tubing can be detrimental to the overall performance. Because this is a land based telescope, this method of pumping cannot be considered.

The use of gravity as a means of pumping the fluid is not practical. This is depicted in Figure 1.5D. First, the requirements specified by DECam indicate that it is imperative that the cooling system be closed loop. Therefore, a proposed cooling system using gravity must return the fluid to reservoir, which requires a pump. Moreover, mounting a cooling system above the telescope imager will obstruct its total viewing angle, have varying flow rates because of varying hydraulic heights, and is susceptible to a vapor lock, which ceases flow. In conclusion, gravity feed pumping will not be considered as an option.

Figure 1.5E displays a centrifugal pump. This is the most common method of fluid transportation. This method of pumping uses a submerged impeller to accelerate the fluid. Accelerating the fluid results in a low and high pressure at the inlet and exit of the pump. This device has many components that are susceptible to failure at cryogenic temperature. Recall, that DECam CCD cooling system utilizes a centrifugal pump. The bearings of this pump fail every 2800hrs. As a result of the bearing failure, the end cap showed signs of score marks, which indicates that the cap was rotating in the pump housing. As a result of this failure, the DES team decided to explore a different pump with mechanical simplicity.

Finally, Figure 1.5B displays a simplex-direct-acting positive displacement (PD) pump. Assume the volume is initially filled with a liquid. As the piston or plunger descends the cylinder, the one way valve at the base remains closed and the liquid exits through the top valve towards its required destination. Despite the PD pump having a reciprocating piston or plunger, it can be easily modified to a simpler mechanism. That is the piston or plunger can be completely removed and replaced with gas. The gas acts as the mechanism to displace the liquid volume out of the cylinder. Thereby, eliminating all high speed mechanical components and using generated gas to displace a fluid volume. This fundamental pumping concept is the basis

of the design of the cryogenic over-pressure pump (OPP).

In conclusion, Figure 1.5A, shows direct lift pump. Due to an external motor required to lift the fixed volumes of fluid, it is deemed unsatisfactory for the application because it is not mechanically simple. Likewise, Figure 1.5D shows a gravity feed pump. This system can be modified for a closed loop system with adding an external centrifugal or PD pump. However, the pumping system must be at an elevation above the telescope on a fixed platform above its zenith, which is 12.2m. This configuration will obstruct the field of view of the night sky, which limits the observed sky. Similarly, the centrifugal pump, Figure 1.5E is the pump that the DES team is attempting to replace with a device that is mechanically simple and innovative. Therefore, the PD pump concept seen in Figure 1.5B is adopted as the basic idea for a new pump. The piston and plunger will be replaced with a moving liquid-gas boundary, where the differential pressure required for fluid flow is generated via an electric heater. The only mechanical devices are the valves needed to regulate the pumping, which can easily placed in parallel to increase the MTBM to 8000 hrs. The concept of the cryogenic over-pressure pump will be described in the next section.

1.4 Positive Displacement Pumps

The cryogenic over-pressure pump (OPP) originated from a piston pump, which is a direct acting positive displacement (PD) pump. The basic operation of this particular pump consists of restoring and displacing a fixed liquid volume cyclically. Typical positive displacement pumps consist of a power pump and direct-acting pumps. The difference between the two is simply the device that drives the piston. For instance, a power pump utilizes a crankshaft with a driver (such as a motor, engine, or turbine). A direct acting pump uses a drive fluid (such as a gas or liquid). The following figure shows a cross sectional view of the two types of pumps.

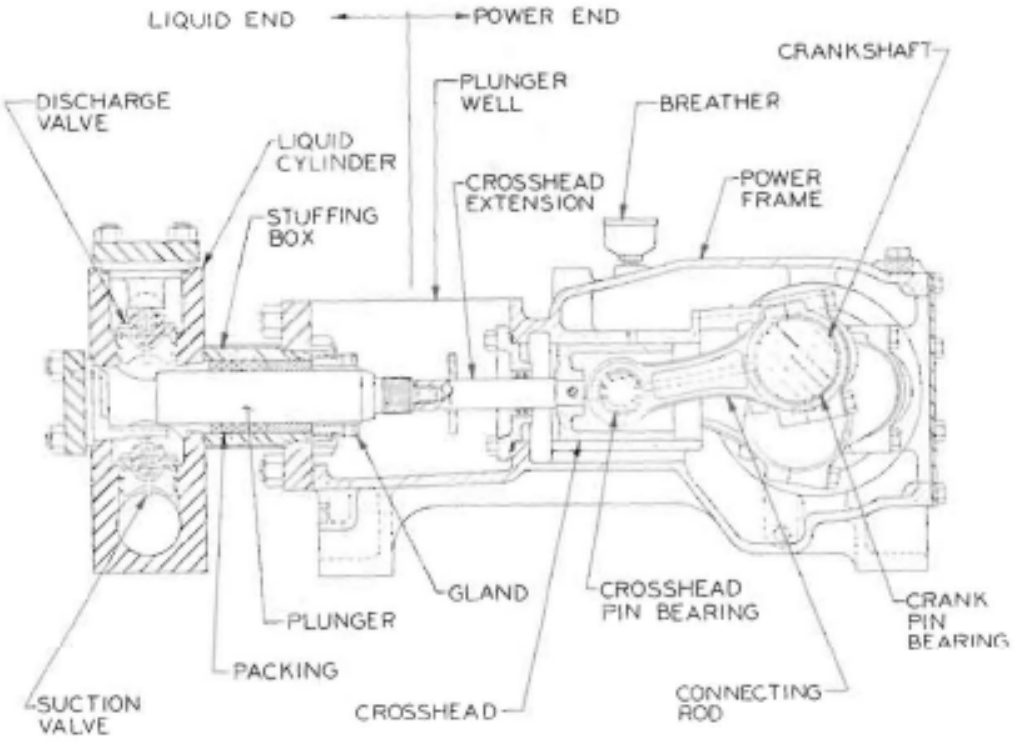

FIG. 2.1. **Components of a power pump. (*Courtesy Union Pump Co.*)**

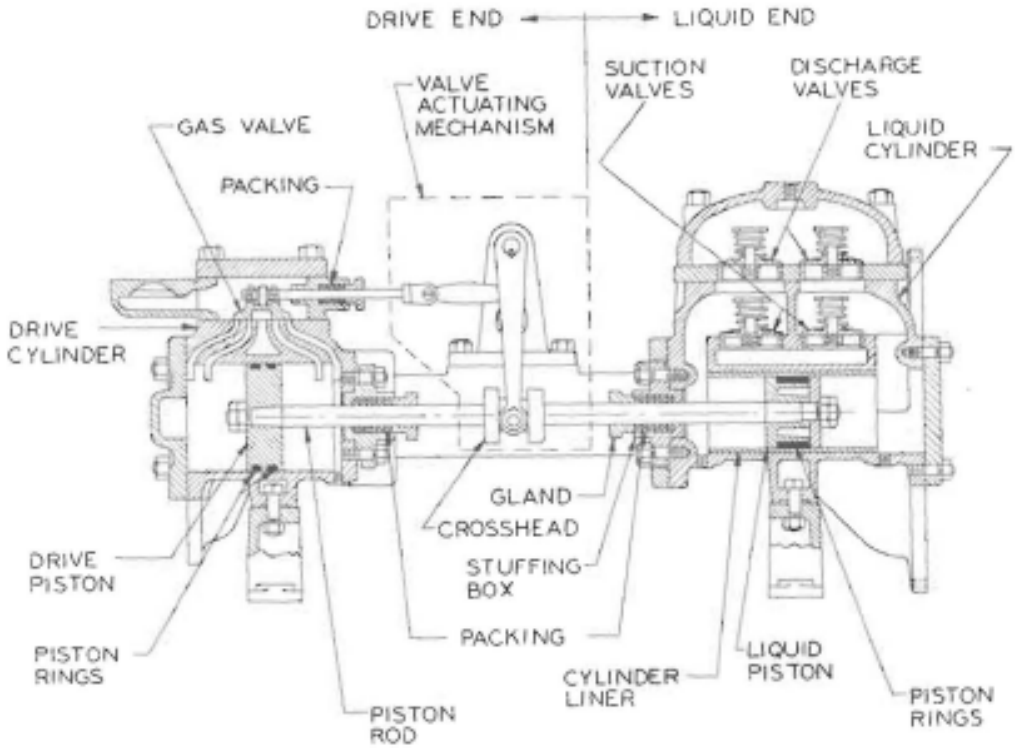

Figure 1.6. Top: Power Pump. Bottom: DirectActing Pump [14]

Figure 1.6 PD pumps are typically used over centrifugal or rotary pumps because of a two-phase fluid. For instance, reciprocating pumps are used to transport slurries from one location to the next. A slurry is a mixture of liquid and solid particles. Because of the solid particles in the mixture, centrifugal pumps would easily be destroyed due to the high velocity of the impeller impacting the hard particles. In addition, two-phase flow of liquid and gas can easily be tolerated by a PD pump. A centrifugal pump can operate with a two-phase (gas-liquid) fluid only during pump priming. Furthermore, Terry Henshaw mentions this in *Reciprocating Pumps*[14],

`The justification for selecting a reciprocating pump, instead of a centrifugal or rotary, must be cost-not just initial cost, but total -including costs for energy and maintenance.`

The main advantage of a power PD pump is the mechanical efficiency. This efficiency corresponds to the power delivered to the driver to be converted to liquid motion. Typical mechanical efficiencies range between 85% and 95%. The typical losses are due to friction in gears, belts, bearings, packing, and valves [14]. For power pumps, the flow rate is independent of discharge pressure. Disadvantages, of this pump are the high initial cost, which will exceed a centrifugal pump cost. Also, the packing maintenance, which occurs every 1440 hrs (60 days). See Figure 1.6 for the image of the packing. Typical maintenance times range between 2500hrs (100 days) to 18000hrs (750 days) for continuous operation for conventionally warm fluids.

Direct-acting pumps have advantages similar to power pumps and additional ones. These units are used for low flow applications. Like in power pumps, the flow rate is independent of discharge pressure. However, the velocity of the liquid side, seen in Figure 1.6, can be regulated via throttling the gas on the drive end. A major advantage of this PD configuration is the absence of a crankcase and other

related mechanical components. These pumps are unaffected by corrosive environments. These direct acting pumps are quiet and have extended lifetimes due to rugged designs. Some disadvantages consists of low thermal efficiencies [14], but high mechanical efficiency. These low thermal efficiencies are a result of the drive gas not expanding during a stroke; the gas remains at a constant pressure throughout the stroke. Therefore, the expansion work at the end of the stroke is not utilized. If a liquid (incompressible) drive fluid is used, it has little expansion work. Hence, higher thermal efficiency.

Recall that the PD pump was selected as the best alternative design for current DECam centrifugal pump as stated in Section 1.3. Two types of PD pumps were investigated. The power PD pump, which has high mechanical efficiency, but poor mechanical lifetime. Thus, it would not be sufficient as the alternative pump design model. However, the direct acting PD pump is relatively promising with the absence of the crankcase, which includes bearings, shafts, lubrication, etc. This pump is mechanically simply as it utilizes a gas, on the drive end, to displace fluid on the liquid end. To even simplify the direct-acting pump, it is proposed to eliminate the valve actuating mechanism and allow the drive end gas be in contact with the liquid end. Therefore, the direct acting pump in Figure 1.6 will now become a vertical cylinder with a varying height interface. This can be seen in the following figure.

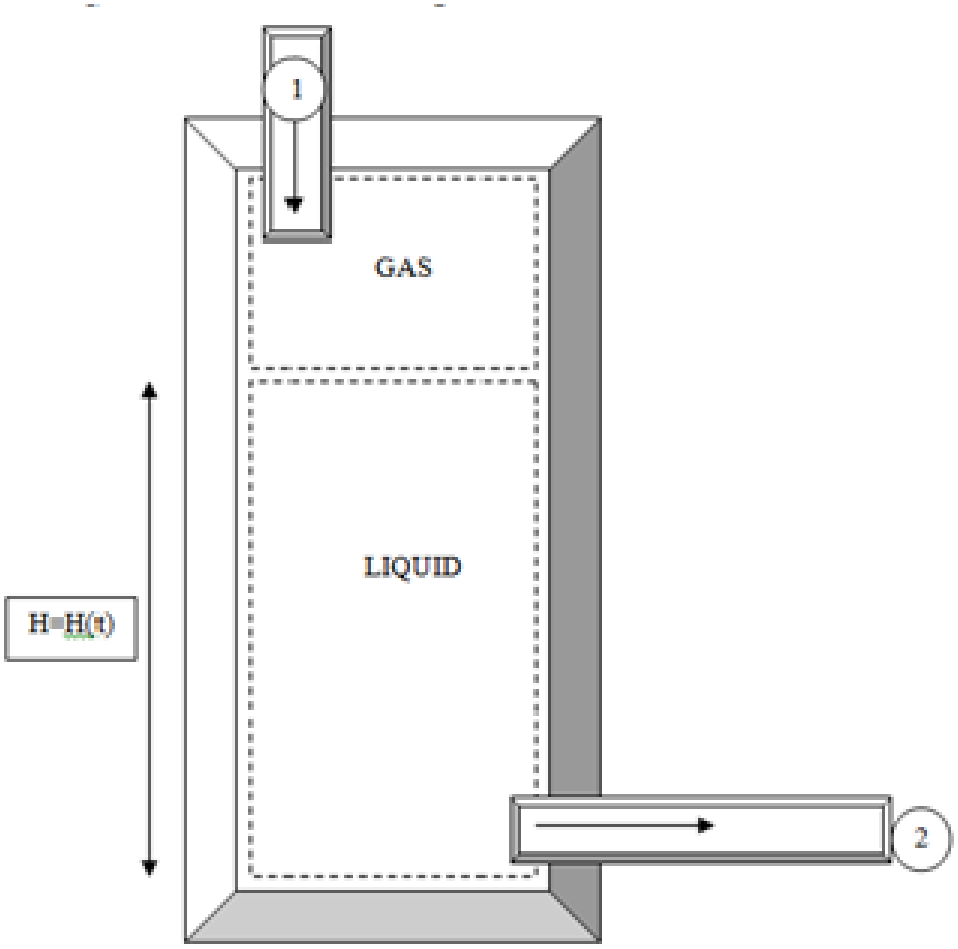

Figure 1.7. Modified Direct Acting Pump

The cylinder in Figure 1.7 is similar to Figure 1.5B in Section 1.3, but with out the piston or plunger. This new concept will eliminate mechanical components associated with most common failures, such as the packing. The basic idea of this device is to inject gas into this chamber to displace a liquid volume. The fluid velocity, similar to a direct acting pump, can be regulated by throttling the injected gas at point 1. Additionally, the stroke height is associated with the liquid height of the liquid-gas interface. The mechanical efficiency of this device is expected to be high as in direct-acting pumps. Further discussion of this concept is made in the next section.

CHAPTER 2

OVER-PRESSURE PUMP

2.1 Concept

Because a direct acting piston pump, seen in Figure 1.5B, requires the use of a valve actuating mechanism, it is recommended that it be removed due to typical failures in the packing [14]. Figure 1.7 shows the fundamental idea behind the cryogenic over-pressure pump (OPP). However, the OPP is not simply a stainless steel tube, it relies heavily on control software. For instance, LabView is used to control valves. The primary components of the OPP, in theory, consist of a process cylinder (PC) as seen in Figure 1.7, one gas generator, and a solenoid valves (SV).

The process cylinder (PC) is the fixed volume from which liquid is discharged. It is simply a tube with capped ends that has ports for injecting and discharging gas and liquid. Additional ports are added to relieve the gas pressure within the cylinder after a single stroke of this PD pump. When the PC is completely filled with gas, it must be refilled with liquid. This can be done by generating an artificial differential pressure or using gravity to feed the liquid into it. The DES CCD cooling system utilizes a 200L cryogenic liquid vessel (CLV) as mentioned in Section 1.1. The vessel is a reservoir for LN2. The PC will be fully submerged inside the LN2 bath. Then the hydraulic head will be used to refill it. Furthermore, the GN2 is buoyant and will rise out of the PC to allow the LN2 to fill it. The idea is similar to a buoyancy driven flow as described in Section 1.3.

The next component is the gas generator. This device provides the motive fluid for displacing the liquid out of the PC. It contains a submerged heater that is used to vaporize the gas. Furthermore, a check valve, that is set to a high opening

pressure, should be used to allow pressure to build. This high pressure is required to better generate the flow needed to discharge the liquid out of the PC. Because the volumetric expansion ratio of liquid to vapor is high, the gas generator will be capable of supplying the PC with sufficient amount of gas prior to it being refilled. In other words, the gas generator has a slower stroke velocity than the PC, which is directly correlated to the volumetric expansion ratio. This stroke velocity is a term used to describe the speed of a piston or plunger of a PD pump when it discharges the fluid from the cylinder. During a refill of the gas generator, a port is opened to allow it to refill using an artificial or gravity induced differential pressure. The CCD cooling system GN2 generator will be submerged in the 200L CLV LN2 bath. This implies that the GN2 will rise out of the GN2 generator and allow LN2 to flow inside (see Fig. 2.1).

The final components that make up the OPP are solenoid valves (SV). These SVs allow for dynamic control of both the PC and gas generator. These valves control how much gas is injected into the PC. Also, the valves control the refills of both the PC and the gas generator. Instead of relying on the control of a variable frequency drive for a centrifugal pump, the OPP is a device that relies heavily on a timing sequence. For instance, changing the refill time of the PC allows for quick adjustments in the flow rates with constant gas injection time. Furthermore, changing the electrical input into the heater allows for changes in pressure, which in turn affect the fluid velocity.

The PC, gas generator, and SVs are the primary components OPP. This pump allows for control over the flow rate, which is directly correlated to the time at which the PC is allowed to refill. In other words, the volume of liquid within the PC can be controlled. Also, the pressure is controlled based on the set pressure of the one way valve on the gas injection line. Finally, the OPP uses solenoid valves to control the

discharge and refill of the PC.

2.2 Basic Components and Operation

This section is not the final design solution, but an example. It is used to convey the overall concept of the pump. The actual test that was conducted only utilized one process cylinder, four solenoid valves, and an improvised gas generator. In order to implement the idea of the OPP into practice, it is important to understand its role in an existing system. The optimal design of the OPP is to integrate it into the DES CCD cooling system at CTIO, which has two AL-300 cryogenic refrigerators. In order to do so, the OPP is installed into the 200L CLV, as seen in Figure 1.1 and 1.2, and fully submerged in the LN2 bath. The PC and the GN2 generator is gravity filled with LN2 after each stroke. Remember that the GN2 generator provides the high pressure GN2 to pump LN2 out of the PC. The discharged LN2 is delivered to the CCD HX. Figure 2.1 illustrates the integral role of the OPP in the CCD cooling system. Notice, that the GN2 generator is vacuum sealed to prevent convection and conduction heat transfer losses, which degrade the thermal efficiency of the OPP. The PC can also be insulated to further reduce thermal losses from the warm GN2.

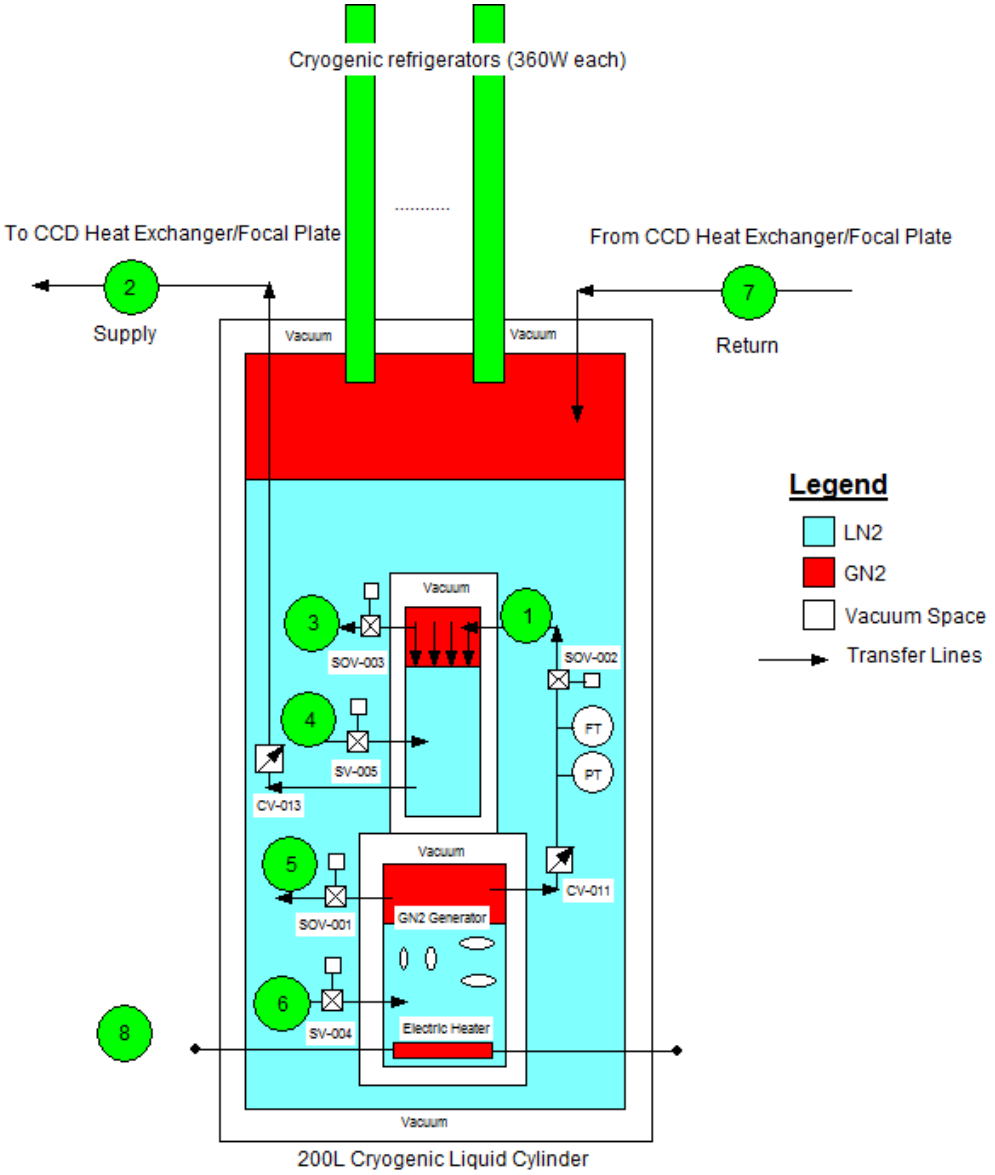

Figure 2.1. Over-Pressure Pumping Schematic

The components shown in Figure 2.1 are a one way valve (CV), solenoid operated valves (SOV), PC, GN2 generator, electrical heater, two cryogenic refrigerators (cryocoolers), and instrumentation. SV-004 and SV-005 allow LN2 to refill the GN2 generator and PC after they complete a stroke. CV-013 prevents back flow of LN2 into the PC. CV-011 is set to a high pressure to allow the GN2 generator to increase in pressure. This high pressure, combined with the low pressure of the 200L CLV, generate a differential pressure to drive the flow. The SOV-001 and SOV-003 are used after the GN2 generator and PC have completely emptied all its contents; these valves are meant to allow the buoyant GN2 to exit through the top of both components. Finally, the cryocoolers are used to condense the generated GN2 via the GN2 generator, CCD heat load, 200L CLV heat load, and the transfer line heat loads.

An electric heater inside the GN2 generator is used to boil LN2 to create GN2, which is injected into the PC. SOV-002 is required to regulate the injected gas. In theory, the PC will complete numerous cycles before all the LN2 within the GN2 generator is consumed. The consumption of LN2 depends on the expansion ratio. For instance, one cubic centimeter of LN2 will expand to seven hundred times to produce GN2 when exposed to atmospheric conditions (see App. D for additional details). This expansion ratio is used as the mechanism for displacing LN2 from the PC. For example, let the PC and GN2 be of the same volume of 100 cm^3. Let it be that it takes $100cm^3$ of GN2 to displace 1 cm^3 of LN2 for cooling. Due to an expansion ratio of 1:100 (LN2:GN2), the GN2 generator, theoretically, can cycle 100 times before it needs to refill with LN2 because each cycle consumed 1 cm^3 of LN2 for GN2 production. In practice, this is much different due to inefficiencies, which require additional GN2 than needed.

In order for the PC to supply LN2 to the CCD HX, GN2 must be injected into it. Therefore, the heater within the GN2 generator is turned on creating the gas.

This gas flows through line 1, when SOV-002 is opened and SOV-001 and SV-003 are closed. Therefore, the GN2 begins applying a pressure over the top of the LN2 within the PC, which begins discharging via line 2. The LN2 enters line 2 at the same temperature as the LN2 within the 200L CLV and returns to it via line 7 as a two-phase flow with a relatively low quality. The two-phase flow on the return line to the 200L CLV is a result of heaters locally boiling LN2. After a single stroke is completed the PC must be refilled.

During the refilling of the PC, the buoyancy of the GN2 causes it to exit through line 3; LN2 fills through line 4. For this to occur, the PC must be isolated from the GN2 generator via closing SOV-002 and opening SOV-003 and SV-005. Closing SOV-002 prevents any residual gas from entering the PC. This refilling cycle is due to the action of gravity, which causes the liquid to exchange volume with the GN2 within the PC. Accordingly, the PC will cycle through this process until the GN2 generator can no longer generate GN2. The orifice of the solenoid valve must be large to allow LN2 to refill the PC better.

Once the GN2 generator consumes the LN2 for generating GN2, it must be refilled similarly as the PC. Likewise, it must be isolated during a fill. Thus, SOV-002 closes and SOV-001 and SV-004 opens, which allows GN2 to exit through line 5 and LN2 to enter through line 6 from the 200L CLV. Again, this device utilizes the force of gravity to displace the GN2 from the fixed volume. This process only requires solenoid valves, which are inexpensive and have long operating lifetimes. Similar to the PC solenoid valves, the orifice size must be large to utilize the hydrostatic pressure of the liquid column.

In conclusion, the OPP control sequence and operation has been discussed. The PC is the device that stores and discharges the coolant to the CCD heat exchanger (HX). Moreover, the GN2 generator provides the driving fluid to displace that LN2.

Both the GN2 generator and PC fill using gravity to allow the LN2, which has a significantly higher density than GN2, to fill the chambers. The OPP relies heavily on the control scheme of the discharge and refill of the both the GN2 generator and PC. These primary components used for the CCD cooling system, given the proper control sequence of the SOVs, will allow for instantaneous control of the volumetric flow rate. Section 1.4, direct-acting pumps, mentions that the speed of the liquid is regulated by throttling the gas on the drive end, as seen in Figure 1.6. Therefore, the GN2 flow rate is governed by the rate at which GN2 is generated within the GN2 generator, which corresponds to the heater power input.

2.3 Ideal Pump Model

The primary components of the OPP is the GN2 generator, process cylinder (PC), and solenoid operated valves (SV). In theory, the OPP is fully submerged within the 200L cryogenic liquid cylinder (CLV). Thus, the pressure of the 200L CLV becomes the initial pressure of the GN2 generator prior to discharging any LN2 from the PC. Therefore, for their to be fluid flow through the MCCD transfer lines, it is necessary to generate a differential pressure. This differential pressure is generated by a heater that is contained within the GN2 generator as seen in Figure 2.1. Recall that the efficiency of the pump depends on the ratio of the pump work to the amount of heat input into the system via the GN2 generator. A final and relatively significant observation is the varying height the LN2 within the PC. In other words, the pump head increases with the decreasing height of the LN2 in the PC and the increasing height of the column of LN2 during startup. Therefore, the pump must be robust to operate in variable working conditions, such as the high pumping pressures required for startup. During normal operations, the pump power is only a function of pipe friction and pipe minor and major losses.

The following equations are used for the ideal use of the OPP described in

Section 2.2.

$$\dot{W}_{pump} = \frac{\dot{m}_{LN2}}{\rho} \left(\Delta P_{column} + \Delta P_{friction} + \Delta P_{minor,major} \right) \tag{2.1}$$

Equation 2.1 shows the work required by the pump to drive the fluid through the system. This equation consists of the pressure drops corresponding to a hydraulic head, fluid friction, and flow obstruction (valves, orifices, elbows etc). When this pump is self priming, the hydraulic head becomes an issue. However, during normal operation of the OPP, the hydraulic head is ignored; it is large during pump priming. The next equation is the electrical power input.

$$\dot{W}_{electrical} = \frac{V^2}{R} \tag{2.2}$$

Equation 2.2 represents the applied electrical power input into the heater. This power input is the product of the voltage and the current. It is required to supply the energy needed to generate the GN2 for displacing LN2 to the CCD heat exchanger. Also, in practice it is important not to exceed the critical heat flux of this heater for it will be destroyed. The next equation is the heat rate needed to vaporize the GN2.

$$\dot{Q}_{in} = \dot{m}_{GN2,injection} \cdot (h_g - h_f) \tag{2.3}$$

Once the power from the heater is applied to the LN2 in the generator, it will begin creating GN2. Equation 2.3 shows that the heat needed to generate GN2 is the product of the mass flow rate of the GN2 and the latent heat of vaporization. Most of the work from the electrical power is supplied for this phase change. Moreover, the power of the heater then equals some fraction for the heat rate input into the system. This can be seen by the electrical efficiency equation seen below.

$$\eta_{pump} = \dot{W}_{pump}/\dot{W}_{electrical} \tag{2.4}$$

Equation 2.4 is the ratio of the power required to displace the LN2 from the PC to the electrical power. This efficiency can be further subdivided into mechanical efficiency, thermal efficiency, and electrical efficiency-Equation 2.7.

$$\eta_m = \frac{\dot{W}_{pump}}{\dot{W}_{drive,fluid}} \tag{2.5}$$

The equation above defines the mechanical efficiency of the OPP. The numerator is defined in Equation 2.1. Nevertheless, the denominator is defined similarly, which is the product of the volumetric flow rate by the differential pressure from the GN2 generator to the process cylinder. In other words, this mechanical efficiency is defined as the ratio of the energy of the LN2 flow to the driver flow of the GN2. The next equation shows the thermal efficiency.

$$\eta_{th} = \frac{\dot{W}_{GN2}}{\dot{Q}_{in}} \tag{2.6}$$

Equation 2.6 is simply the ratio of the fluid power of the GN2 to the latent heat of vaporization of the GN2. Physically, this means that the heat energy via the electrical heater is transformed into a pressure and temperature, which generates a flow. This equation determines the effectiveness of the heat rate that is used to generate gas power. The electrical efficiency can be seen in the next equation.

$$\eta_e = \frac{\dot{Q}_{in}}{\dot{W}_{electrical}} \tag{2.7}$$

Equation 2.7 shows the effectiveness of the electrical power being converted into heat needed to vaporize GN2. This phase transition governs the response of

the OPP. Throttling the gas for different LN2 discharge velocities is governed by Equation 2.7. In theory, the electrical efficiency, Equation 2.7 is set equal to unity. Furthermore, the mass balance can be seen in the following equation.

$$\Delta m = 0 \tag{2.8}$$

The mass balance of the system is governed by drawing a control volume around the inner portion of the 200L CLV and on the inner walls of the tubing of line 2 and line 7 of Figure 2.1. Subsequently, the control volume has zero mass leaving or entering the boundaries. Instead, heat and work energy rates enter and leave the control volume (CV) as seen in the next equation.

$$\dot{Q}_{CCD} + \dot{W}_{electrical} = \dot{Q}_{cryo} \tag{2.9}$$

Because the mass within the CV of the entire 200L CLV and the transfer lines is always constant, heat via the CCD components and electrical heater enter the CV. The cryogenic refrigerators remove the heat that is added to the system by removing the sensible heat and/or latent heat of the GN2. Equations 2.9 and 2.8 simply state that the mass in the closed loop system is constant and the energy can only be added or removed via heat or work.

In order for the theoretical model to replicate the system, certain assumptions must be made. First, the analysis assumes that the calculated energy rates and corresponding parameters are based on averages of temperature, pressures, and flow rates from the actual system. Averages are needed because the pump, in a simplex single cylinder configuration, provides a modulating flow. This modulated flow occurs after a single stroke. Moreover, in theory, the system is assumed to be adiabatic. In this particular case, heat added via the transfer lines and the 200L CLV is ignored. The

only energy crossing the boundary is from the CCD components ($\dot{Q}_{CCD}$), and the electrical heater ($\dot{W}_{electrical}$). Also, energy that is added to the system is removed via the cryocooler, $\dot{Q}_{cryo}$. Table 2.1 outlines the specified variables for the theoretical analysis of the OPP. The detailed circulation loop for the closed-loop CCD cooling

Table 2.1. Design Specifications for CCD Cooling System [8]

200L CLV Average Pressure: 110 [kPa]
GN2 Generator Average Pressure: 155 [kPa]
LN2 Temperature: 77 [K]
Volumetric Efficiency (LN2/GN2): 100%
Swing Check K_L: 2
Globe Valve K_L: 10
Elbows K_L: 0.7
Length of Flexible hosing: 31 [m]

system can be found in *Thermodynamic and Transport Conditions in Nitrogen Circulation Loop*[21]. The flow coefficients were determined both from the manufacturer as well as in the *Fundamentals of Fluid Mechanics*[7]. The volumetric efficiency of the LN2 to GN2 volumetric flow rates (injection and discharge) in a theoretical positive displacement pump is 100%. In other words, this states that for every liter of GN2 injected into the PC, it will displace and equal amount of LN2. This simply states compressibility effects of the GN2 can be ignored. This was determined experimentally due to almost negligible compressibility effects (i.e. compressibility factor ranges between 98-99 for different refill times).

The following figure was cropped by varying only the $\dot{V}_{GN2,injection}$. The saturation pressure of the GN2 generator was fixed at 155 kPa due to the high volumetric expansion ratios associated with lower pressures as compared to higher pressures. Further discussion of the importance of the expansion ratio can be found in the Appendix D. Also, pump work, as seen in Equation 2.1 is determined by utilizing fluid

dynamic equations and constants. Figure 2.2 shows a contour plot using the mul-

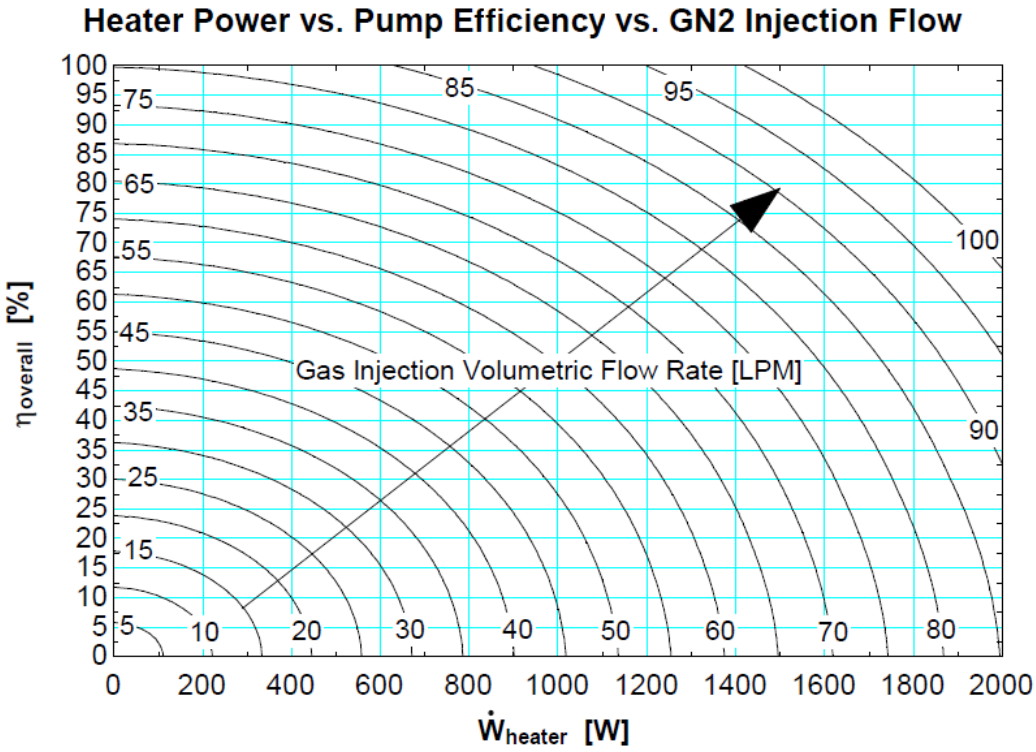

Figure 2.2. Heater Power versus Pump Efficiency versus GN2 Injection Volumetric Flow Rate

tiquadric radial basis function. It uses a function to fit the data according to the GN2 injection volumetric flow rate contours. This figure shows that as the GN2 injection volumetric flow rate increases, so does the heat needed to vaporize the LN2 within the GN2. Moreover, as the heater input decreases along a GN2 contour line, the efficiency increases. The overall efficiency is governed by Equation 2.4. In order to navigate this graph, the efficiency and heater power must be specified. However, given the current differential pressure drop of the current CCD cooling line, an orifice must be added to prevent the pump from operating with insufficient head pressure, which implies the pump work is too low for the designated efficiency.

In order to traverse upward along the constant GN2 injection flow rate contours, an orifice can be installed. This increases the efficiency by increasing the

differential pressure across the pump and lowering the heater power proportionally. A small diameter orifice plate allows the pump to work more (see Eqs. 2.4, 2.5, 2.6, and 2.7). Furthermore, to traverse vertically along the y-axis for a constant heater input, a small decreasing diameter orifice plate can be used to work the pump. Additionally, to traverse the graph horizontally at constant efficiency, an orifice plate can be used and adjusted accordingly to an increasing heater input. Therefore, in order to control where the pump operates an adjustable valve or an orifice plate can be used to regulate the flow accordingly, which would directly change the pump work. Also, the heater power can be changed accordingly.

In conclusion, the theoretical pump model is a simple concept. Given the proper assumptions of the pump, the model can be implemented into a system model to determine the operational points for different flow rates. This theoretical model uses Equations 2.1-2.7 to generate Figure 2.2. The only difference between the OPP and a centrifugal pump, in theory, is the addition of a thermal efficiency term that contributes to the overall pumping efficiency, Equation 2.6. This term provides the necessary information in designing a heating element for optimal heat transfer.

2.4 Defined Operating Characteristics

Due to the similarity between direct acting PD pumps and the OPP, the operating characteristics that describe direct-acting pumps can also be used to describe the OPP. Thus, the mechanical efficiency, volumetric efficiency, stroke, slip, and plunger speed are some of the terms that are used. This section will compare the trends and equations related to a direct acting pump as discussed in *Reciprocating Pump* [14].

The cryogenic over-pressure pump (OPP), for simplicity, is similar to a simplex, single-acting, reciprocating power positive displacement pump without the stuffing box and other mechanical components, seen in Figure 1.6. This implies that the drive end gas will be in direct contact with the liquid end. Still, the modulating flow

seen in a simplex, single-acting, direct-acting pump can also be observed in the OPP. In a simplex, single-acting, direct-acting pump, the drive piston only displaces liquid in an extension and not a retraction. A double-acting direct-acting pump implies that any extension or retraction of the drive piston displaces a liquid volume. Therefore, the OPP will suffer from a discontinuous flow as partly seen in the following figure.

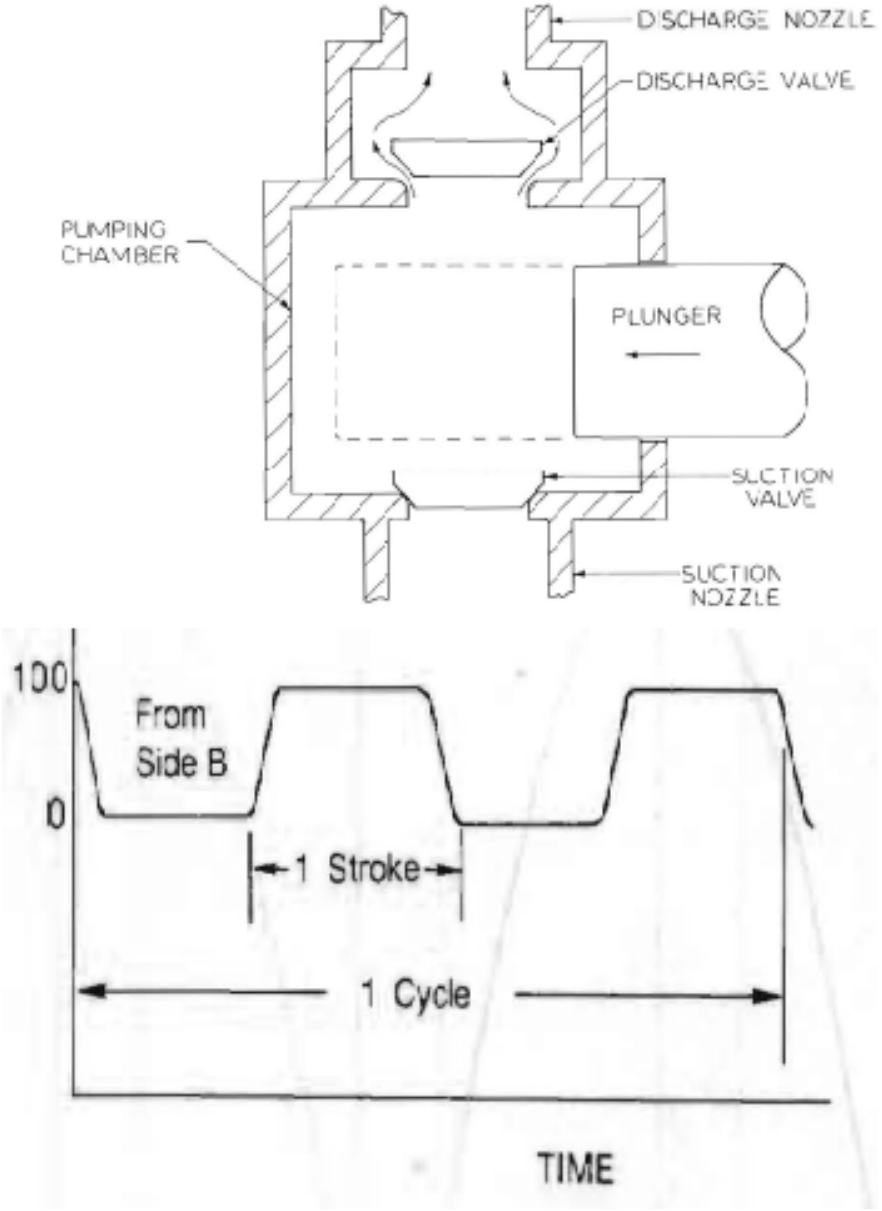

Figure 2.3. Top: Liquid end of Simplex, Single-Acting, Reciprocating Pump. Bottom: Flow Velocities of a Simplex, Single-Acting, Direct-Acting Pump [14]

The bottom of Figure 2.3 shows the percent maximum flow velocity versus time. Notice the acceleration at the beginning and end of a single stroke. As the plunger enters the fixed cylinder volume, it discharges the liquid volume through the discharge nozzle; the velocity of the fluid exiting the chamber reaches the maximum velocity until the end of the stroke. At the end of the stroke, the velocity is zero until the plunger is fully retracted. While the plunger is retracted, liquid begins entering through the suction nozzle. The OPP operates slightly different than this type of piston pump; the plunger is replaced by gas and the filling operation occurs via gravity. Notice, that a plunger or piston perform the same task of displacing a fluid volume. The next aspect of a direct-acting pump is its mechanical efficiency.

The mechanical efficiency of a direct acting pump is simply the ratio of the liquid to drive end piston areas multiplied by the ratio of the liquid to drive end differential pressures. The OPP mechanical efficiency is slightly different. It is defined as the required fluid work to pump liquid through the transfer lines to the drive gas work into the process cylinder, see Equation 2.5. The reason for this difference in mechanical efficiencies is the OPP is expected to operate in a closed loop system, where the mechanical work associated with drive fluid is needed for an overall heat load analysis. If the OPP operates in an open loop fashion, then the following equation will be used to define the mechanical efficiency.

$$\eta_m = \frac{A_L}{A_{dr}} \cdot \frac{\Delta P_L}{\Delta P_{dr}} \tag{2.10}$$

Where A_L is the liquid plunger area, A_{dr} is the drive end plunger area, ΔP_L is the liquid end differential pressure, and the ΔP_{dr} is the drive end differential pressure. The next equation shows the definition for stroke length.

$$L = \frac{V_{fluid}}{A_L} \tag{2.11}$$

Where L is the stroke length, V_{fluid} is the volume of the fluid, and A_L is the cross sectional area of the pumping chamber of the liquid end. Finally, the last PD characteristic to be discussed is the plunger speed. This next equation provides an estimate of the service life of the pump [14].

$$S_p = 2 \cdot L \cdot N \tag{2.12}$$

Equation 2.12 contains parameters in determining various other characteristics of the pump. For example, it can be used to determine the velocity of liquid flowing through a valve opening. Additionally, it is used to determine the gas consumption rate for industrial direct-acting pumps.

In conclusion a simplex, single-acting, direct-acting pump is similar to the basic operation of the OPP. The major differences between the two is the stuffing box and the various mechanical components that are used in a simplex, single-acting, direct-acting PD pump. Likewise, many similarities between these pumps can be made through the equations that describe their performance. Equations 2.10-2.12 are used to outline areas of enhancing the performance, which can also be used in describing the performance of the OPP.

CHAPTER 3

EXPERIMENTAL SETUP

The test in Lab A was completed over a three day period in February 2012. The primary goal of the test is to determine whether an assembled OPP can cool the multi-CCD (MCCD) test vessel in SiDET Lab A building at Fermi National Accelerator Laboratory (FNAL). This test vessel is vacuum sealed; its primary components are bayonet connections for the transfer lines, focal plate, and copper braids with resistance heaters. The MCCD vessel is stationed on a cart that is on ground level. Supply and return transfer lines are routed from the MCCD test vessel indoors to the 200L CLV outside Lab A. This can be seen by the following figure.

Figure 3.1 shows the MCCD test vessel inside Lab A and the CCD cooling system. The CCD cooling system provides LN2 to the MCCD focal plate. Various resistance temperature detectors (RTDs) are recorded in heater data files. Additionally, the flow rates, pressures, and temperatures required for the test are recorded in the cooling data files in the FNAL Dark Energy Survey document database. All files will be analyzed using Matlab 7.10.0.499 (R2010a), Engineering Equation Solver (EES) V8.874-3D, or Microsoft Excel (V. 14.0.6112.5000 (32-bit)).

The OPP is composed of three major components: GN2 generator, process cylinder (PC), and solenoid valves (SV). In order to fulfill the objective of cooling the focal plate, the OPP was partially tested in a quasi-closed loop test. The PC was designed and installed with the SVs. The GN2 generator was replaced by a 160L low pressure CLV. This low pressure CLV supplies the LN2 to a vaporizer. This vaporizer generates the needed GN2 to displace the LN2 within the PC for cooling the CCD focal plate. The 160L low pressure CLV and the GN2 injection tubing is meant to

Figure 3.1. MCCD Test Vessel (left) and the Closed-Loop CCD Cooling System (right)

serve as the GN2 generator. Additionally, the OPP was tested in a quasi-closed loop CCD cooling system. This implies that the GN2 injected and generated into and within the system was released to atmosphere after a discharge (40s) and a delay (15s).

Finally, it is imperative to note that a previous OPP test conducted, in the CCD cooling system at FNAL near Lab A, indicated that the OPP would not operate closed-loop (see *DECam LN2 Over-Pressure Pump Process Cylinder Testing Dec. 20-22, 2011*[1]. This was a result of the pressure within the 200L CLV rising significantly than that which can be controlled via a regulator during the discharge time of 40s. The cryogenic refrigerator could not reduce the pressure of the 200L CLV quickly

enough. Additionally, the process cylinder (PC) had difficulty filling as well. This was indicated via a liquid level probe. Modifications to the prototype CCD cooling system at FNAL were limited as it was a test facility for other prototype and modified pumps.

3.1 Experimental Objectives

The process cylinder is tested in a quasi-closed loop (QCL) cooling system, which is the modified equivalent of the CTIO CCD cooling system in Chile. The primary difference between the QCLCS and the CCD cooling system is that the QCLCS is operated in open loop and it has one cryogenic refrigerator. That is the GN2 injected into the PC will be ejected to atmosphere, to lower the pressure in the 200L CLV to its initial conditions and refill the process cylinder. Previous tests conducted in December 2011 indicated failures in filling the PC and regulating the 200L CLV in a closed-loop. Further discussion of this topic can be found in *DECam LN2 Over-Pressure Pump Process Cylinder Testing Dec. 20-22, 2011* [1].

The objectives of the process cylinder test can be seen in the following list.

1. Cool the focal plate down to 173K using the quasi-closed loop CCD Cooling system
2. Attain a correlation of the average flow rates of the injection and discharge ports of the PC.
3. Determine the LN2 loss per hour from the 200L cryogenic liquid vessel.
4. Determine the number of cryocoolers needed to operate the system closed loop in Lab A.
5. Determine the amount of LN2 passing through the transfer lines.

The first objective in the list will show that the OPP is capable of cooling the focal plate to 173K. Therefore, it would be considered as a successful alternate design that requires further study. Completing this objective will prove the fundamental concept of the OPP is significant. Furthermore, the OPP is a simplified design of a simplex, single-acting, direct acting pump seen in Figure 2.3. Moreover, meeting this objective will show the process cylinder refilling and discharging. The cooling of the focal plate will be seen in the RTD data files that are recorded. Furthermore, the refilling and discharging processes are captured in the liquid level sensor data file. The second objective is meant to determine the required GN2 that is needed to displace LN2 within the process cylinder. From this information, various GN2 injection flow rates can be extrapolate from this curve. It is a special characteristic flow rate curve of the PC. The general form of the correlation can be seen in the following equation.

$$\dot{V}_{injection} = \dot{V}(\dot{V}_{discharge}) \tag{3.1}$$

Where $\dot{V}_{injection}$ is the GN2 volumetric flow rate into the PC and $\dot{V}_{discharge}$ is the LN2 volumetric discharge flow rate exiting the PC. The third objective is to calculate the overall efficiency of the OPP. This efficiency encompasses the mechanical and thermal efficiency, as seen in Equations 2.4-2.6. A more detailed form of Equation 2.4 is shown in Equation 3.2.

$$\eta_I = \eta_{pump} = \frac{\dot{W}_{pump}}{\dot{Q}_{in}} = \frac{\dot{V}_{discharge}\Delta P_{discharge}}{\dot{V}_{injection}\Delta P_{injection}} \frac{\dot{V}_{injection}\Delta P_{injection}}{\dot{Q}_{in}} \tag{3.2}$$

Where $\dot{Q}_{in}$ is the heat input via the vaporizer, $\Delta P_{injection}$ is the differential pressure of the GN2 injection line, and $\Delta P_{discharge}$ is the differential pressure of the transfer lines to and from the MCCD test vessel. Recall that the electrical efficiency in theory is assumed to be 100%. Thus, the vaporizer heat input in the experimental

setup can be equated to the heat input via an electrical heater. The fourth objective is needed to determine the number of cryogenic refrigerators required to operate the system closed loop. A liquid level probe will provide the information. Furthermore, the fifth objective will be revealed in the probe data. The peeks and troughs will be analyzed to determine this.

In conclusions, the objectives are meant to abide by DES demand for an alternate pump design. Therefore, the primary goal is to cool the focal plate by any means possible. All other objectives are secondary. The OPP in the experiment is only composed of two of three primary components: process cylinder and solenoid valves. The heater size of a future GN2 generator can be determined from this experiment via heat input from the vaporizer. Additionally, the design of the GN2 generator (i.e. dimensions, materials, etc.) will have a similar function to the PC, but discharge GN2 and contain a submerged heater. It will also need to be refilled via gravity.

3.2 System Diagram: Quasi-Closed Loop CCD Cooling System

The control sequence that governs the pump operation consists of a delay, fill, and discharge. The delay allows the process cylinder pressure to equalize its pressure with the tank prior to a fill. A fill operation allows LN2 to enter the process cylinder. Furthermore, the discharge operation uses GN2 to displace LN2 out of the PC to cool the focal plate. Figure 3.2 shows the basic instrumentation used in the experiment. Figure 3.3 shows the process during the discharge of the PC. The last diagram, Figure 3.4 shows the process during the refill of the PC.

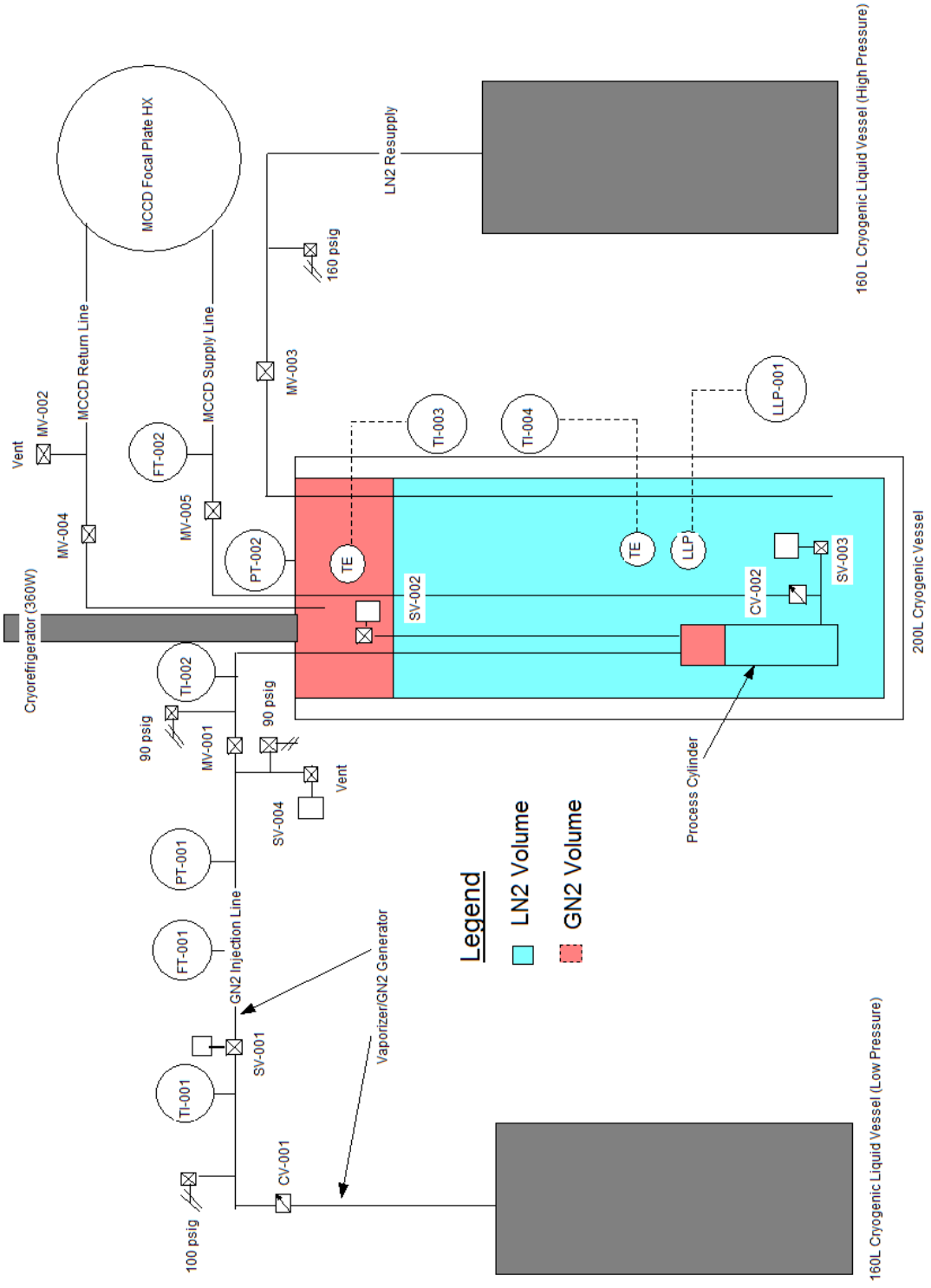

Figure 3.2. Experimental Setup and Instrumentation: General Diagram

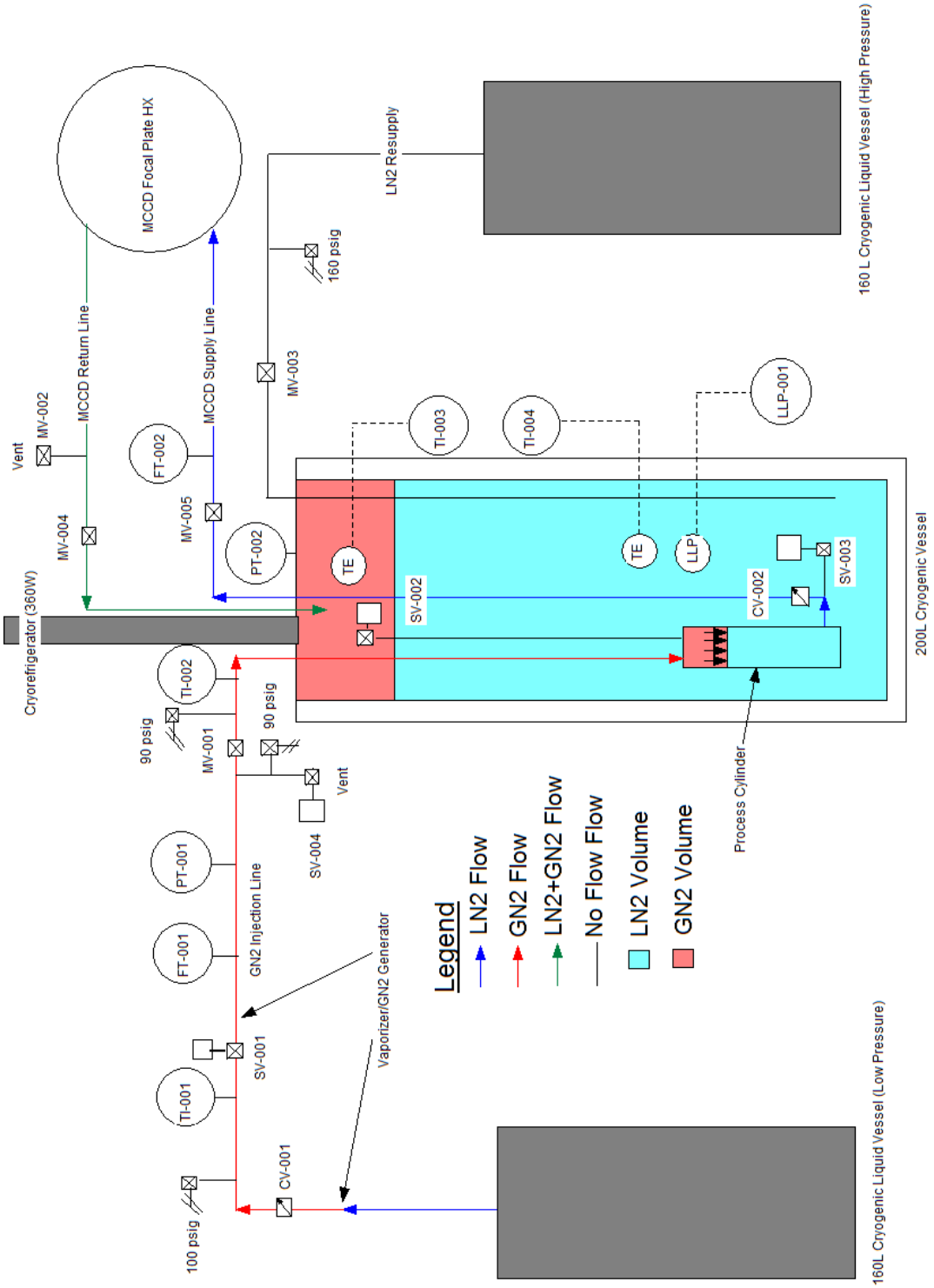

Figure 3.3. Experimental Setup and Instrumentation Discharge

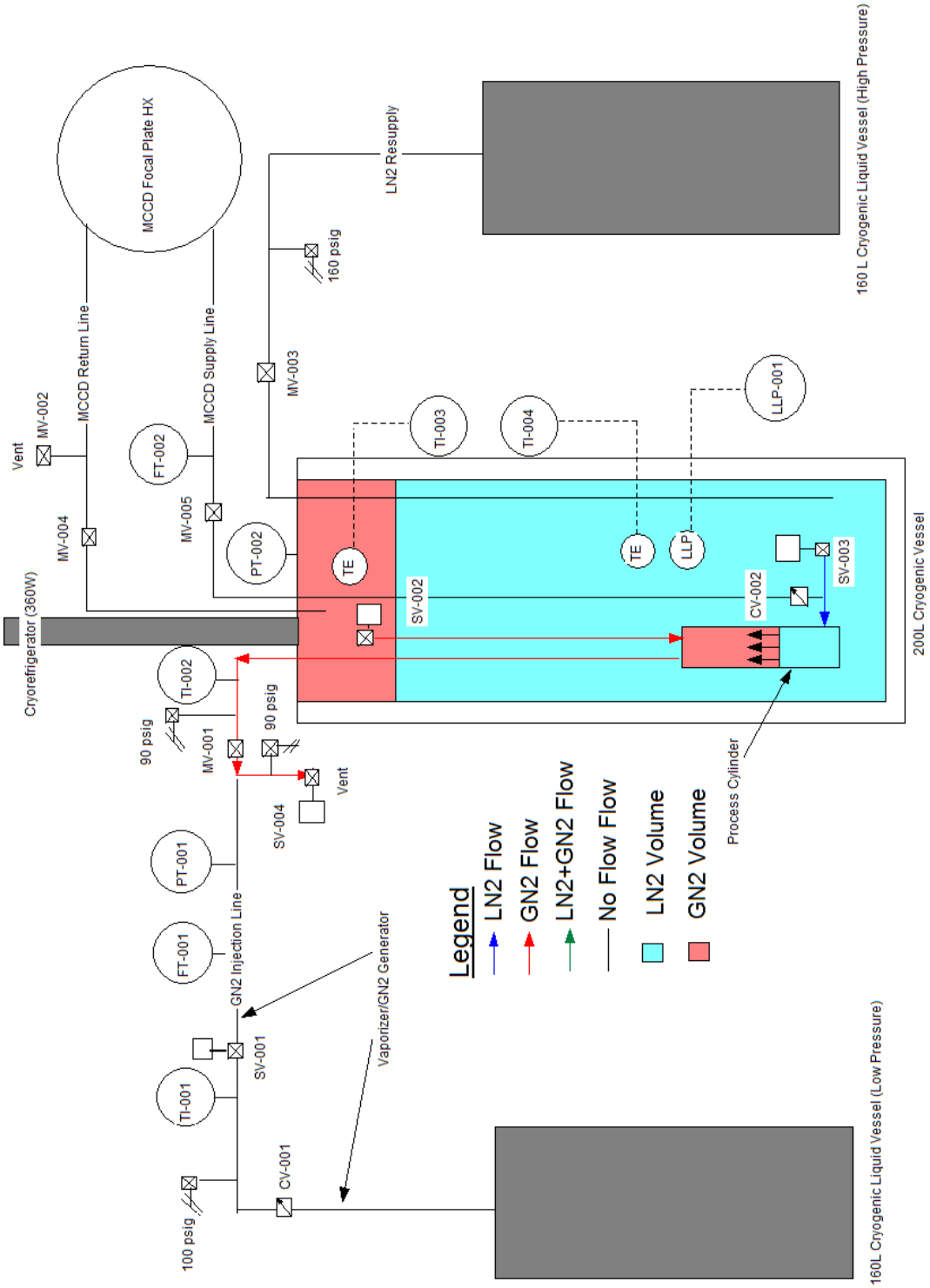

Figure 3.4. Experimental Setup and Instrumentation: Refill

The process and instrumentation diagram seen in Figures 1.1 and 1.2 is similar to Figure 3.2. The primary difference is that in the cryogenic OPP test, it was necessary to operate the pump in quasi-closed-loop instead of a closed-loop. The reason for not installing the OPP in the closed-loop prototype CCD system at FNAL was the difficulty in regulating the 200L CLV pressure, which contributed to the inability to refill the PC (see *DECam LN2 Over-Pressure Pump Process Cylinder Testing Dec. 20-22, 2011*[1]). Figure 2.1 shows the instrumentation needed to meet the objectives specified in Section 3.1. TI-001 temperature measurements are used in adjusting the output flow rates from FT-001. TI-001-TI-004, and PT-001 and PT-002, are used to estimate thermodynamic properties. Additionally, LLP-001 is used to measure the volume of LN2 within the 200L CLV. The cryogenic refrigerator is used to assist in regulating the pressure via condensing GN2 within in the 200L CLV. A 160L low pressure CLV is needed to supply LN2 to the vaporizer. A 160L high pressure CLV is required to resupply LN2 to the 200L CLV. The resupply of LN2 only occurs after each test run. The next figure shows the process of discharging the PC.

The discharge process involves utilizing the generated GN2 from the vaporizer to displace LN2 from the PC (see Fig. 3.3). Notice the blue to red arrow on the GN2 injection line. That section of tubing up to the TI-001 is meant to serve as the vaporizer such that the bulk fluid temperature is above the saturation temperature of the fluid. Any temperature above the critical temperature for nitrogen is always gas. Additionally, the rest of the GN2 injection line serves as sensible heating to add additional energy to the fluid. Once the warm GN2 enters the PC, it begins displacing the LN2 out through the MCCD Supply Line towards the MCCD Focal Plate Heat Exchanger. The returning fluid, the green arrows, is two-phase, which consists of GN2 and LN2. This discharge process occurs for 40s and it remains constant throughout the experiment. This process increases the pressure within the 200L CLV due to the

excess GN2 within the system. Therefore, the pressure within the 200L CLV must return to its initial pressure. This is performed via the refill cycle.

During the refill of the PC the system is open loop, which discharges the gas that has accumulated and generated via the GN2 injection and the system heat loads. Figure 3.4 shows this refill process, which varies from 60s to 120s. During this process, SV-002 to SV-004 are opened. Opening SV-002 relieves the cold GN2 within the tank. Notice that the cold GN2 within the 200L CLV is not only ejected to atmosphere, but also pre-cools the GN2 injection line to a certain degree. Opening SV-003 allows LN2 to flow inside the PC via the hydraulic head pressure. SV-004 allows the excess GN2 pressure to escape from the 200L CLV and the PC.

This next list summarizes the control sequence that govern the process cylinder refill and discharge of LN2.

- Delay Before Fill
  - During a delay all valves are closed (SV-001 to SV-004) and the process cylinder is allowed to reach an equilibrium pressure with the tank. LN2 and GN2 do not flow during this time period.
- Gas Injection or Discharge
  - A discharge of the process cylinder requires that GN2 be injected into the tank to displace LN2. Therefore, SV-001 remains open and SV-002, SV-003, and SV-004, remain closed. In other words, the injected GN2 displaces the LN2 within the PC, which in turn increases the pressure within the 200L CLV.
- Tank Refill

- During a refill of the process cylinder, SV-001 is closed and SV-002 and SV-003 are open. The PC is refilled via the hydraulic head of the LN2 within the 200L CLV. Flow ceases in the GN2 injection line via closing SV-001.

In conclusion, the QCL cooling system is open loop when the PC is refilling with LN2 and relieving the pressure within the 200L CLV. During a stroke, the PC is operated closed-loop. The OPP in the QCL cooling system has three parts to a single cycle. The first is the refill of the PC with LN2. The second is the discharge of the PC to flow the coolant through the MCCD transfer lines. Lastly, the third is the delay, which is used to allow the system to reach equilibrium as well as provide a slight delay between each cycle of the PC. The following section will discuss the instrumentation of the QCL system in more detail.

3.3 Valve and Instrumentation List

Recall that in order to meet the objectives in Section 3.1, pressure, temperature, and flow rates must be measured. Highly accurate instrumentation is used in order to meet those objectives. The following list shows the various instrumentation needed to measure the inlet and outlet flow conditions of the process cylinder. Refer to Figure 3.2 for the location of the following pieces of equipment.

1. GN2 injection Instrumentation
   (a) Solenoid Valve (SV-001 & SV-004)
      i. Vendor: McMaster-Carr
      ii. Catalog #: 4710T12
      iii. Power: 25W
      iv. Operating Range: minimum (-320F/-194C)

(b) Pressure Transducer (0-200 psig)(PT-001)

i. Manufacturer: Setra Sensing Solutions

ii. Model #: 2561-0200P-G-2M

iii. Range: 0-200psig

iv. Accuracy RSS: ±0.25%

(c) Flow Transmitter (FT-001)

i. Manufacturer: Sponsler

ii. Model #: SP3/8-CB-NL-B-4

iii. Range: 0-4 CFM

iv. Accuracy: ±3.5% [4]

(d) Thermocouples

i. Manufacturer: Lake Shore Cryotronics

ii. Model #: PT-103

iii. Range: 14-873 K

iv. Accuracy: ±0.20%

2. LN2 Supply Line

(a) Flow Transmitter (FT-002)

i. Manufacturer: Sponsler

ii. Model #: SP3/8-CB-NL-B-4

iii. Range: 0.75-5gpm

iv. Accuracy: ±0.25%

(b) Tank Pressure Indicator (PT-002)

i. Manufacturer: NOSHOK

ii. Model #: 615-200-1-1-2-6

iii. Range:0-200psig

iv. Accuracy: ±0.25%

(c) GN2 and LN2 Temperature Elements (TI-002 & TI-003)

i. Manufacturer: OMEGA

ii. Model #: PT-103

iii. Sensing Length: 14K to 873K

iv. Accuracy: ±0.25%

(d) Liquid Level Probe

i. Manufacturer: Teragon

ii. Model #: LP7

iii. Sensing Length:0-10FT

iv. Accuracy: $<$ 1% full scale range

3. Process Cylinder

(a) Solenoid Valves (SV-002 & SV-003)

i. Manufacturer: ASCO

ii. Catalog #: 822G003LT

iii. Power: 17.5W

(a) Electrical Cabinet

i. National Instruments Compact Field Point(CFP-1808)

ii. National Instruments CompactRIO (cRIO-9014) (CRIO)

For additional details of the valve and instrumentation, refer to *DECam Over-Pressure Pump Cryogenic Safety Review Documentation* [2]. Firstly, the GN2 injection instrumentation consists of solenoid valves, flow transmitter, and platinum RTDs.

The SVs are used to regulate the amount of GN2 injected into the PC. This type of valve is a direct-acting piston SV. The flow transmitter was calibrated at FNAL to 3.5 % [4]. The temperature, pressure, and flow meter readings will be used to calculate the needed thermodynamic properties for later calculations.

The LN2 supply line contains a flow transmitter, which was calibrated by the manufacturer. Additionally, the pressure indicator and the temperature elements will be used to calculate fluid properties to provide an estimate of the work associated with driving the fluid through the piping system. The liquid level probe (LLP) provides the volume of LN2 within the 200L cryogenic liquid vessel (CLV). The LN2 volume will be used to estimate the liquid loss and the flow rate of LN2 into the process cylinder (PC).

Finally, the PC is a welded assembly of 316 SS tubing and piping. The dimensions and description of the PC will be discussed in a later section. The PC provides the pumping volume for the OPP. It has a total of three ports. The first port is used to supply the GN2 into the PC. The second port relieves the GN2 within the PC. Finally, the third port discharges the LN2 as well as supplies LN2 into the PC, refer to Figure 3.2.

In conclusion, the instrumentation listed above are necessary to meeting the objectives discussed in Section 3.1. Pressure, temperature, and flow rates will be used to determine the fluid and thermodynamic properties of the system. Additionally, the liquid level probe (LLP) is used to determine the exact volume of LN2 within the 200L CLV. The entire list of the instrumentation can be found in the Appendix C. The next section discusses the pump priming of the OPP.

3.4 CCD Cooling System Cool Down and Pump Priming

Prior to testing the pump, it was necessary to cool the focal plate down to 173K

and allow the OPP to maintain the temperature of the focal plate. The copper braids used to assist in cooling the focal plate to 173K via conduction heat transfer also have individual heaters. The CCD focal plate heater control will remain operational during the test.

First, the 200L vessel must be filled with LN2 before pumping can commence. This requires at least two 160L high pressure cryogenic liquid vessels. One is used to cool the 200L cryogenic vessel and the components inside. The second one is used to fill the 200L vessel and maintain the liquid level as the focal plate is cooled down. Likewise, the LN2 supply for the 200L vessel comes from a high pressure 160L cryogenic liquid vessel, see Figure 3.2. During the priming process, the high pressure 160L cryogenic liquid vessel is connected to the fill line and MV-002, MV-003, SV-002, and SV-003, are opened and MV-001 and MV-004 are closed. This valve arrangement allows one to generate a differential pressure through the high pressure cryogenic supply vessel, through the process cylinder, out to the focal plate and out to atmosphere. This cool down process prevents the LN2 from vaporizing within the transfer lines to and from the focal plate, which can result in a vapor lock.

Once the 200L vessel and the transfer lines are cool, it necessary to pre-cool the GN2 injection line. This is performed by first closing MV-001 to shield the process cylinder form the warm gas. Secondly, SV-001 and SV-004 solenoid operated valves will be opened. This allows the low pressure 160L cryogenic liquid vessel to pass cold gas through the injection line and out to atmosphere. Once this is completed, the LabView process cylinder valve control program may begin. It is necessary to allow the CCD cooling system to reach a steady pumping state. This is where the temperatures, pressures, and flow rates of the CCD cooling system oscillate repeatedly or remain relatively constants.

3.5 Process Cylinder Engineering Drawing

The over-pressure pump (OPP) requires three major components. The first is the process cylinder or pumping chamber. The second is the GN2 generator. Lastly, the third is the arrangement of solenoid valves used to control the refill and discharge of the PC. This sections will discuss the simple design of the process cylinder.

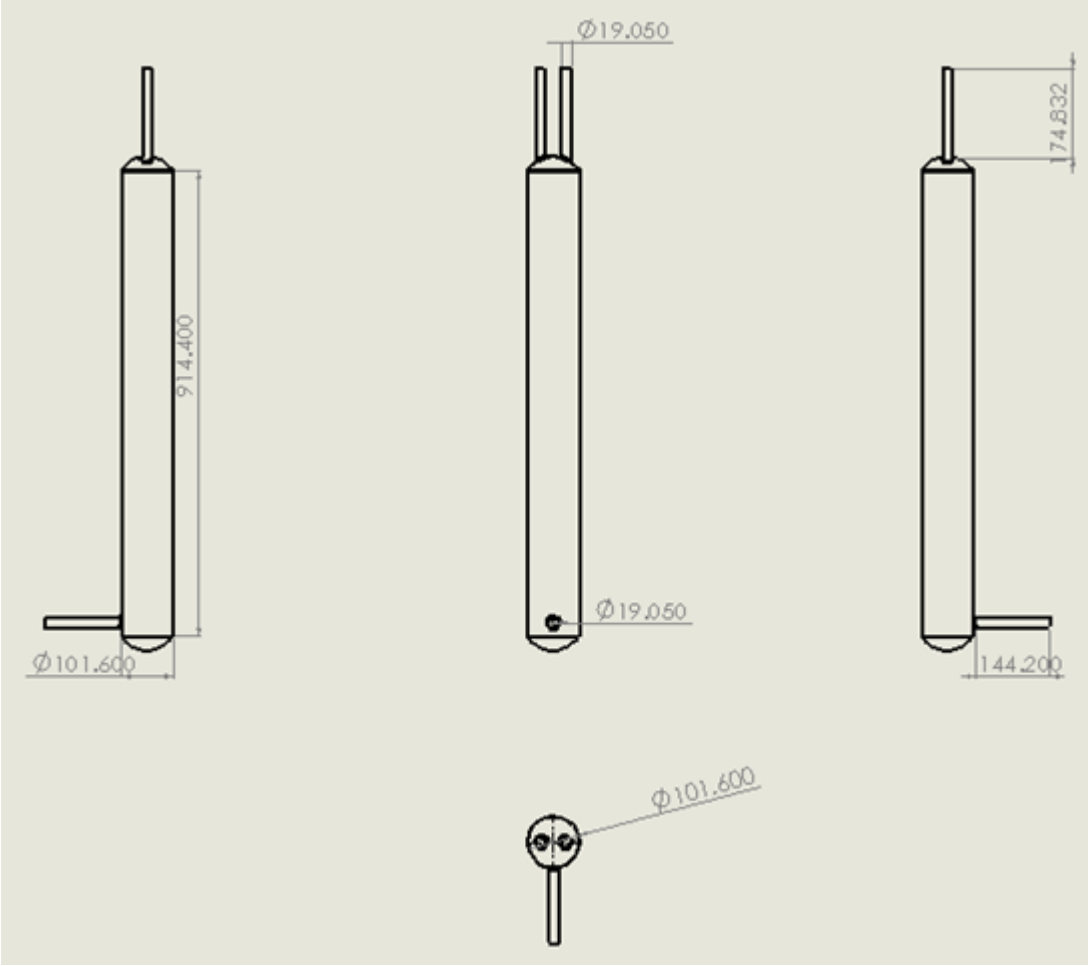

Figure 3.5. Process cylinder Dimensions (Units in millimeters)

The two ports at the top of the process cylinder in Figure 3.5, represent the GN2 injection and exit port for the GN2 within the process cylinder. When the liquid level is above 65.5% the GN2 injection port simply enlarges the refill orifice size from 19mm to 48mm. The port at the bottom of the process cylinder is used to discharge

LN2. Also, it is used to refill LN2 due to a T-joint between the supply line to the MCCD and the refill solenoid valve SV-003, as seen in Figure 3.2 This cylinder has a total volume of 6.79L (1.75gal). The construction of the PC consists of the following components.

Construction Components

1. Tubing Sanitary, 4" OD
   (a) Material: 316L Stainless Steel
   (b) Length: 3 ft
   (c) Maximum Pressure: 1000 psig
   (d) Wall Thickness: 0.083"
   (e) Item #: 2FGG6
2. Cap, 4", Butt Weld
   (a) Material: 316L Stainless Steel
   (b) Item #: 1RUB1
3. Hose Clamps
   (a) Material: 301 Stainless Steel, 201 Stainless Steel, Zinc-Plated Steel
   (b) Minimum/Maximum Diameter: 4"/6"
   (c) SAE number: 88
   (d) Item #: 2PA75
4. Standard-Wall Stainless Steel Threaded Pipe Nipples and Pipe
   (a) Material: 316 Stainless Steel
   (b) Pipe size: 3/4"

(c) Length: 18”

(d) Maximum Pressure: 150 psig

(e) Item #: 4816K125

3.6 Data Acquisition

Once all the instrumentation and the process cylinder are installed in to the quasi-closed loop CCD cooling system at FNAL, the data must be attained using the following steps. The software used to acquire the data as well as control the solenoid valve sequence is LabView 2010 V10.0 (32-bit). The data acquired as a result of this section is stored in cooling and heating data files within the LabView program directory.

1. Complete the steps in Section 3.4 to cool the focal plate to 173K. The transfer lines must be pre-cooled as well.

2. Turn on the computer and start LabView Thermal-pump-cooling control _v9_PC_LV2010.vi

   (a) Set sample rate to 2Hz

      i. Thermal-pump-cooling control _v9_PC_LV2010.vi>LN2 Front Panel> Data log loop time(s)

3. Go to Heater_LVPID_Test_V10LV2010.vi on the Windows XP taskbar

   (a) Change Data second=1

4. Adjust timing sequence of solenoid valves to the following

   (a) Delay before fill (D): 15s

   (b) Refill first tap: 0s

(c) Tank Refill Seconds (R): *set*

(d) Gas Injection Seconds (I): 30

5. Turn on timing solenoid push button in LabView graphical user interface

   (a) Thermal-pump-cooling control_v9_PC_LV2010.vi >LN2 Front Panel> timing solenoids (ON)

6. Allow the GN2 injection line as well as the 200L vessel tank pressure to reach a steady and repeatable pattern before collecting data

7. Collect Data by recording the start time

   (a) Runtime for cycle 'n'

   (b) n=(D+R+I) minutes, where n is the number of cycles

8. Change flow meter readout of the LN2 supply line with GN2 injection line

9. Repeat 7 for FT-001 flow meter

10. Adjust the Tank Refill Seconds time for different fill times of the process cylinder and repeat 4, 6, 7, 8, and 9 for four different refill times

11. Once data has been collected for four different refill times turn off the following

    (a) Timing solenoids

        i. Thermal-pump-cooling control_v9_PC_LV2010.vi > LN2 Front Panel > timing solenoids (OFF)

    (b) Over-pressure pump

        i. Turn off rank power to place the CCD cooling system in a safe mode.

In summary, the original CTIO cooling control file is modified for the OPP quasi-closed loop (QCL) cooling system. The sample rate of the cooling related data

is set to 2 Hz. The solenoid valve timing sequence delay before fill, refill first tap, tank refill seconds, and gas injection seconds are set to constant values. Delay before fill, tank refill seconds, and gas injection seconds are associated with the previously discussed delay, fill, and discharge. The following subsection discusses the LabView graphical user interface (GUI).

3.7 LabView Graphical User Interface (GUI)

National Instruments LabView 2010 Version 10.0 (32-bit) is used to collect the temperature, pressures, and flow rates required for this experiment. The graphical user interface (GUI) was previously created and modified slightly to add additional pressure and temperature gages at the inlet of the process cylinder. Furthermore, the solenoid timing sequence was designed to actuate the solenoid valves via relay switch control. The following image shows the layout of the GUI of the "LN2 Front Panel.vi."

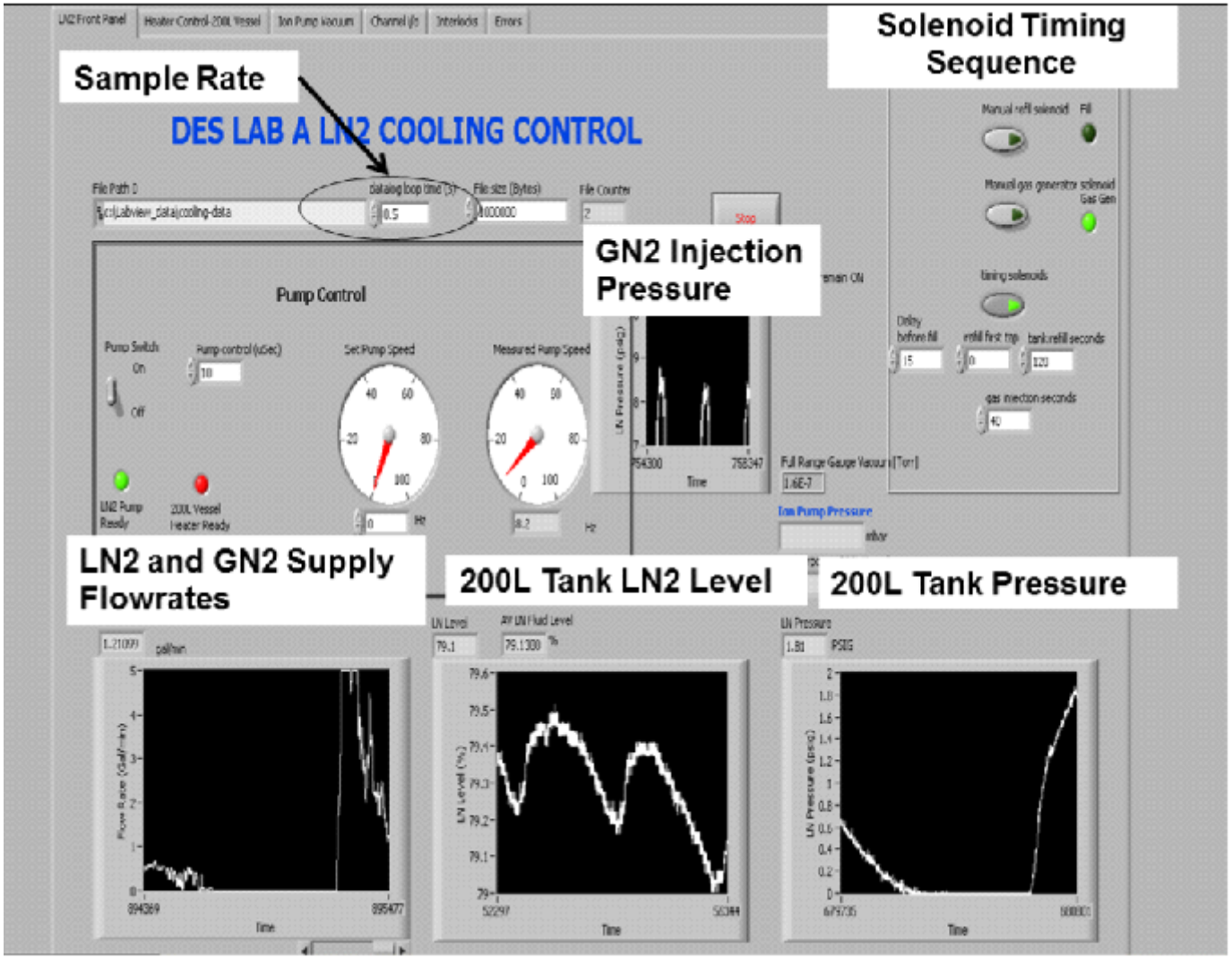

Figure 3.6. LabView LN2 Front Panel.vi

Figure 3.6 displays the "LN2 Front Panel.vi." During the test of the over-pressure pump, the LN2 and GN2 supply flow rates, liquid level, and tank pressure were referenced periodically. The dynamic plots seen at the bottom of the window are used to indicate stable and repeatable data. The location, file size, sample rate, and file count for the cooling data files are listed near the top of the screen under the title of the window. All dynamic plots are sampled at one hertz. Additionally, the values collected and stored in the data cooling files are sampled at two hertz.

The solenoid timing sequence box, seen at the top right of the window, allows for adjusting the three major timing schemes, delay, refill, and discharge, of the process cylinder solenoid valves. The delay and discharge times, in this test, remain constant. The only variable that does change is the refill time. The timing solenoid push button activates the solenoid sequence. When the solenoid sequence is off the refill and gas generator solenoid valves can be manually controlled. Typically, the manual push buttons are not utilized unless the gas injection line is required to be cooled due to the radiation heat transfer into the system.

The next GUI "Heater_LVPID_Test_v10_LV2010.vi" is the focal plate temperature control panel. The following window displays the various RTDs and voltages related to the CCD focal plate. Additional details of the GUI can be found in *Imager Cooling Operations, User Manuals, LabView VI* [9].

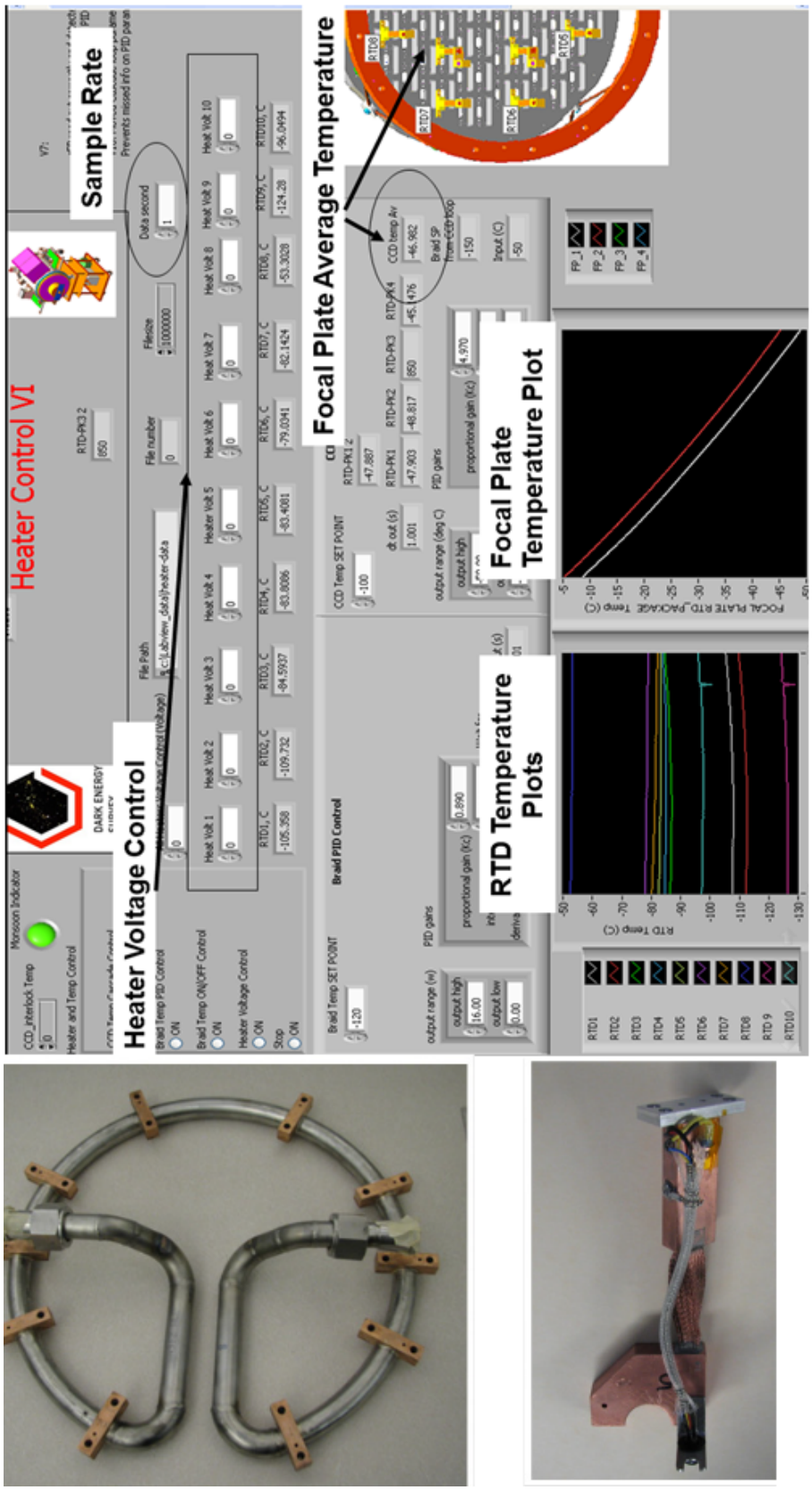

Figure 3.7. Top: LabView Heater GUI. Bottom left: LN2 Focal Plate Heat Exchanger. Bottom Right: Copper Braid

Figure 3.7 displays the focal plate resistive temperature detectors (RTDs) and heater voltages. A total of ten copper braids attach to the focal plate from a 'horse-shoe' like heat exchanger. Each copper braid acts as a thermal conductor, as well as, a heater to regulate the temperature of the focal plate. In other words, the heating function of the copper braid adds additional temperature control of the focal plate. Each copper braid is outfitted with a 16W heater. The heating voltages are listed as 'Heater 1' to 'Heater 10'. The temperatures of the copper braids are listed below the heater voltage control as RTD1-RTD10. A proportional-integral-derivative (PID) controller is used to regulate the temperature of the focal plate. As the focal plate temperature nears 173K, the feedback loop turns on to activate the heaters. Therefore, the heating elements on the copper braids begin warming the focal plate in and around 173K. This control loop maintains the temperature within ± 0.25K [8].

Similar to the "LN2 Front Panel.vi," the location, file size, sample rate, and file count for the cooling data files are listed near the top of the screen under the title of the window. Also, the dynamic plots of the RTDs and the average temperature of the focal plate can be seen at the bottom of the GUI. A cooling trend of the copper braids and focal plate RTDs are typically a negative slope. Additional details of the GUI can be found in DES document database *Imager Cooling Operations, User Manuals, LabView VI* [9].

CHAPTER 4

DATA

This particular chapter describes and displays the data from February 17 & 21 2012. The over-pressure pump (OPP) utilizes three different time delays that control the overall function of it. The data is collected in two separate data files. The 'coolingdata_201202' data files store temperature, pressure, and flow rates that correspond to the cooling action of the CCD cooling system. In addition, the 'heater-data20120217T11' data file corresponds to temperature readings on the focal plate and copper braids. Also, the voltages applied to the heaters on the copper braid are stored in this file. This chapter displays the data from multiple different process cylinder refill times. Below shows an image of the solenoid valve control in LabView.

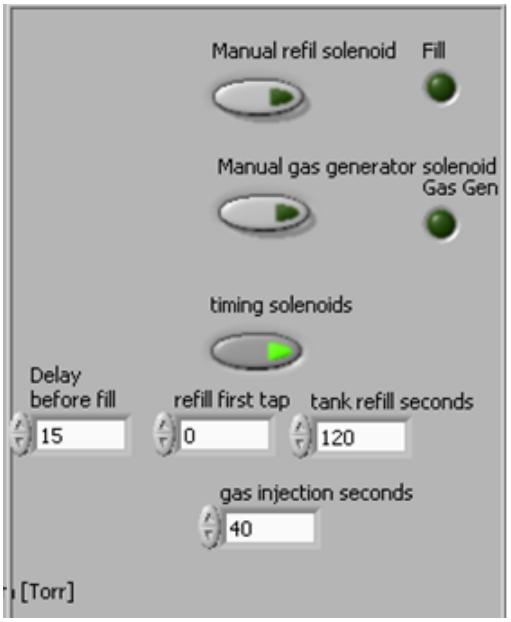

Figure 4.1. LabView GUI Solenoid Timing Sequence Box

Finally, the cryogenic over-pressure pump (OPP) was installed in an existing prototype system. Therefore, modifications to cater towards the OPP could not be

made because other pumping tests were being conducted. Previous tests of the OPP indicated that the CCD prototype cooling system was unfit to operate the pump closed loop. Therefore, the system was operated in the new quasi-closed loop cooling system, where the GN2 pressure in the 200L CLV is vented to atmosphere. This was needed to maintain the pressure within the tank at a relatively constant pressure. The data presented in this section is meant to depict the trends expected for an over-pressure pump.

4.1 Delay Before Fill, Tank Refill, and Gas Injection

The over-pressure pump timing sequence, as seen in Figure 4.1, is required to properly control this positive displacement device for its optimal performance. A three part cycle is used in the test, which was conducted in February 2012. Each time delay serves a particular function in the overall operation of the pump, which can be seen in the figures below.

The first part of the cycle is the discharge. A discharge corresponds to GN2, or the drive fluid, being injected into the PC to displace the LN2. During this discharge process LN2 begins flowing through the MCCD transfer lines. The LN2 enters as single phase fluid and exits as a two phase fluid with a fraction of it being GN2. During this part of the cycle, both the drive fluid, GN2, and the process fluid, LN2, are flowing through the system. Also, this part of the cycle is conducted as closed-loop.

The second part of the cycle, is a called a delay before fill. This part is typically fifteen seconds, as is allows the system to equalize in pressure, as well as provide a clear distinction between each cycle. Because the system operates in a quasi-closed loop cooling system, the delay is short. In an ideal system, the delay before fill will be greater than the tank refill seconds (see Fig. 4.1). For the ideal operation of the OPP, the delay is longer to allow the cryogenic refrigerators to condense the gas generated,

via the GN2 generator. Finally, the gas injection timing sequence encompasses the GN2 injection to displace the LN2 out of the process cylinder. Each aspect of the solenoid timing sequence will be described and correlated to the raw data taken on February 17, 2012. The times associated with a discharge, delay, and refill are 40s, 15s, and 100s for these following figures.

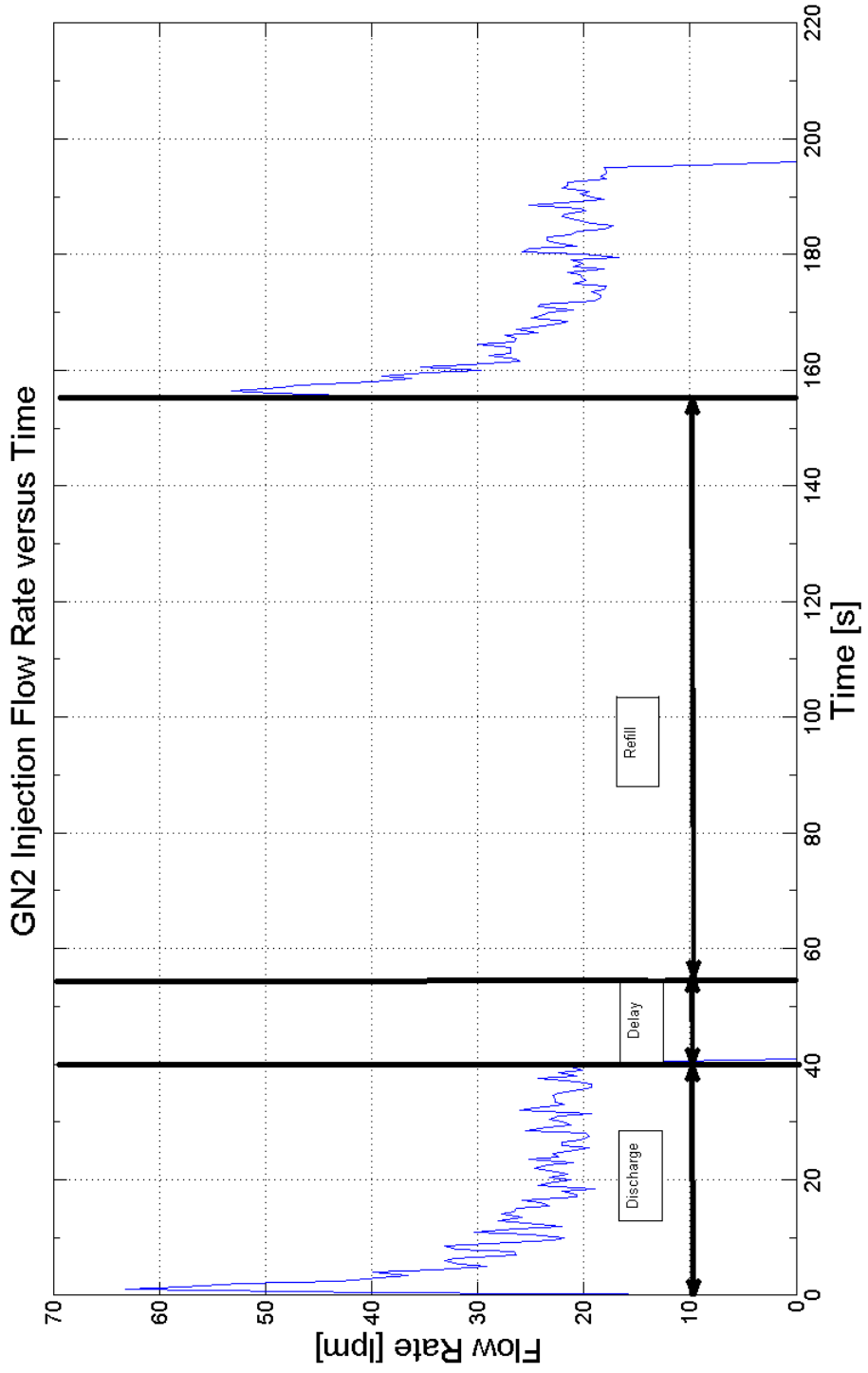

Figure 4.2. GN2 Injection Flow Rate vs. Time (Refill=100s)

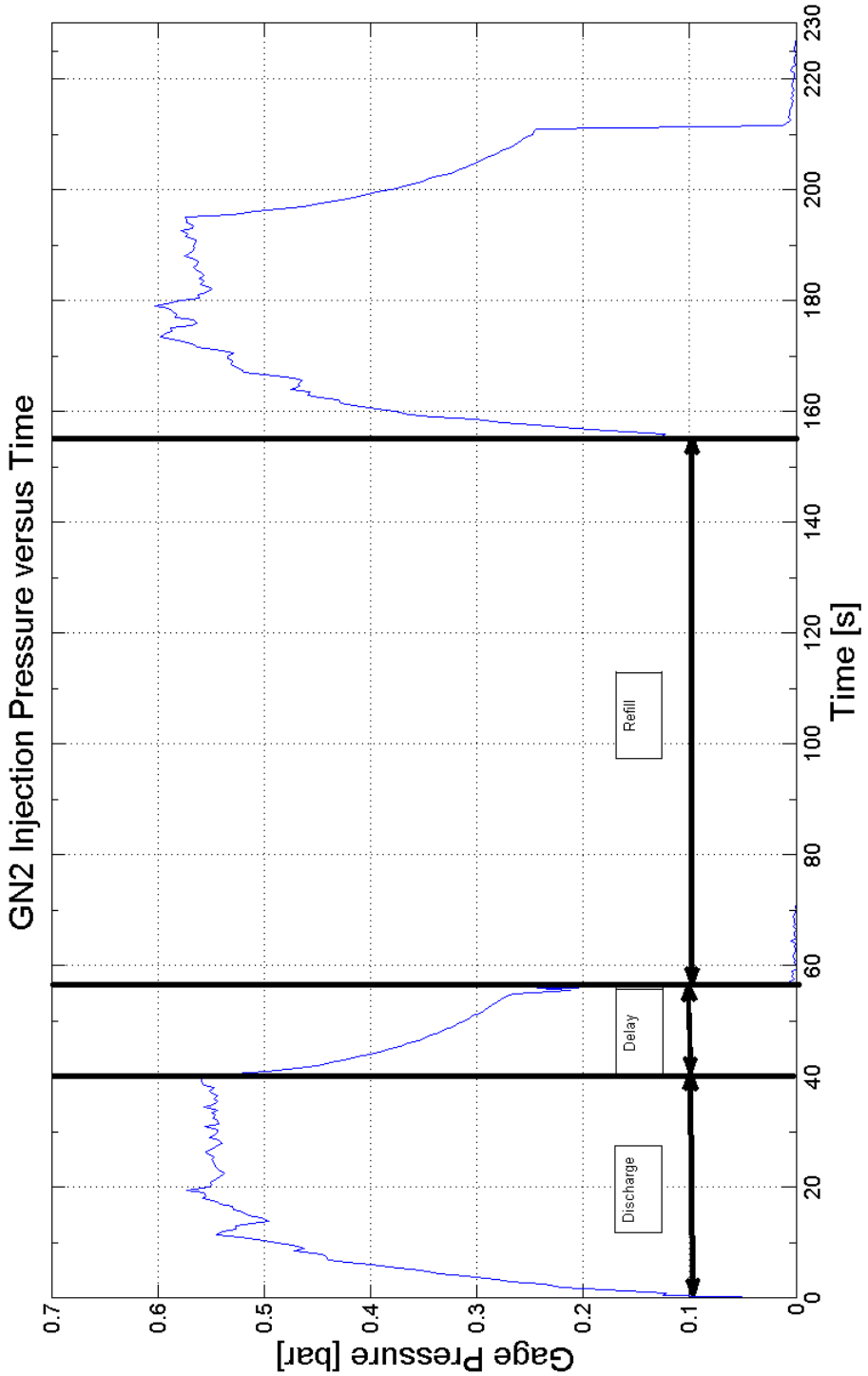

Figure 4.3. GN2 Injection Pressure vs. Time (Refill=100s)

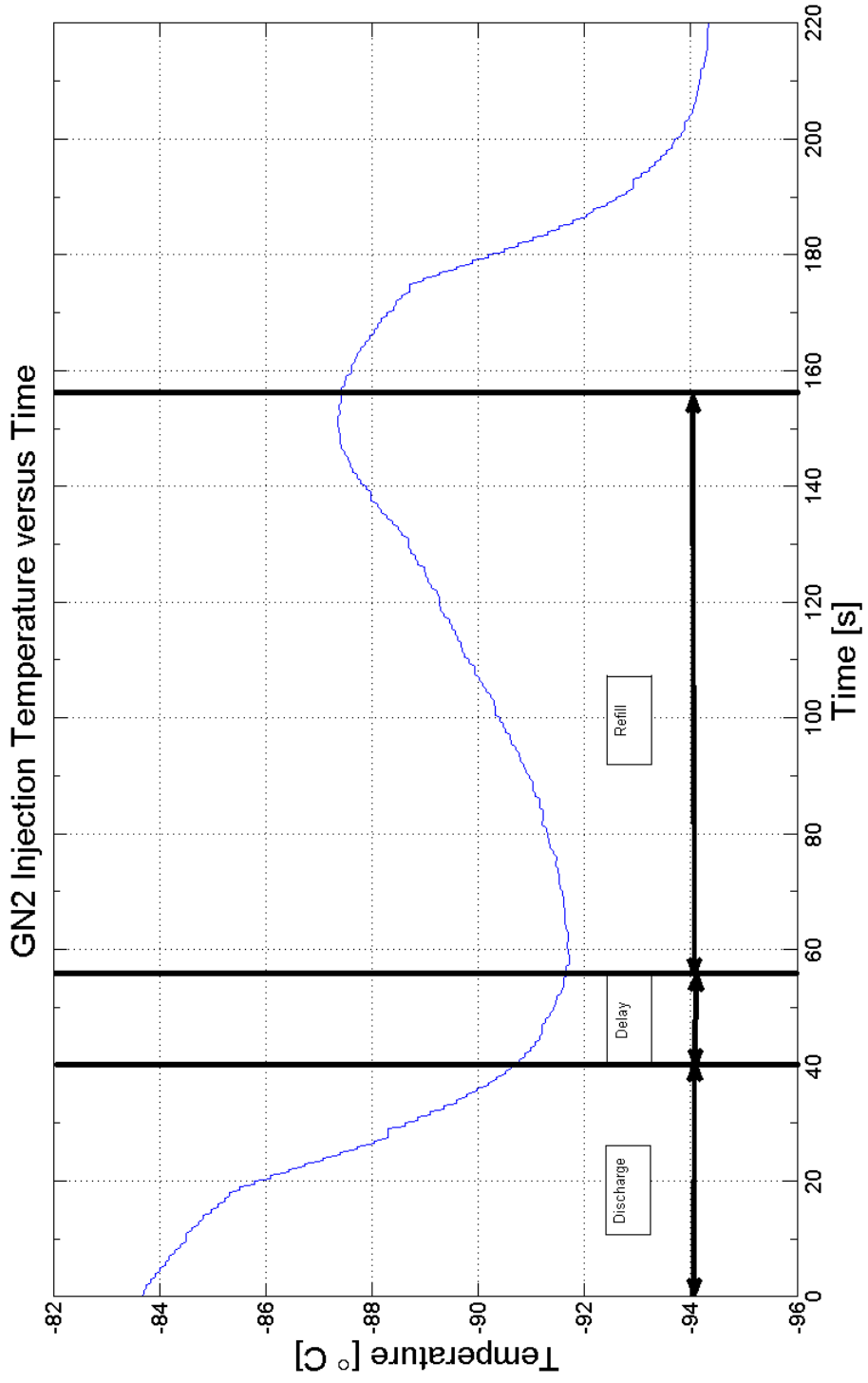

Figure 4.4. GN2 Injection Temperature vs. Time (Refill=100s)

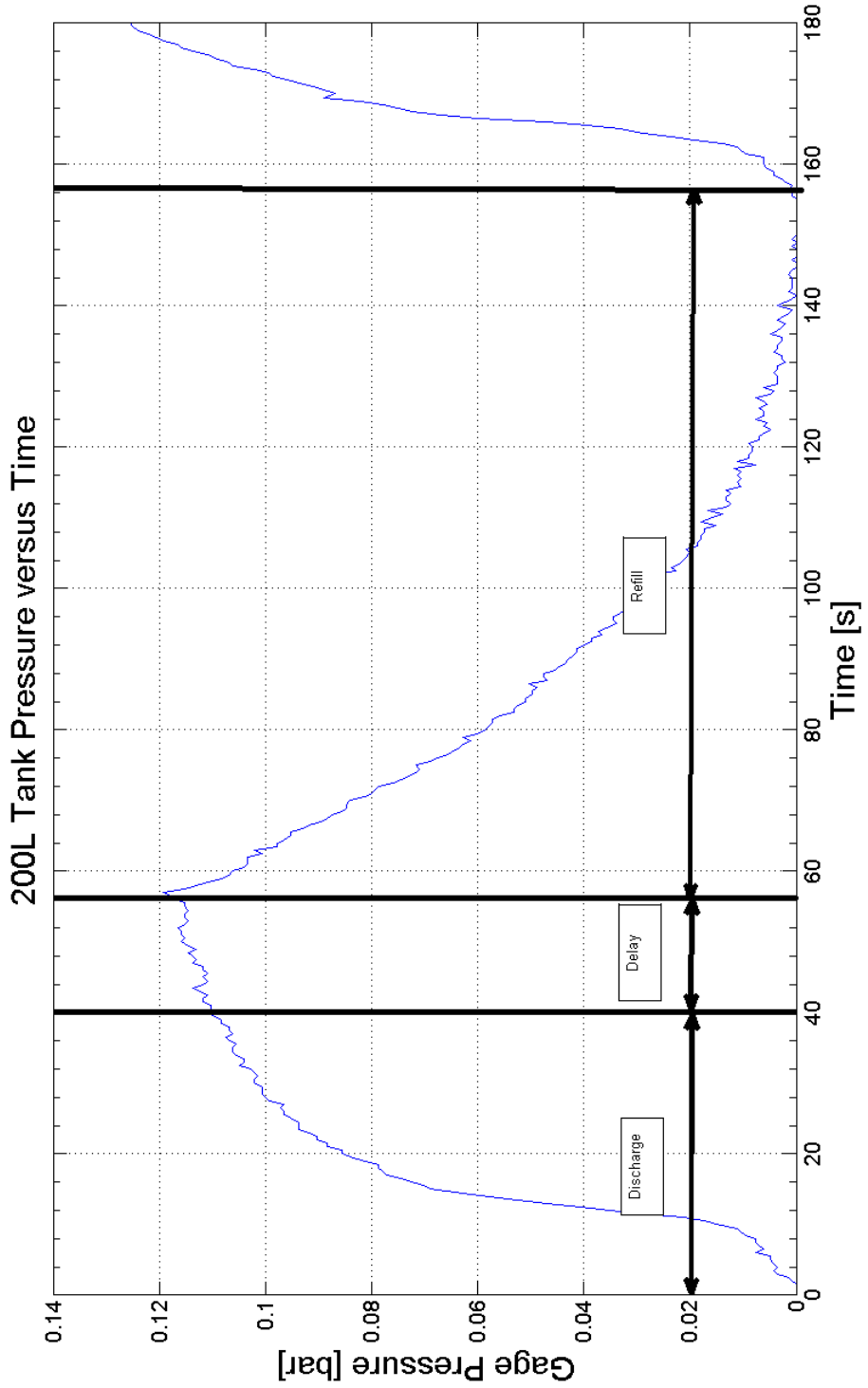

Figure 4.5. 200L Tank LN2 Volume vs. Time (Refill=100s)

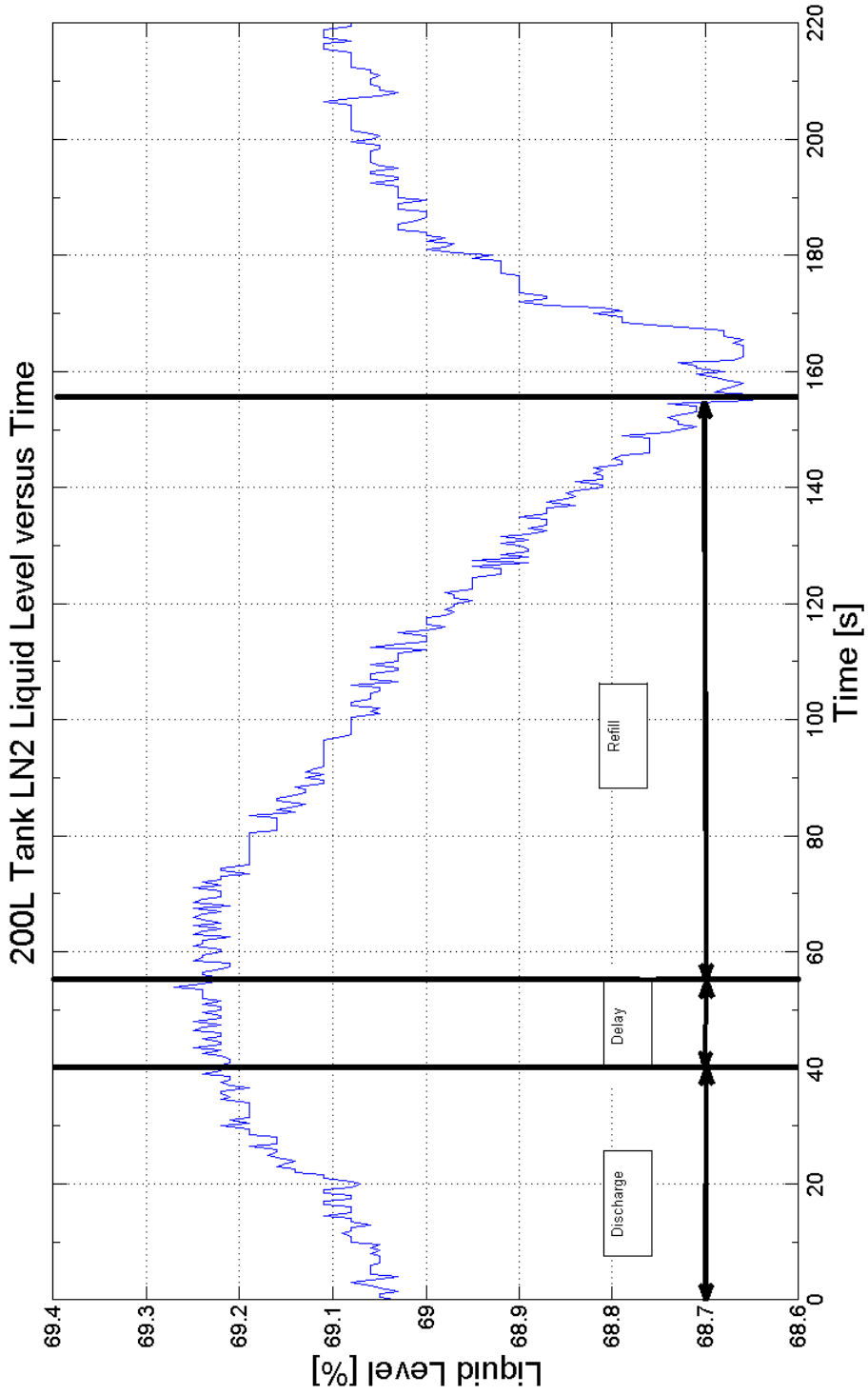

Figure 4.6. 200L Tank LN2 Volume vs. Time (Refill=100s)

Notice that in Figure 4.2 that all three parts of the solenoid timing sequence are displayed in the figure above with the double arrows. The gas injection only lasts forty seconds. Notice that the flow rate is high and decays to a constant value, which is associated with a constant differential pressure in the line. This continues until the delay before fill control sequence closes all solenoid valves (SV-001 to SV-004), which corresponds to zero flow rate in the gas injection process for fifteen seconds. After the fifteen seconds, the tank refill is started by opening SV-002-SV-004 (refer to Figure 3.2). This tank refill timing does not initiate flow because SV-001 is closed. The next figure shows the GN2 injection pressure versus time.

Figure 4.3 shows gas injection, delay before fill, and tank refill during one cycle, which lasts for one hundred fifty-five seconds. During the gas injection, the pressure in the GN2 injection line increases abruptly and plateaus for the majority of forty seconds. Furthermore, the delay before fill show a slight decay in pressure. It is then followed by the refill time, which is associated with a sudden pressure decline to 0 bar. The next figure shows the GN2 injection temperature versus time.

Figure 4.4 temperature trend is associated with the platinum RTD, or TI-001 in Figure 3.2. Notice that during the discharge of the PC, the temperature of the GN2 injection line becomes colder. This is associated with the cold GN2 gas flowing through the line. Furthermore, the delay is associated with the beginning of a warming trend, which is a result of the cessation of GN2 flow via SV-001. Because flow in the GN2 injection line stops, radiation heat transfer begins to dominate, which causes the line to warm. The next figure shows the overall trend of the 200L tank pressure.

In Figure 4.5, notice that the pressure increases during the injection process. This a result of the system being closed loop during the gas injection procedure. The delay before fill shows a slight increase in pressure during the fifteen seconds as a

result of the pressure wave. The tank refill shows a drop in pressure because SV-004 opens to vent the GN2 within the process cylinder to atmosphere. The next figure shows the liquid level versus time.

Figure 4.6 graphically depicts the gas injection, delay before fill, and tank refill. Notice that the gas injection corresponds to a slight increase in the LN2 level of the 200L tank. This corresponds to LN2 returning to the 200L tank because the LN2 volume that was in the PC is forcing the existing fluid through the transfer lines. A delay before fill shows a plateau or constant liquid level, which corresponds to no liquid displacement. Finally, the tank refill shows a decrease in liquid level, which corresponds to LN2 filling the process cylinder volume.

4.2 Raw Data

The data was recorded in two types of data files. The first data file contains pressure, temperature, and flow rate measurements regarding the 200L vessel. Moreover, the second data file contains the heating data, which corresponds to focal plate RTD temperature readings, voltages, and a GN2 injection line thermocouple reading. The data recorded involves maintaining the delay before fill and gas injection constant and varying the tank refill from 60, 100, to 120 seconds. The raw data files can be found in *Lab A Over-Pressure Pump Test February Tests* [3]. The figures presented below will show the data for a refill time of 100s. Trends for pressure, temperature, and flow rate will be discussed.

The data collected for the tank refill time of one hundred seconds can be seen in the following figures. The solenoid timing sequence consists of the gas injection, delay before fill, and the tank refill, which corresponds to 40, 15, and 100 seconds. The figures presented below involve 200L CLV LN2 level, GN2 injection pressure (PT-001), 200L CLV tank pressure (PT-002), GN2 injection flow rate (FT-001), GN2 injection temperature (TI-001), and GN2 injection temperature flange (TI-002) (see

Fig. 3.2). The first figure shows the trend of the LN2 liquid level versus time.

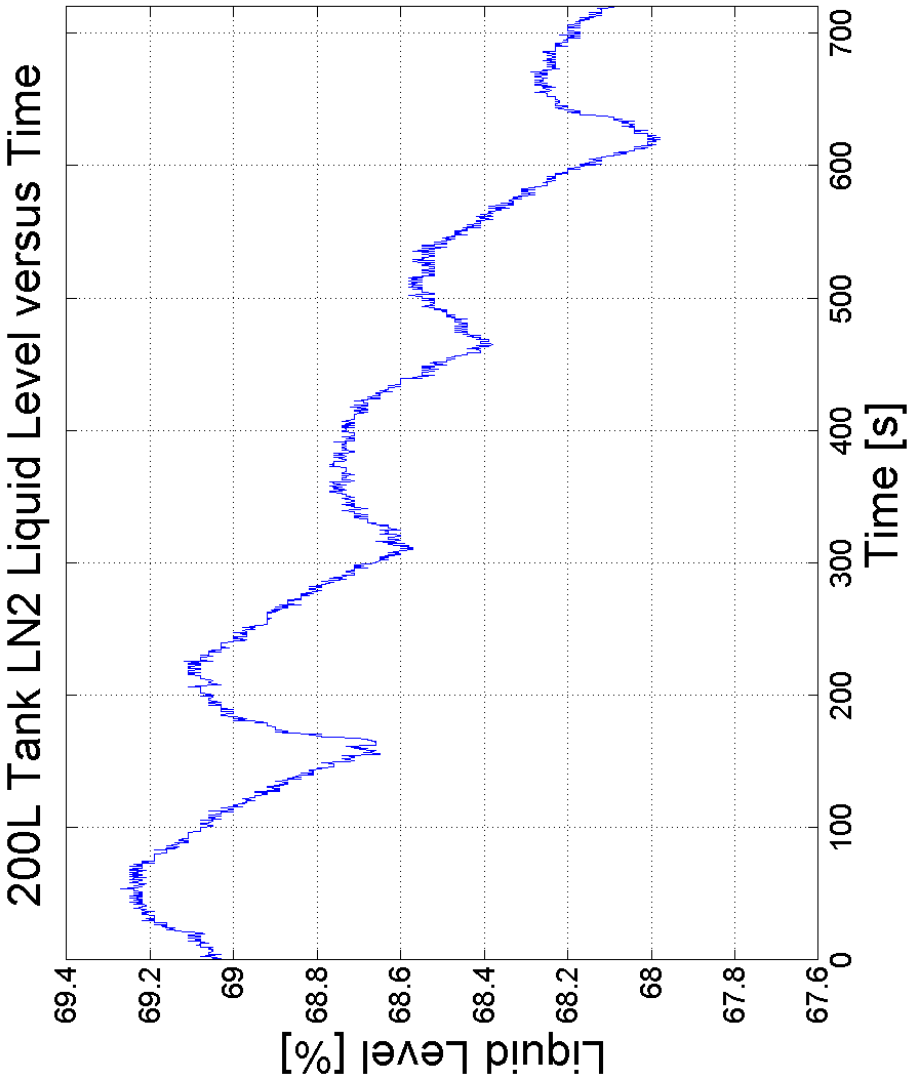

Figure 4.7. 200L Tank Liquid Level vs. Time (refill=100s)

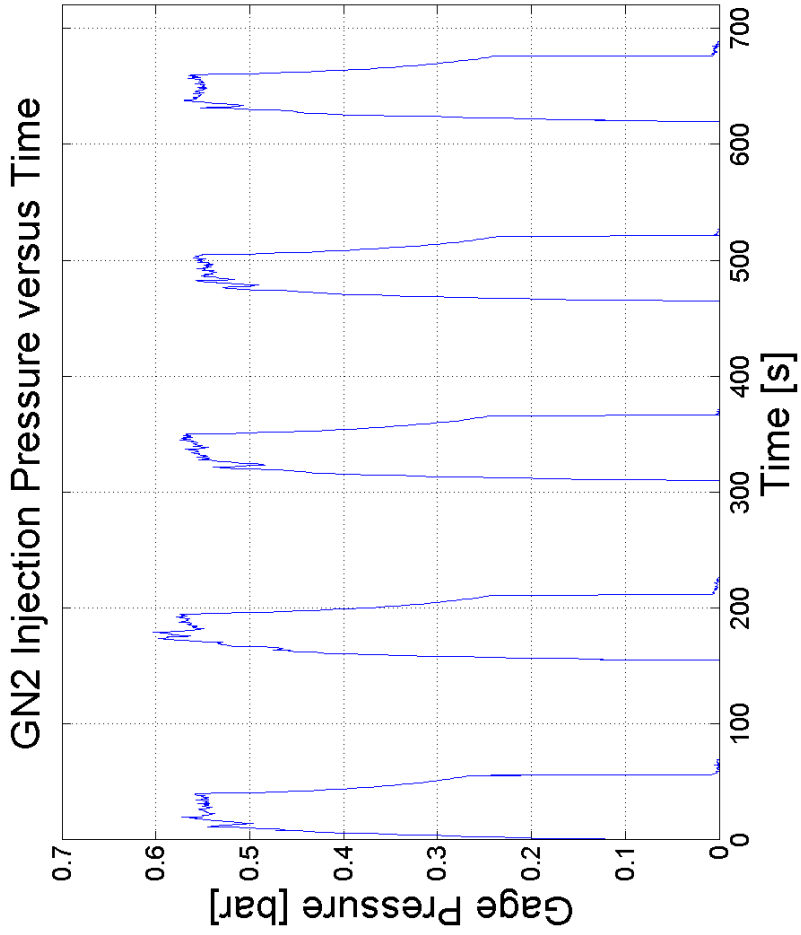

Figure 4.8. GN2 Injection Pressure vs. Time (refill=100s)

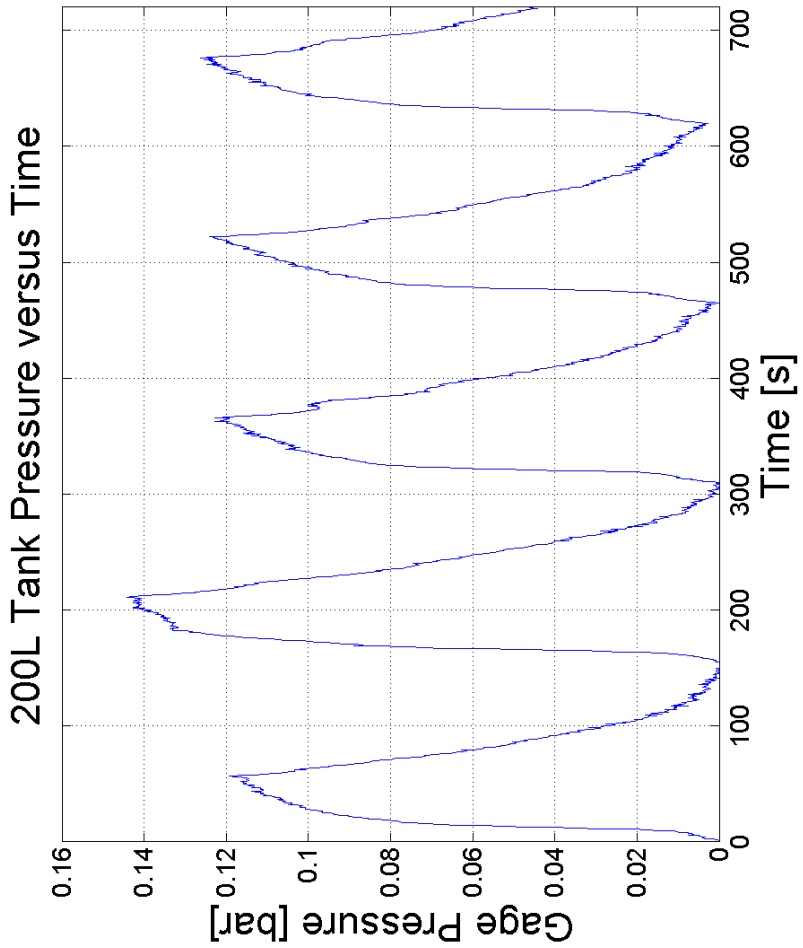

Figure 4.9. 200L Tank Pressure vs. Time (refill=100s)

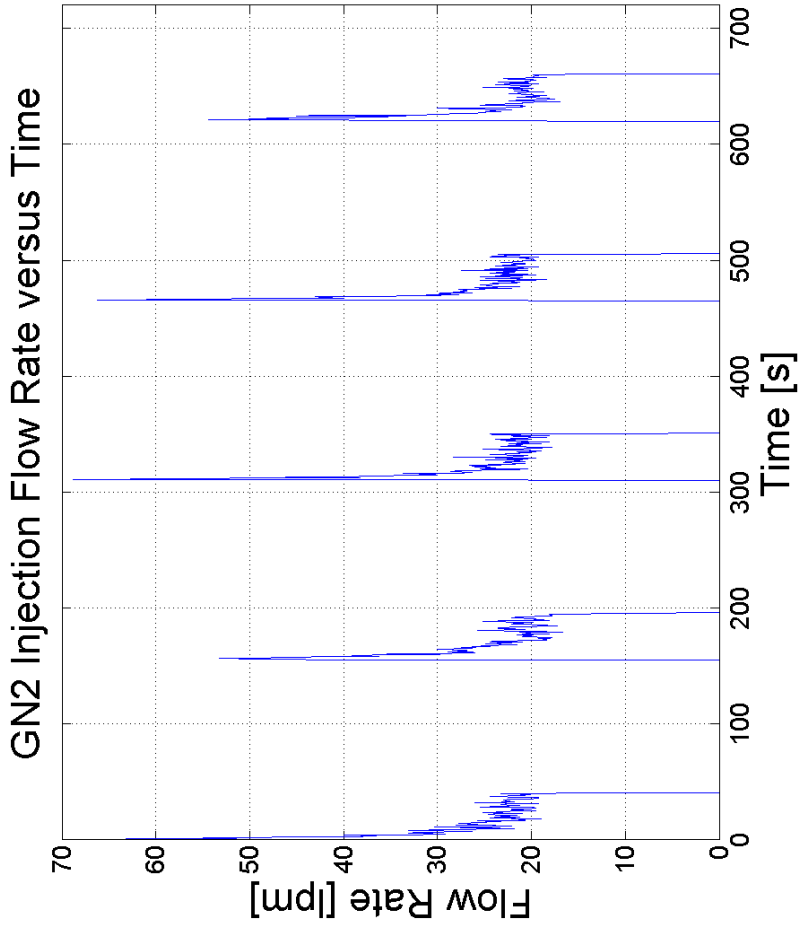

Figure 4.10. GN2 Injection Flow Rate vs. Time (refill=100s)

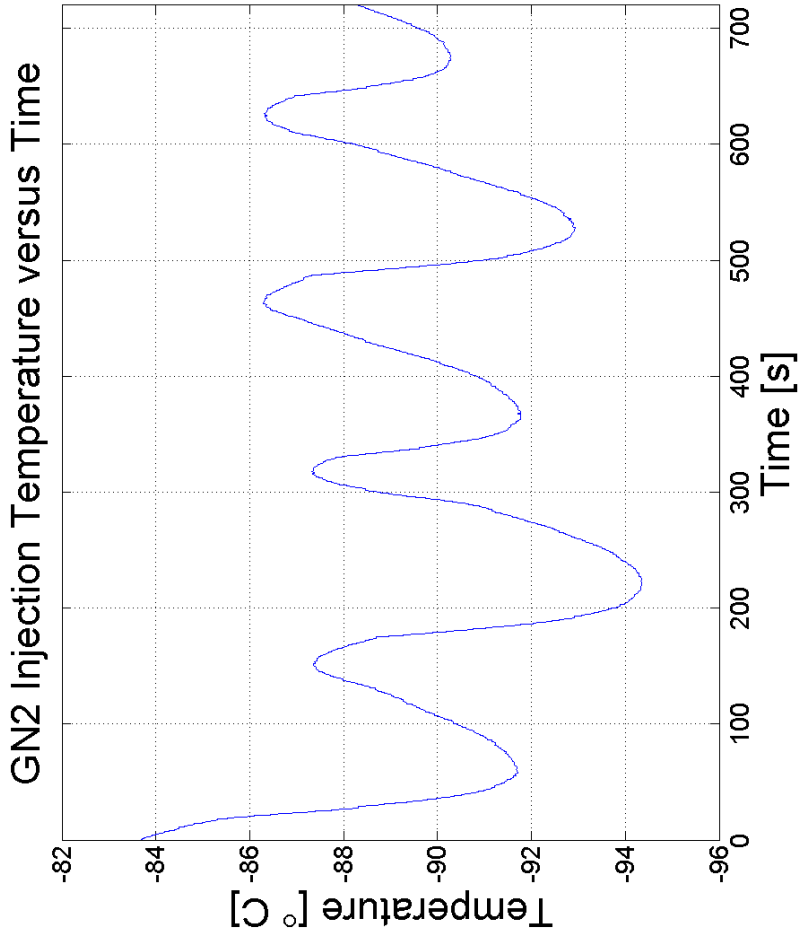

Figure 4.11. GN2 Injection Temperature vs. Time (refill=100s)

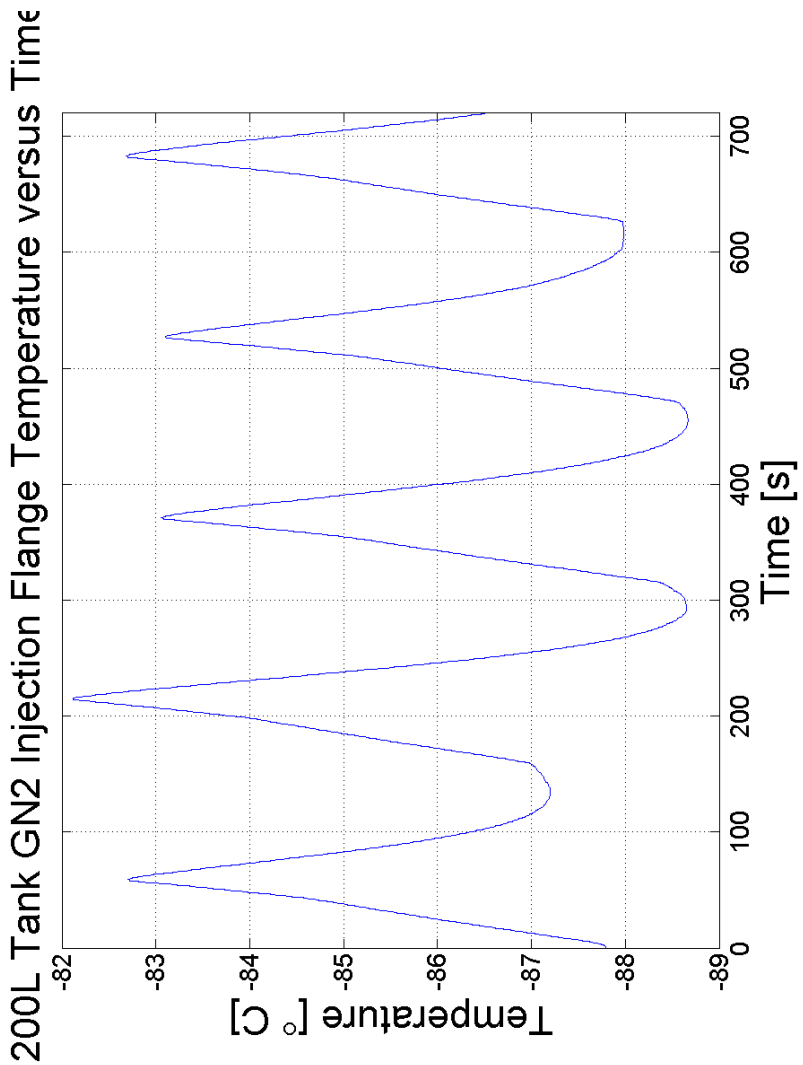

Figure 4.12. 200L Tank GN2 Injection Flange Temperature vs. Time (refill100s)

Figure 4.7 displays an increasing liquid level during the discharge process of the LN2 from the PC. After the discharge and the time delay finish, the PC begins refill. Notice that the liquid level decreases after 100s, but it does not return to its original level. Overall, the liquid level decreases over time. This is a result of the cryogenic refrigerator being unable to condense the gas generated via heat loads onto the system. Furthermore, the system is operated quasi-closed loop (see Sec. 3.2). The second figure displays the GN2 injection line pressure versus time (PT-001).

Notice that during a discharge of the PC, the pressure in the GN2 injection line plateaus at 0.55bar (see Fig.4.8). This sudden increase in pressure is associated with SV-001 opening, which injects GN2 into the PC from a 160L low pressure CLV. The pressure in Figure 4.8 decays during a delay and then abruptly drops to 0 bar during a refill. Recall that SV-004 opens, which vents the excess GN2 to atmosphere. This implies that PT-001 measures atmospheric pressure. The next figure shows the pressure in the 200L CLV.

Similarly, Figure 4.9 shows an increasing trend until nearly 0.12 bar. Notice the logarithmic trend. It is associated with the 200L CLV tank pressure approaching the 160L CLV tank pressure, which is 1.50 bar. In other words, if GN2 continues being injected, the 200L CLV will equal the pressure of the 160L CLV. Recall that the flow through the transfer lines is a result of this differential pressure, which decays over time. The same can be said about the GN2 injection flow rate. The next figure shows the GN2 injection flow rate vs. time.

Figure 4.10 shows a sudden spike in flow rate. This is a result of the SV-001 abruptly opening, which results in flow. The flow plateaus at roughly 20LPM. Because this flow is driven by pressure, the flow rate will decay to 0 LPM over time. Also, notice the oscillations as the flow steadies to around 20LPM. These oscillations are associated with the LN2 in the vaporizer flashing. This sends surges of flow through

the GN2 injection line. The next figure shows the GN2 injection temperature (TI-001) located before the turbine flow meter.

Figure 4.11 shows the temperature trend of the GN2 injection line. During a discharge of the PC, the temperature of the GN2 injection line cools. This is associated with cold gas flowing through the line. When the 40s cycle is over, the line begins warming as a result of radiation, convection, and conduction effects that act on the GN2 injection line. Notice that the temperature oscillates steadily. This steady oscillations allow for an average temperature to be taken to estimate thermodynamic properties. The final figure shows the temperature of the GN2 injection line at the 200L CLV flange feedthrough (TI-002).

Figure 4.12 shows a warming trend during the GN2 injection process. In contrast, the cooling trend in Figure 4.11 implies that the GN2 is cold at that point and becomes significantly warmer when it reaches TI-002. This is a result of the entire GN2 injection line being uninsulated and completely exposed to radiation, conduction, and convective effects. During the refill of the PC, the temperature in Figure 4.12 begins lowering. This is associated with the cold GN2 (142K) from the top of the 200L CLV being vented through that line.

In conclusion, the data collected for different refill times (60s, 100s, and 120s) will be used to determine the thermodynamic, fluid, and heat transfer properties. These properties will then be used to show that the focal plate was cooled to 173K. Additionally, this data will be used to show that the experimental objectives were achieved (see Sec. 3.1). The GN2 and LN2 flow rates are strongly related to the differential pressures between the 160L CLV and the 200L CLV. Furthermore, the additional data not presented in this section can be found in *Lab A Over-Pressure Pump Test February Tests* [3].

CHAPTER 5

RESULTS

Once the data was collected, it was converted to the International System of Units (SI). Some of the data was corrected and will be discussed in detail below. The sections below will be devoted to displaying evidence that the objectives were met. For a summary of the objectives, refer to Section 3.1. Furthermore, some of the data is adjusted for error or improper calibration. This can be found in the Appendix G. Lastly, the calculations involving thermodynamic properties are purely estimates and should not be taken as a highly accurate value.

5.1 173K Focal Plate

The primary objective in the quasi-closed loop cooling system was to determine whether the OPP was cooling the focal plate to 173K. Because no liquid level probe (LLP) was installed within the process cylinder (PC) to indicate a stroke; other data must be investigated to indicate this. The focal plate RTDs, copper braid RTDs, and the liquid level probe data will be presented below.

Focal Plate RTDs

The focal plate RTDs are surface mounted on the CCD focal plate. The copper braids also have RTDs mounted on them, which are nearer to the tube heat exchanger (see Fig. 3.7). A total of 10 copper braids are required to conduct heat through a vacuum space to the CCD cooling system heat exchanger. Each copper braid contains a resistance heater to add additional temperature control of the CCD focal plate. One of the copper braid heaters and RTD (HV8) was damaged during the installation; the values will be ignored. Additionally, each copper braid contains a platinum RTD. The temperature readings are presented below. The following figure

shows the average temperature of the focal plate versus time and the heater power for each of the copper braids.

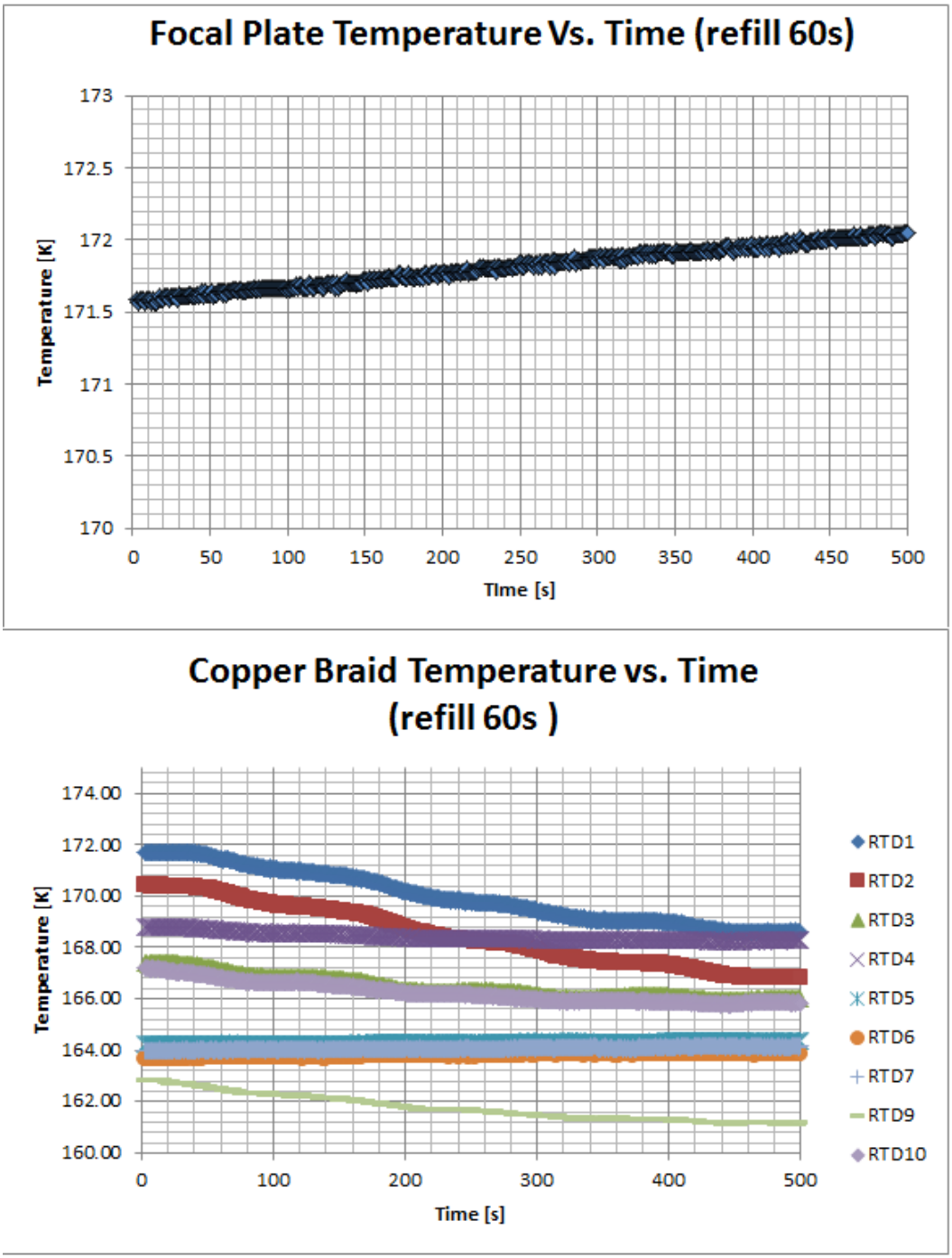

Figure 5.1. Top: Focal Plate Temperature vs. Time. Bottom: Copper Braid Temperature vs. Time (refill 60s)

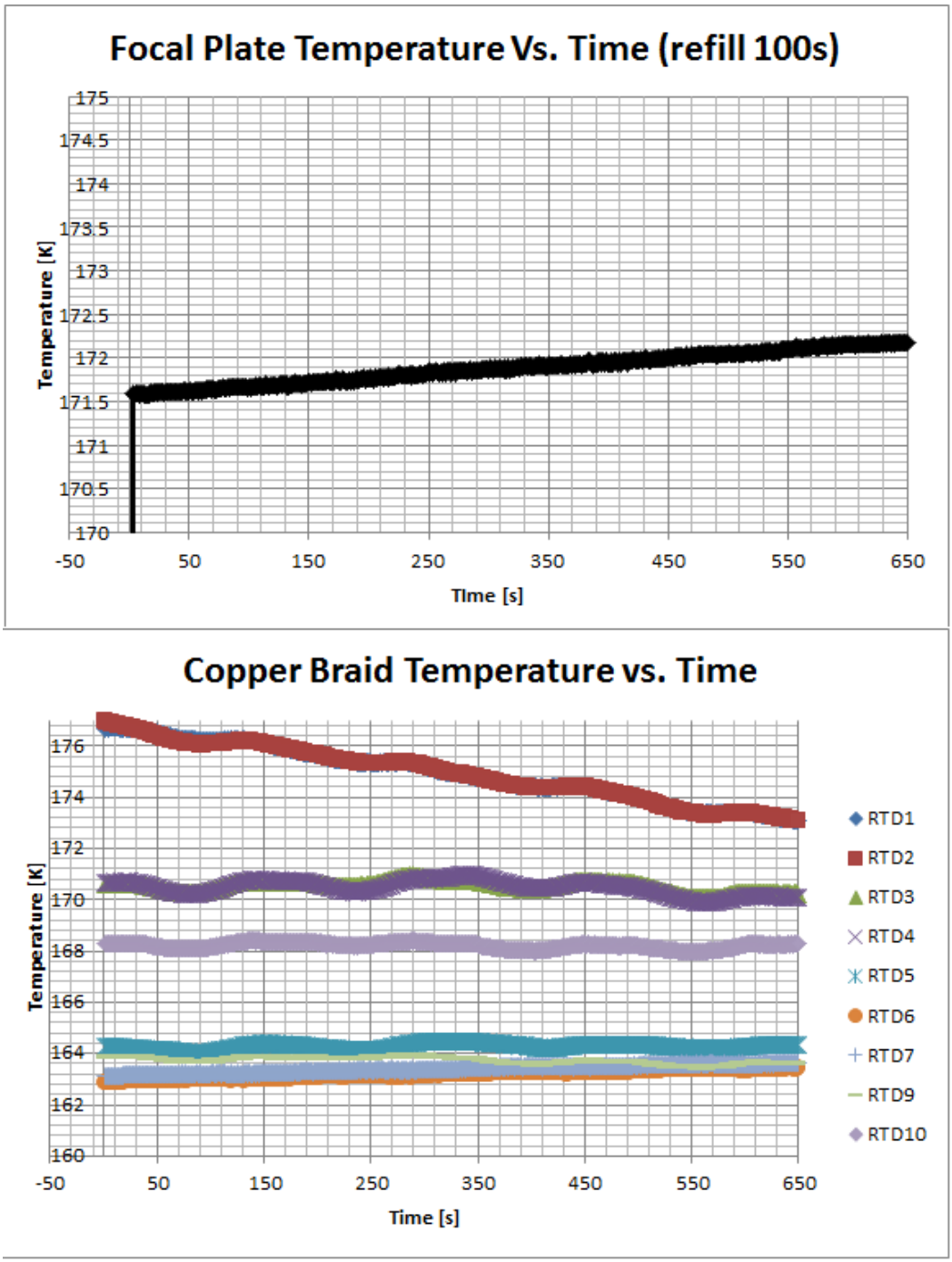

Figure 5.2. Top: Focal Plate Temperature vs. Time. Bottom: Copper Braid Temperature vs. Time (refill 100s)

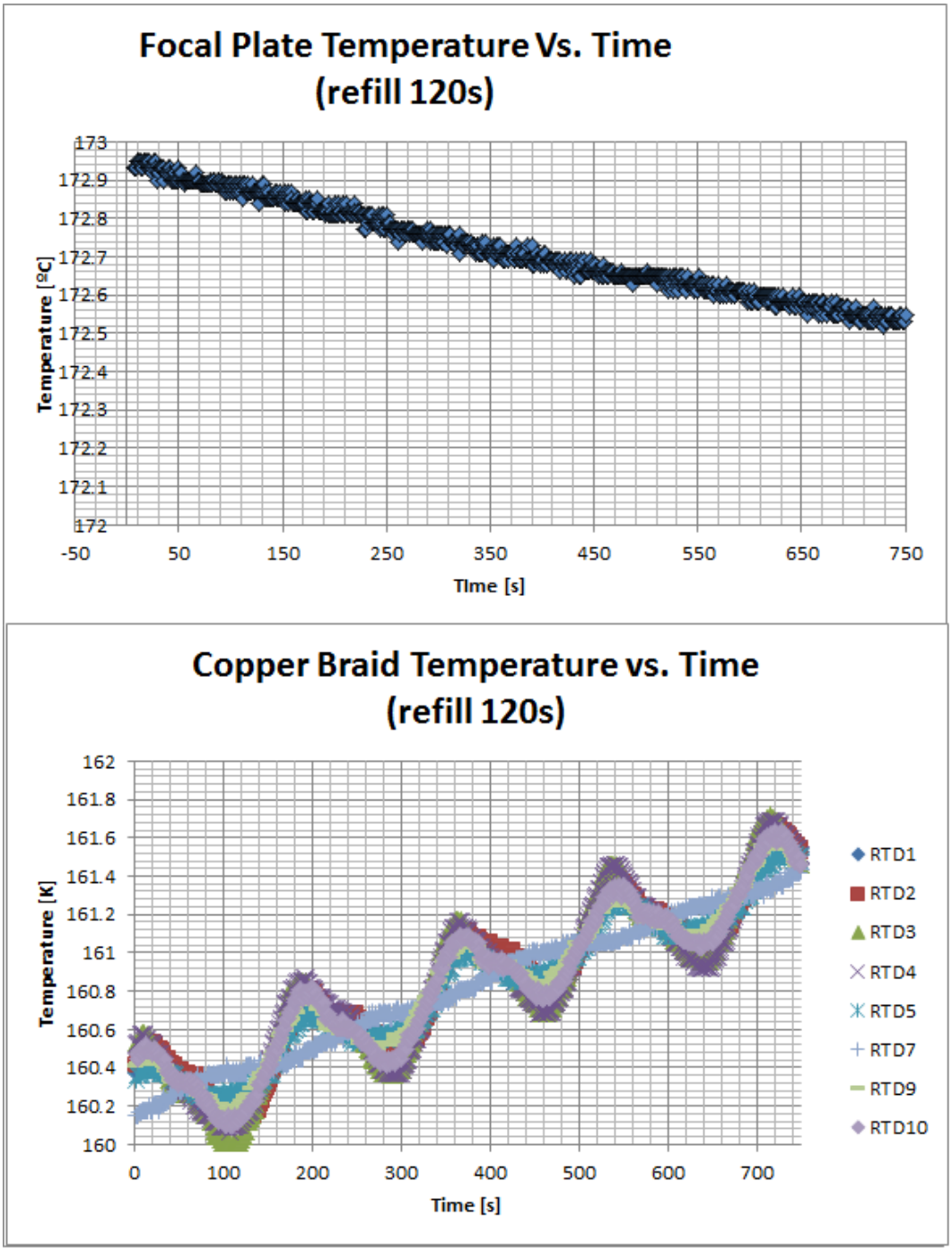

Figure 5.3. Top: Focal Plate Temperature vs. Time. Bottom: Copper Braid Temperature vs. Time (refill 120s)

In Figure 5.1, the focal plate temperature is ascending to 173K, which is the set point temperature of the focal plate. The focal plate average temperature is based upon RTDs that are mounted to the surface of the focal plate itself, which are averaged. This ascension indicates that the focal plate is warming. Notice that the copper braid RTDs measure temperatures that are lower than the set point temperature of 173K (see Fig. 5.1 *Bottom: Copper Braid Temperature vs. Time (refill 60s)*). This indicates that the LN2 is flowing through tube HX and providing sufficient cooling. The cool LN2 turns on the heater control on the copper braids, which regulate the temperature on the focal plate to 173K.

The ascending temperature of the focal plate indicates that the heaters on the copper braids are activated. The heaters are meant to regulate the temperature of the focal plate. Furthermore, notice that in Figure E.5, the temperature of the injected GN2 is significantly above 173K. This implies that the GN2 injected into the system cannot cool the focal plate, but it would rather warm it. The only way that the focal plate is being cooled is through a LN2 supply. Lastly, notice that the RTDs show different temperature measurements. This is a result of imperfect contact between the copper contacts and the tubing (see Fig. 3.7). Hence, the difference in temperature of RTD10 and RTD2 in the Figure 5.1.

Figure 5.2 displays a similar trend as in Figure 5.1. Again, the focal plate temperature shows a warming trend. The figure above shows slight oscillations within the temperature readings. These oscillations are a result of LN2 flow during a 40s discharge cycle, which corresponds to a decrease in temperature. Moreover, no flow exists during a refill and delay of the OPP. Thus, the temperature of the RTDs will increase in temperature, which is a result of the copper braid heaters being turned on to regulate the CCD focal plate temperature. The next figure shows the temperature and power trends for a refill time of 120s.

Despite a converse focal plate temperature in Figure 5.3 as compared to Figures 5.1 and 5.2, the overall trends are similar. That is the focal plate is cooling rather than warming. If a longer of period of time was captured, a warming trend of the average focal plate would be captured in the data. In summary, the heaters regulate the temperature in and around the set point temperature of 173K. The oscillations during a discharge and refill can be seen in the figure above. Again, flow through the tube heat exchanger cools the focal plate; no flow corresponds to the warming of the focal plate.

In conclusion, Figures 5.1 to 5.3 show that the focal plate cools for varying refill times. The focal plate has been cooled to 173K and lower. When the focal plate is cooler than the set point, the heaters on the copper braids are turned on. Conversely, if the focal plate is warm, the copper braid heaters are turned off or set to a lower power state. Overall, the heaters assist in regulating the temperature of the focal plate in and around 173K. Lastly, the RTDs mounted on the copper braids indicate that the LN2 within tube heat exchanger is well below the set point of the focal plate, which means the LN2 supply from the OPP is sufficient. Furthermore, the oscillations seen in the Figures 5.1 to 5.3 show that during a discharge cycle the focal plate cools and warms during a refill cycle.

Liquid Level

This part investigates the liquid volume in the 200L CLV during the entire cycle of the PC. Data was recorded using a Teragon LP7 liquid level probe (see Sec. 3.3). The liquid level was recorded as a percentage fill of the 200L CLV. During a discharge, delay, and refill, significant tank volume can be observed. Each refill time 60s, 100s, and 120s, will be discussed below. Four continuous cycles were extracted from the liquid level data.

The first figure represents an overlay of data from each of the four cycles observed in Figure E.1. The second figure represents an overlay of data from each of the four cycles observed in Figure 4.7. The third figure represents an overlay of data from each of the four cycles observed in Figure E.7.

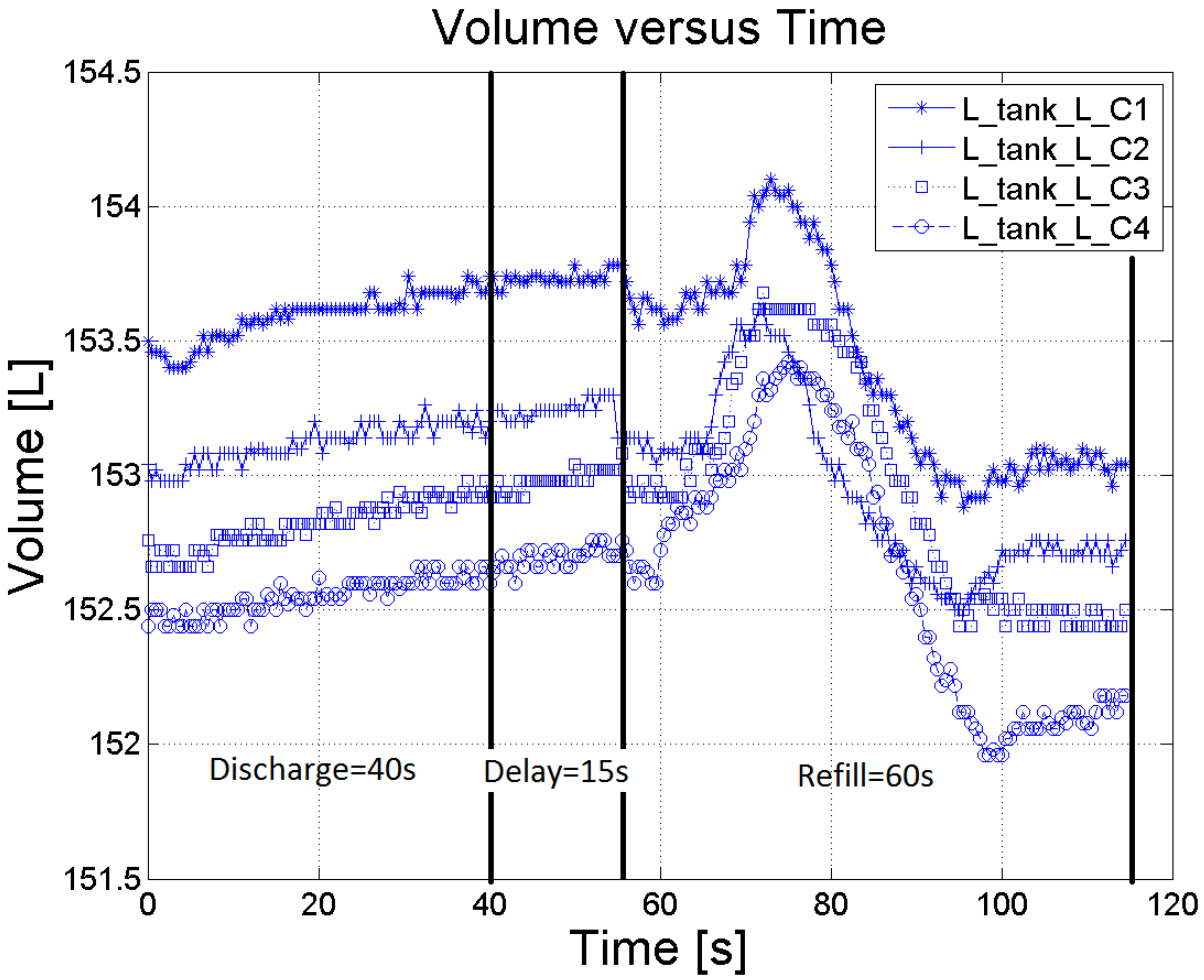

Figure 5.4. Four Cycle Overlay of 200L Tank Volume Versus Time (refill 60s)

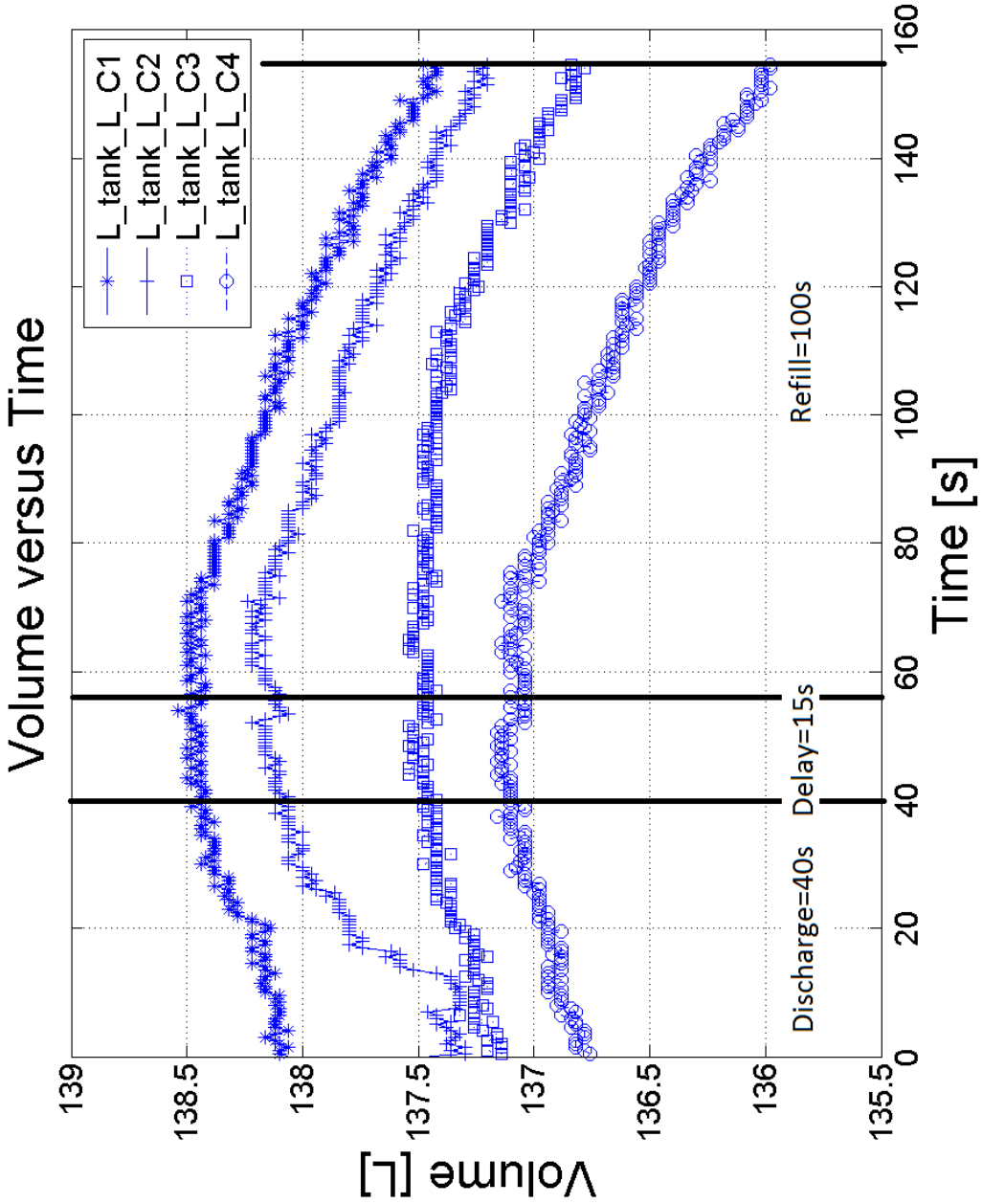

Figure 5.5. Four Cycle Overlay of 200L Tank Volume Versus Time (refill 100s)

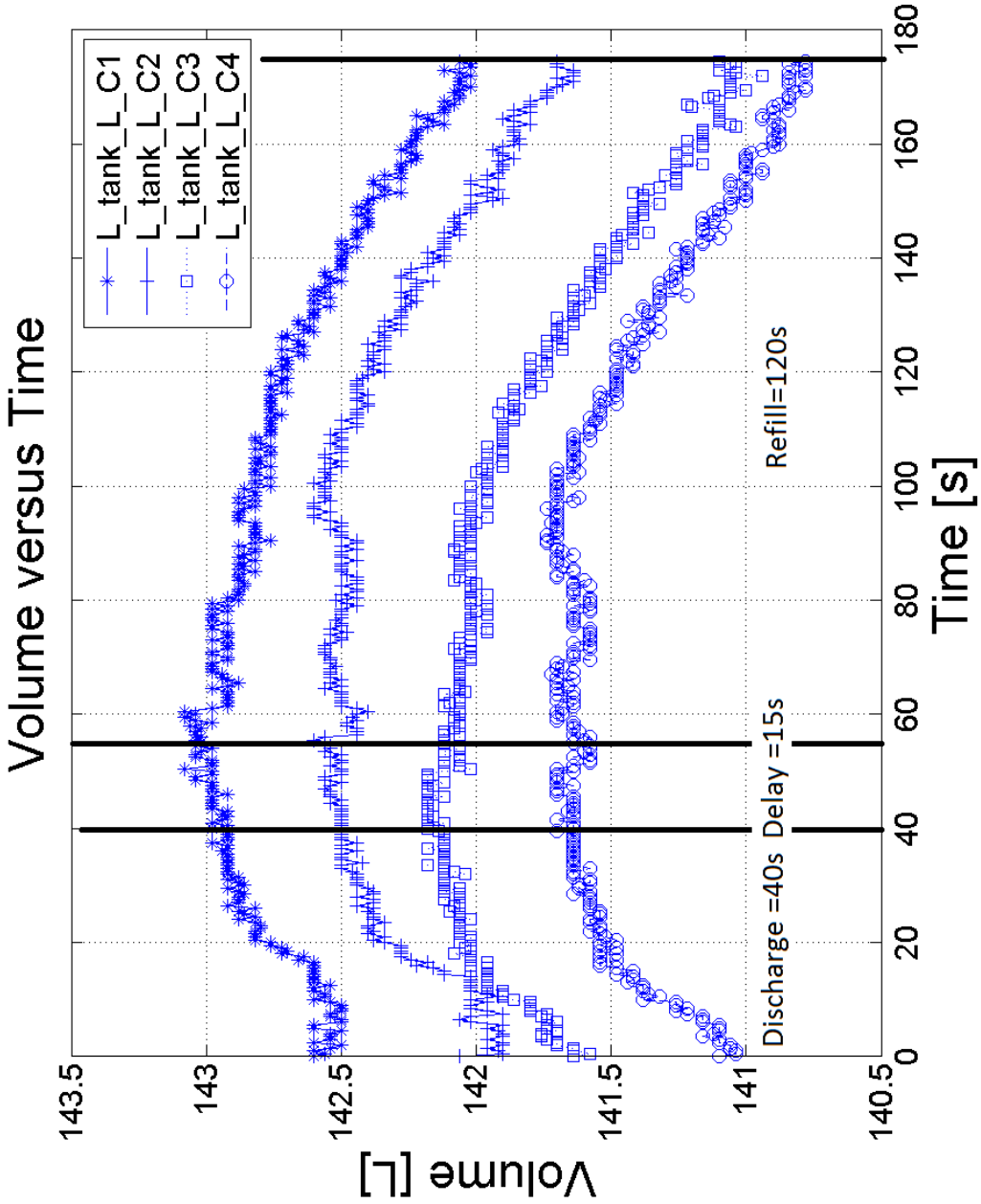

Figure 5.6. Four Cycle Overlay of 200L Tank Volume Versus Time (refill 120s)

Figures 5.4 to 5.6 show four cycles overlayed on top of one another. The curve at the top of each of the figures show an earlier discharge, delay, and refill cycle of the process cylinder. Recall that the first 40s is associated with flow through the transfer lines and the remaining part of the cycle their is no LN2 flow. Notice that the curves do not overlap each other, but progressively decrease. This decline in the liquid level is associated with the open loop portion of the PC (see Sec. 3.2). Thus, the 200L CLV is continuously losing LN2 during a refill.

Figures 5.4 to 5.6 show flow rate associated with the 200L CLV changing volumes during a single cycle. Notice that after 40s the LN2 level within the 200L CLV increases. This is associated the injected GN2 into PC displacing the LN2 volume out from it through the MCCD transfer lines. A LN2 volume increase is associated with LN2 returning to the tank via the transfer lines. Recall that the discharge of the PC is performed closed loop. Therefore, the mass of nitrogen in the tank remains fixed for the discharge (40s) time as well as the delay (15s), which is for a total of 55s. During a delay, or after the 40s, the figures show a steady liquid level for 15s. The delay is performed closed loop as well. Lastly, the refill, which is open loop, results in a decrease in LN2 within the tank. Figure 3.4 is slightly unusual during the refill time of 60s. This is associated with the release of a slug of LN2 when the system is exposed to atmosphere during the refill. In other words, a GN2 pocket is allowed to expand and push LN2 through the lines. This occurs when SV-004 is opened, which lowers the 200L CLV pressure. Additionally, the pressure initially within the 200L CLV is used to generate a differential pressure to assist in the refill of the PC. This flow returns LN2 to the 200L CLV, which is associated with the increase in the tank volume during a refill.

From the information in Figures 5.4 to 5.6 the average volumetric flow rate through the transfer lines is simply the difference between the initial point and the

final point of the volume after the discharge time of 40s. Then the value is divided by the time during the discharge. The following equation illustrates this.

$$\Delta V_{discharge,PC} = V(40) - V(0) \tag{5.1}$$

Where $\Delta V_{discharge,LN2}$ is the LN2 flow rate through the transfer lines, $V(40)$ is the $V(0)$ is the volume at the beginning of the cycle. This difference is taken for each of the four cycles displayed in the figures above. Then an average volume is determined and divided by the discharge time to attain the flow rate. The following table shows the flow rates through the transfer lines.

Table 5.1. Average LN2 Supply Line Flow Rate

Refill Time [s]	Cycle Number for Volume [L]				Average	Standard Deviation	Flow Rate	
	1	2	3	4	Volume [L]	Volume [L]	Volumetric [LPM]	Mass [kg/min]
60	0.18	0.10	0.22	0.22	0.22	0.05	0.33	0.27
100	0.38	0.64	0.28	0.32	0.45	0.14	0.67	0.54
120	0.32	0.44	0.50	0.60	0.50	0.10	0.75	0.60

Table 5.1 shows the volumes calculated using Equation 5.1 for each of the four cycles. It also displays the average volume during a discharge taken for all four cycles. Lastly, the LN2 flow rate through the transfer line is determined by dividing the average volume for each refill time by the discharge time of 40s. Notice, that the PC discharges less volume with a lesser refill time. This is associated with the amount of LN2 initially inside the PC. Finally, the average volume in the table above was corrected to account for the boiling off of LN2 during the 40s interval (see App. G LN2 Discharge Flow Rate Volume Correction).

Table 5.1 shows an increasing volumetric flow rate trend with an increasing refill time. This indicates that for longer times to refill the process cylinder, the higher the flow rate and the more volume fills the PC. It is known that the injected GN2 is supplied at a constant 22psig from the 160L LP CLV. This increasing flow rate is directly associated with a varying heat input via the LN2 vaporizer or GN2 injection line. Furthermore, a varying heat input via the vaporizer will affect the amount of drive gas being injected into the PC. Additionally, a refill of the PC is performed open-loop. This implies that GN2 injection line up to SV-004 (see Fig. 3.2), will become cooled and is dependent upon the refill time. The GN2 within the tank is significantly cooler than the GN2 injected. So there exhibits a dependence upon the length of time of the refill and the GN2 injection volumetric flow rate into the PC. The temperature of the GN2 within the 200L CLV typically ranges between 143-145K for all three refill times, which is lower in temperature than the GN2 injection flange temperature seen in Figures E.6, 4.12, and E.12.

Also, the rate at which LN2 refills the PC can be determined as the difference between the initial and terminal point of the refill cycle.

$$\Delta V_{fill,PC} = V(40) - V(15 + t_f) \tag{5.2}$$

Where $\Delta V_{fill,PC}$ is the volume that enters the LN2 during a fill, $V(15 + t_f)$ is the final volume after a complete cycle of the process cylinder, and t_f is the refill time. Using the equation and averaging the data within the liquid level curves, the following table is produced.

Table 5.2. Average LN2 Refill of PC Flow Rate

Refill Time [s]	Cycle Number for Volume [L]				Average	Standard Deviation	Average
	1	2	3	4	Volume [L]	Volume [L]	Refill Rate [lpm]
60	0.64	0.38	0.48	0.48	0.50	0.09	0.50
100	0.96	0.92	0.64	1.12	0.91	0.17	0.55
120	0.86	0.80	1.04	0.92	0.91	0.09	0.45

Equation 5.2 is used to calculate the average volumes seen in the sixth column in Table 5.2. Notice that the average volume per fill begins to plateau at 0.91L. The plateau effect is associated with the SV-002 being in the GN2 within the 200L CLV. Furthermore, the SV-003 is the only valve that is fully submerged. SV-003 uses only the hydrostatic pressure of the liquid to refill the PC. SV-002 lowers the pressure within the 200L CLV to atmospheric pressure.

Notice that the volume during a fill in Table 5.2 is larger than the volume that is returned into the tank during the 40s discharge of the PC (see the volumes in Tab. 5.1). Typically, the volume during a refill should equal the amount that returns to the tank. This is not the case. The difference is associated with the boil off of LN2 as it flows through the MCCD transfer lines. Evidence of boiling or low contact resistance can be seen in the copper braid RTD data. Notice some of the copper braids are at lower temperatures than others. This can be seen in Figure 5.2. Lower temperature RTDs can indicate fully wetted sections of the tubing or low contact resistance between the copper connector and the tube heat exchanger.

5.2 The Number of the Cryogenic Refrigerators

The number of cryogenic refrigerators (cryocoolers) will be determined. The single cryocooler within the quasi-closed loop CCD cooling system was incapable of condensing the injected GN2 fast enough to maintain a steady pressure. Therefore, the number of cryocoolers will be determined. It is simply the sum of the injected GN2 and the LN2 lost during a single hour. The maximum cryocooler capacity will be determined and the sensible heat is neglected because it is negligible as compared to the latent heat.

LN2 Loss per Cycle

The LN2 loss is determined from the liquid level probe data (LP). The LN2

loss per cycle is found from subtracting the initial point by the final point of each cycle of the LN2 curves seen in Figures 5.4, 5.5, 5.6. The following equation describes the LN2 loss per cycle of the PC.

$$\Delta V_{LN2,Loss} = V(0) - V(55 + t_f) \tag{5.3}$$

Where $\Delta V_{LN2,Loss}$ is the LN2 loss per cycle and $V(55 + t_f)$ is the final LN2 volume at the end of the entire cycle. The following table shows the average volume loss per cycle.

Table 5.3. Average LN2 Loss Per Cycle

Refill Time [s]	Cycle Number for Volume [L]				Average	Standard Deviation	Average
	1	2	3	4	Volume [L]	Volume [L]	Loss Rate [lpm]
60	0.46	0.28	0.26	0.26	0.32	0.08	0.32
100	0.58	0.28	0.36	0.80	0.51	0.20	0.30
120	0.54	0.36	0.54	0.32	0.44	0.10	0.22

Table 5.3 shows the loss per cycle. The average LN2 volume lost is averaged across the four different cycles, which can be seen in the sixth column. The standard deviation between each measurements shows that it is relatively low. Finally, the average loss rate is determined by dividing the average volume by the total cycle time of $(55 + t_f)$. This loss rate becomes a function of refill time.

Notice that the average loss rate is higher for the refill time of 60s. It is lowest with refill time of 120s. This is a result of the extended cycle time. The loss rate is associated with LN2 boiling off and being discharged to atmosphere. The QCL CCD cooling system operates open loop during a refill. Furthermore, the CCD heaters used to regulate the temperature of the focal plate and the transfer line boil off LN2.

Results

After determining the LN2 loss, EES is used to approximate the number of cryogenic refrigerators needed to operate the system closed loop. The LN2 loss data from Table 5.3 will be used along with the LN2 equivalent of the GN2 injected into the system. The 200L CLV tank pressure and the LN2 and GN2 volumes within it will be used as well. The following table shows the parameters used in estimating the number of AL-300 cryogenic refrigerators needed.

Table 5.4. Input Parameters for Estimating the Number of Cryocoolers

Refill time[s]	LN2 Loss	GN2 Injection Line		Volume	Pressure	Tank Temperatures	
		GN2	LN2	Expansion	Tank	LN2	GN2
	[LPM]	[LPM]	[LPM]	Ratio	[bar]	[K]	[C]
60	0.32	13.33	0.07	182.4	1.14	78.4	144.6
100	0.30	27.57	0.19	146.6	1.09	77.9	141.7
120	0.22	60.38	0.49	122.1	1.08	77.7	141.5

Notice that in Table 5.4 the injected GN2 is converted to the equivalent form. This is done by dividing the GN2 injection gas by the volume expansion ratio to obtain the equivalent liquid form seen in column four. The 200L CLV tank temperatures for the GN2 will be used to account for the sensible cooling required by the cryocooler. This will further reduce the effectiveness of condensing the GN2 within the 200L CLV. Also, the LN2 tank temperature will be used in determining the work output of the cryocooler, given a manufacturer provided curve fit equation. Using an equation similar to Equation 5.6, but for condensing, the required work output via a theoretically sized cryocooler can be determined.

Table 5.5. Number of Cryogenic Refrigerators

Refill time[s]	Theoretical Cryocooler		Experiment Cryocooler		Additional Number of Cryocoolers	Total Number of Cryocoolers
	Condense [LPH]	Heat [W]	Condense [LPH]	Heat [W]		
60	23.4	1035	7.2	317	4	5
100	29.4	1305	7.1	315	5	6
120	42.6	1892	7.1	314	7	8

Table 5.5 shows the estimated theoretical cryogenic refrigerator needed to maintain the system in closed loop. This calculation was performed by summing all LN2 volumes leaving and entering the system. LN2 entering the system is referring to the equivalent volume of the GN2 injected into the system. Furthermore, the LN2 leaving the system is associated with the LN2 that is boiled within the transfer lines due to radiation, convection, and conduction heat loads. The experimental and theoretical cryocooler utilize both latent heat and sensible heat in the calculation. The experimental cryocooler uses the temperature of the LN2 within the 200L CLV to calculate the power required. Then the actual condensation rate for a single cryocooler could be extrapolated given the results of the theoretical cryocooler. The experimental cryocooler column refers to a single AL-300 model mounted during the QCL CCD cooling system experiment. Finally, the number of cryocoolers required is the ratio between the theoretical work divided by the capacity of the experimental cryocooler, which is rounded up. Also, an additional cryocooler is added to account for the one that was operating during the experiment.

Notice that the condensation rate as well as the work for the theoretical cryocooler increases with increasing refill time. This is directly associated with colder GN2 being injected into the PC for longer refill times (see Figs. E.5, 4.11, and E.11). Recall that the differential pressures are roughly constant throughout all refill times. Therefore, GN2 enters the system at lower temperatures which implies more mass enters the system in gaseous form than at warmer temperatures. Thus, a larger or numerous cryocooler is required because more GN2 and heat is added to the system. Therefore, the number of cryocoolers increases with increasing $T_{GN2,injection}$.

In conclusion, the fourth and fifth objective in Section 3.1 were met. The LN2 loss per cycle was determined in investigating the liquid level data for a single cycle. Furthermore, it was used in determining the number of cryocoolers required to

cool and condense the GN2. The single cryocooler capacity and condensation rate is found int Table 5.5. The number of cryocoolers increases with amount of GN2 mass input into the system (see Tab. 5.6). Therefore, the colder the gas temperature the more cryocoolers are needed to condense the GN2 because the latent heat has a larger contribution to the overall work than the sensible heat.

5.3 Injection and Discharge Flow Rate Correlations

This section discusses the procedure in determining the curve fit equation needed to correlate the GN2 injection and the LN2 discharge of the process cylinder. The LN2 discharge volumetric flow rate was determined in Section 5.1. Moreover, the GN2 injection instantaneous volumetric flow rate data will be averaged over the entire interval. A plot of the relationship between the GN2 injection and LN2 discharge flow rates will be developed.

GN2 Injection Flow Rate Averages

The flow rates for the GN2 injection must be averaged over the discharge time. In doing so, this would provide a reasonable estimate of the pump efficiency. In order to approximate the GN2 injection, the data from Figures E.4, 4.10, and E.10 will be numerically integrated over the discharge interval. The numerical integration used is 1/3 Simpson's Rule, which uses quadratic polynomials to approximate the total volume during the discharge of the PC. In order to use this formula, the data must be equally spaced and the number of subintervals must be an even number. The data was adjusted slightly to meet the requirements. Recall that four flow rate curves were extracted and the total volume was estimated for each and then averaged. The following equation represents the 1/3 Simpson's Rule.

$$I(f) = \frac{h}{3} \cdot [f(a) + 4 \cdot \sum_{i=2,4,6}^{N} f(x_i) + 2 \cdot \sum_{j=3,5,7}^{N-1} f(x_j) + f(b)]; h = \frac{b-a}{N} \tag{5.4}$$

Where $f(a)$ and $f(b)$, are the dependent values at the end points of the interval, h is the step size defined as the difference of the independent values a and b over the number of points in the interval N. Finally, the volume $I(f)$ will be summed for each interval of time and divided by 40s, which is the discharge time; this would allow for an estimated flow rate over the PC discharge time. The following code is used to estimate a GN2 injection flow rate. The following table shows the approximate volumes for each of the four cycles seen in Figure G.1, G.2, and G.3 and the corresponding average volumes and flow rates.

Table 5.6. GN2 Injection Average Volume and Volumetric Flow Rates

Refill Time [s]	Cycle Number For Volume [L]				Average	Standard Deviation	Flow Rate	
	1	2	3	4	Volume [L]	Volume [L]	Volumetric [LPM]	Mass [kg/min]
60	8.1	8.3	10.0	9.1	8.9	0.8	13.3	0.024
100	18.7	18.2	18.3	18.3	18.4	0.2	27.6	0.061
120	40.3	39.6	39.9	39.7	40.3	0.2	60.4	0.176

Table 5.6 shows the estimated total volume for each of the four cycles using Equation 5.4 and the coding above. The average of the four cycles was taken. Then that volume was divided by the total injection time of 40s. The standard deviation can be seen in the seventh column. Furthermore, the mass flow rate is provided in the last column of the table. It was calculated using the averaged value of the $T_{GN2,injection}$ GN2 injection temperature (see Figures E.5, 4.11, and E.11). The average flow rates in the table above will be used to estimate the overall pump efficiency as well as derive a flow rate correlation.

The volumetric flow rate in Table 5.6 shows that it is dependent upon the refill time. With increasing refill time the both the mass and volumetric flow rate increases. Recall that the GN2 injection process is fixed at 40s. Therefore, the mechanisms behind this dependance between the refill time and the flow rate is the temperature of the GN2 injection flange temperature (TI-002). The colder this GN2 injection line the lower the temperature. This lower temperature of the GN2 allows more mass into the system than at higher temperatures. This is only true if the supply tank pressure is held constant, which it is. The 160L low pressure CLV supplies GN2 at 22psig continuously and is maintained at that pressure via a pressure relief valve.

Volumetric and Mass Flow Correlations

Using the flow rates for LN2 supply line and the GN2 injection line from Tables 5.1 and 5.6, a correlation between the volumetric and mass flow rates can be found. A correlation can be determined for the inlet and outlet conditions of the PC for a fixed discharge and delay time of 40s and 15s. This correlation can be used to extrapolate different flow rates given the current quasi-closed loop CCD cooling system and PC volume. The figures below will consists of three points, which represent each of the refill times. It is important to understand that the refill time not only controls the volume of LN2 that enters the PC, it also governs the temperature of the GN2

injection line. In other words, a cold GN2 injection line implies less sensible heating to the injected gas and higher flow rates. However, their is a limit for the refill time. This limit is governed by the maximum fill of LN2 within the PC, which is controlled by the orifice of SV-003 (see Fig. 3.2). This will be described in detail below.

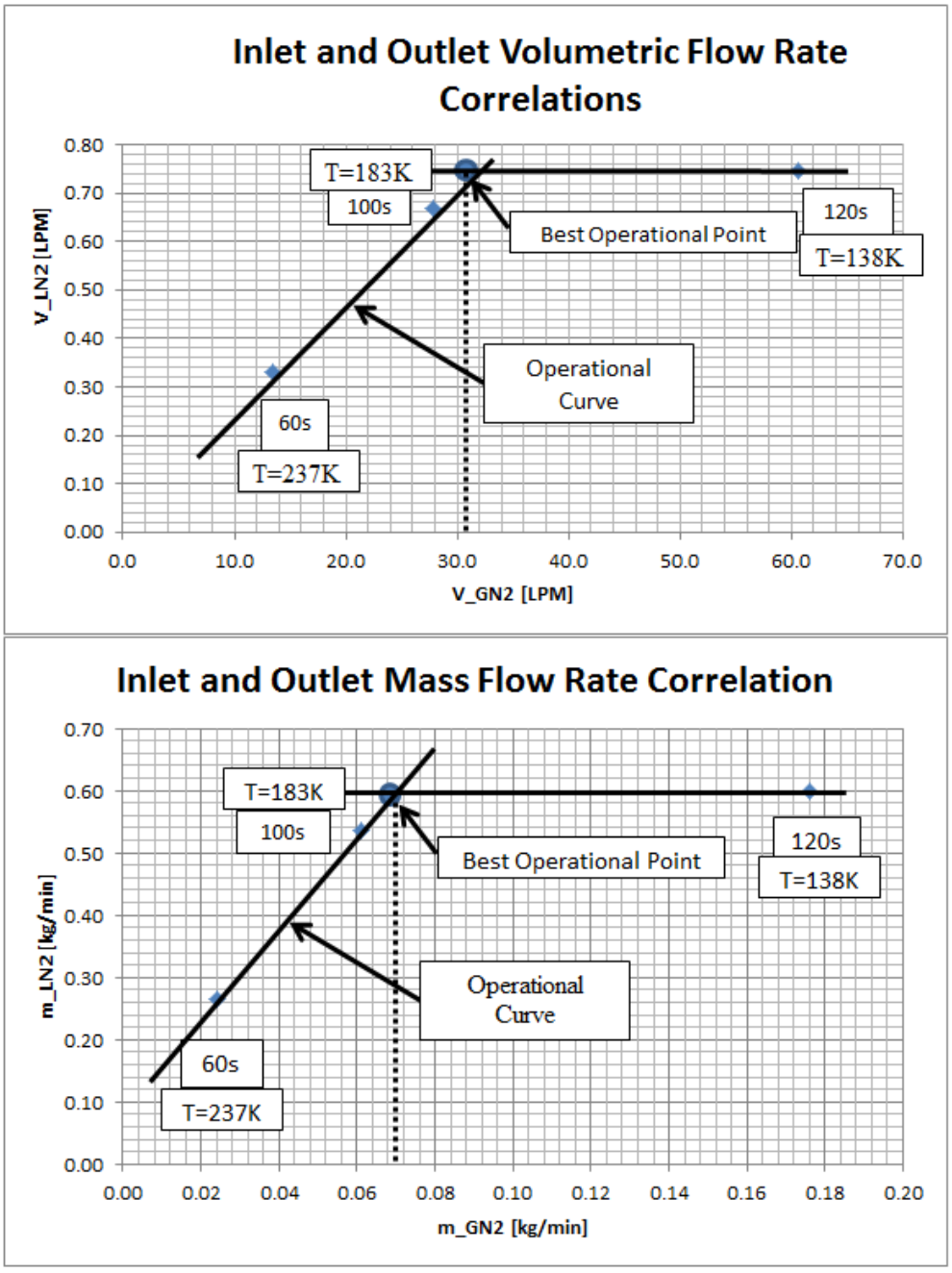

Figure 5.7. Top: Volumetric Flow Rate correlation. Bottom: Mass Flow Rate Correlation

Figure 5.7 shows the flow rate of the required inlet and outlet conditions of the process cylinder for each refill time. The volumetric flow rate is located at the top of the figure and is a strong function of temperature, which affects the curve fit equation used in the calibration process. The bottom portion of the figure represents the mass flow rate of PC given the measured temperature of GN2 injection line fluid. The volumetric flow rate correlation can be used to extrapolate different LN2 flow rate correlations within the 60s to 100s range. These correlations provide a way of estimating the amount of GN2 that is needed to displace a fixed amount of LN2 from the process cylinder.

Notice that their is abrupt rise in flow rate between refill times 60s and 100s. This abrupt change is directly associated with the increase in the time to refill the process cylinder (PC). However, their seems to be almost no increase in LN2 flow rate from refill times 100s to 120s. This is directly associated with the suction end of the process cylinder. In other words, the orifice size of the PC restricts it from refilling further. The maximum fill of the PC occurs at 0.91L, which is independent of the refill time (see Sec. 5.1 *Liquid Level*) after 100s. This independence is a result of the orifice size during a refill, which restricts further flow into the PC. Notice the line intersecting the points of refill times 60s and 100s. This black line provides evidence that their is a linear relationship between the GN2 injected into the PC and the discharged LN2. This linear relationship provides an operating curve that is specific to the process cylinder and current differential pressures for the GN2 injection line and the MCCD transfer tubing. Additionally, notice a horizontal black line drawn through refill time of 120s. Because it is understood that for refill times greater than 120s, the displaced volume will always be 0.91L. This simply states that the LN2 flow rate for any GN2 injection flow rate will peak at 0.6 kg/min or 0.75LPM. The correlation between the refill time and the injection GN2 is simply the temperature. The next section discusses the relationship between injection gas flow rate and the

temperature of this drive gas. Thus, a best operational point can be extrapolated from these points, which maximizes the LN2 flow rate and minimizes the GN2 injection flow rate for this specific case. Recall that the refill process not only fills the PC, but also pre-cools the GN2 injection line. Thus, the best operational point provides sufficient cooling of the GN2 injection line as well as the minimal amount of GN2 for cooling the CCDs. Lastly, the operational curve is valid between the temperature range of 183K to 237K.

In conclusion, this section achieved the second experimental objective in Section 3.1. The GN2 injection flow rate was determined by integrating over the entire discharge time of the measured data. In doing this, Equation 5.4 was used to determine the total volume underneath the GN2 injection curve seen in Figures E.4, 4.10, and E.10. That total volume was divided by the 40s discharge to attain average flow rates for each of the refill times. Finally, the LN2 discharge flow rate was attained by analyzing the liquid level data as seen in Section 5.1. A linear curve fit equation can be used simply by using the points which correspond to refill times of 60s and 100s. While the point corresponding to 120s indicates that the discharge LN2 is independent of the drive gas.

5.4 Overall Pump Efficiency

The overall pump efficiency is the product of the mechanical and thermal efficiencies associated with pumping LN2. The mechanical efficiency is defined in Equation 2.5. Moreover, the thermal efficiency associated with the heat energy transferred to moving the fluid is seen in Equation 2.6. This section will briefly discuss the pressure averages and the differential pressures associated with pumping. Also, the procedure to estimate the heat input via the vaporizer will be discussed. Finally, the overall efficiency will be provided.

Before continuing any further, certain variables must be defined. The first two

variables $\dot{W}_{pump}$ and $\dot{W}_{GN2}$ correspond to the work associated with pumping the LN2 through the transfer lines and the work associated with the GN2 needed to displace the LN2 from the PC. The third variable is $\dot{Q}_{in}$ is the heat input via the vaporizer. The pump work is already defined in Equation 2.1. The fluid work of the GN2 can be defined as the following.

$$\dot{W}_{GN2} = \dot{V}_{GN2,injection} \cdot \Delta P_{GN2,injection} \tag{5.5}$$

Where $\dot{V}_{GN2,injection}$ is the volumetric flow rate of the GN2 measured in FT-001 and $\Delta P_{GN2,injection}$ is the differential pressure that drives this flow. The next equation defines the heat input via the vaporizer.

$$\dot{Q}_{in} = \dot{m}_{GN2,injection} \cdot (h_g - h_f) + \dot{m}_{GN2,injection} \cdot C_p \cdot (T_{GN2,injection,flange} - T_{160LCLV}) \tag{5.6}$$

Where $\dot{m}_{GN2,injection}$ is the mass flow rate of the injected GN2, $T_{GN2,injection,flange}$ is the temperature from the TI-002, and $T_{160LCLV}$ is the temperature of the cold LN2 within the 160L CLV. Lastly, the differential pressure associated with pumping LN2 through the transfer lines is represented by the following equation.

$$\Delta P_{GN2,injection} = P_{160LCLV} - P_{GN2,injection} \tag{5.7}$$

$$\Delta P_{LN2,discharge} = P_{GN2,injection} - P_{200LCLV} \tag{5.8}$$

Where $P_{160LCLV}$ is the constant pressure measured on the 160L low pressure cryogenic liquid vessel, $P_{GN2,injection}$ is the pressure of the GN2 in PT-001, $P_{200LCLV}$ is the pressure measured via PT-002, and $\Delta P_{LN2,discharge}$ is the differential pressure associated with cooling the CCDs.

Average Differential Pressures

The pressure is averaged across the four cycles and the difference is taken, yielding the differential pressure associated with pumping LN2 to the MCCD test

vessel. The data associated with $P_{GN2,injection}$ comes from Figures E.2, 4.8, and E.8. The data associated with $P_{200LCLV}$ comes from Figures E.3, 4.9, and E.9.

$P_{200LCLV}$,The following table shows the discharge differential pressures for four cycles and different refill times, where Equation 5.8 is used. The 160L lower pressure cryogenic liquid vessel (CLV) was maintained at 1.516 bar above atmospheric conditions. Furthermore, the pressures measured via PT-001 and PT-002 are averaged and the difference is taken to determine the average differential pressures. The following table shows the average differential pressures for the GN2 injection line.

Table 5.7. $\Delta P_{GN2,injection}$ Averages for Each Cycle

Refill Time [s]	Cycle Number for Pressure [bar]				Average	Standard Deviation	Average
	1	2	3	4	Pressure [bar]	Pressure [bar]	Pressure Rate [bar/min]
60	0.96	0.96	0.97	0.98	0.97	0.008	1.45
100	1.03	1.02	1.03	1.03	1.03	0.006	1.54
120	1.01	1.01	1.01	1.01	1.01	0.002	1.52

Table 5.8. $\Delta P_{LN2,discharge}$ Averages for Each Cycle

Refill Time [s]	Cycle Number for Pressure [bar]				Average	Standard Deviation	Average
	1	2	3	4	Pressure [bar]	Pressure [bar]	Pressure Rate [bar/min]
60	0.41	0.42	0.42	0.43	0.42	0.006	0.63
100	0.42	0.41	0.42	0.42	0.42	0.002	0.63
120	0.44	0.44	0.44	0.44	0.44	0.002	0.66

Heat Input via the Vaporizer

This portion will briefly cover the input parameters in estimating the heat input via the vaporizer. The heat input via the vaporizer provides the mechanism of creating GN2 that assists in driving the fluid. During the experiment the fluid temperature was monitored closely to assure that the GN2 temperature was above the saturation temperature of the LN2. In other words, the superheated GN2 was passed through the GN2 injection line only. The heat input via the vaporizer is estimated using Equation 5.6. The following table lists the averaged temperatures for TI-001 and TI-002. Data from Tables 5.9, 5.7, 5.8, 5.2, and 5.6 is used in estimating the heat input $\dot{Q}_{in}$.

Table 5.9. $T_{GN2,injection,flange}$ Average Temperatures for each Refill Time

Refill Time [s]	GN2 Injection Temperatures [K]	
	TI-001	TI-002
60	237.0	168.8
100	183.3	186.9
120	138.1	186.3

Results

Table 5.10. Vaporizer Input and Pump Efficiencies

Refill Time [s]	Heater Input [W]	Efficiency [%]		
	Vaporizer	Mechanical	Thermal	Overall
60	258.6	1.48%	8.52%	0.13%
100	715.1	1.04%	6.76%	0.07%
120	1870	0.46%	5.46%	0.03%

Table 5.10 shows the heat input power estimates. Notice that the mechanical efficiency and thermal efficiency decrease with increasing refill times. The overall efficiency is the product of the thermal and mechanical efficiency. Recall that the vaporizer is similar to the GN2 generator electrical input (see Eq. 2.7). The equiva-

lence between the electrical input and the vaporizer is simply the difference between the forms of energy (i.e. work and heat). Also, one of the major assumption regarding Equation 2.7 is that it equals 100%, which means that all the electrical work is transferred into heat energy used to generate GN2. Furthermore, the vaporizer heat estimate does not account for the radiation and convection effects. If it did, the overall efficiency would be significantly less.

Notice that the refill time of 60s has the highest efficiency across all categories. The mechanical efficiency is defined in Equation 2.5. This high efficiency is simply a result of a relatively constant $\Delta P_{GN2,injection}$ and $\Delta P_{LN2,discharge}$ across all refill time samples (see Tabs. 5.7 and 5.8). Therefore, the flow rate, given the relatively steady differential pressures, varies only by temperature of the fluid. Notice that in Table 5.9 shows the temperature of TI-001. This indicates that for refill time of 60s, 237K GN2 is being injected at the lowest flow rate. Thus, the lower the flow rate of the GN2 injection the higher the efficiency. The increased volumetric flow rate affects the velocity of the fluid given the fixed cross section of the existing piping system. Therefore, the higher the velocity of the fluid the higher the heat transfer. In contrast, the lower the temperature of the injected gas; the higher the GN2 flow rate and the lower the overall efficiency. The lower overall efficiency is associated with a higher speed fluid, which enhances the heat transfer of the vaporizer to some degree. The pump efficiency can be increased if the PC could refill and discharge correctly.

In conclusion, the third objective in Section 3.1, which is to attain the pumping efficiency, has been completed. The GN2 flow rate was determined using Simpson's rule and dividing that by the total 40s interval for an injection. The differential pressures was determined and averaged over the entire interval. The overall efficiency is dependent on the temperature provided via the vaporizer. The vaporizer efficiency was estimated using know the LN2 temperature of the 160L LP CLV and

the $T_{GN2,injection,flange}$. Recall that the longer the fluid remains stagnant during a refill within the 160L CLV and the SV-001 (see Fig. 3.2) the more heat energy is added. Hence, the refill time of 120s has the highest energy added to the fluid because it has the longest stagnant flow time in the GN2 injection line. Also, it has the highest flow velocity, which increases the convection coefficient or. The heat added to the fluid via the vaporizer would be the thermodynamic equivalence to the heater input for a complete cryogenic OPP. Also, the overall efficiency (see Tab. 5.10) would become significantly less if the radiation and convection heat transfer effects were factored in.

CHAPTER 6
DISCUSSION

6.1 Measurements

The data has shown consistent trends with the theory and engineering principles. Discharge LN2 flow rate is an estimate and not to be taken as a highly accurate measurement. Thus, the calculated data are simple estimates consistent with the theory and engineering principles. The other measurements taken were from highly accurate instrumentation, which were routed to a computer via a cFP and cRIO (see Sec. 3.3). The compact field point (cFP) sends a signal to a relay switch to actuate the solenoid valves. Also, it provides voltages to the heaters and so forth. The cRIO provides power to the temperature, pressure, and flow meters. Both cFP and cRIO accept the output signals from the instrumentation to be interpreted in LabView and recorded into a data file.

The flow meters (FT-001 and FT-002) were calibrated slightly different. FT-002 on the GN2 injection line was calibrated in house in similar conditions [4]. This was performed using a 160L CLV LN2 supply dewar and a large section of copper pipe for a vaporizer. Similar experimental temperatures and pressure were recorded. The flow rates in which the output data of the FT-001 is correlated with is with a Dwyer 0-200SCFH. The Dwyer flow meter is calibrated with air, but can be converted to N2 gas using the manufacturer provided equations. The overall accuracy of this measurement is 3.5%. Therefore, the GN2 injection measurement is not as accurate as typical turbine flow meters. However, the measurement is acceptable as the overall flow rate trend is captured. The FT-002 measurement was ignored due to a two-phase flow passing through the meter. Any two-phase flow entering a turbine flow meter produces erroneous measurements.

Therefore, data collected from this turbine flow meter (FT-001) was ignored. Recall that this flow meter measures the discharge flow rate of LN2. It could be accounted for by analyzing the liquid level during the various parts of the cycle (see Sec. 5.1). The LLP was calibrated by Teragon and is capable of recording the liquid level fill height to 1% accuracy [11]. Also, the flow through the MCCD transfer lines and the CCD heaters causes some LN2 to boil as it travels through the line. The LN2 level was corrected to account for the boiled gas, which made up nearly 35% of the total measurement. This being the most indirect measurement in the experiment forces the calculated data to become estimates not accurate measurements.

The pressure transducer (PT-001 and PT-002) data is recorded with relatively high accuracy of 0.25%. The only issue that has arisen is the calibration constant associated with $P_{200L,CLV}$ data (PT-002), which was off by nearly 33% (see Figures G.4, G.5, and G.6. The data collected in $P_{160L,CLV}$ (PT-001) is accurate to 0.25% and can be seen in Figures E.2, 4.8, and E.8.

The RTDs (TI-001 to T-004) are platinum and are accurate to 0.20 % [11]. TI-001 and TI-002 are surface mounted on copper and stainless steel tubing. Insulation is wrapped around the platinum RTDs. Copper with its relatively high thermal conductivity represents the temperature of the nitrogen gas or liquid inside of it. TI-002, being surface mounted on stainless steel and insulated provides a sufficient reading due to the low temperatures of the GN2. TI-003 measures the temperature of the GN2 and TI-004 measures the temperature of the LN2. Overall the platinum RTDs depict the temperature trends very accurately. Furthermore, the RTDs mounted on the CCD focal plate are exactly the same platinum RTDs used for TI-001 to TI-004.

Error Bars

The various measurements taken were averaged in order to attain the needed

data to calculate the efficiency, heat input, or density. Of the recorded data for each parameter, a total of four cycles were averaged. The standard deviation was found. Therefore, the following figures show the various data for refill time of 100s, which include error bars. Appendix F shows the raw data as in Section 4.2.

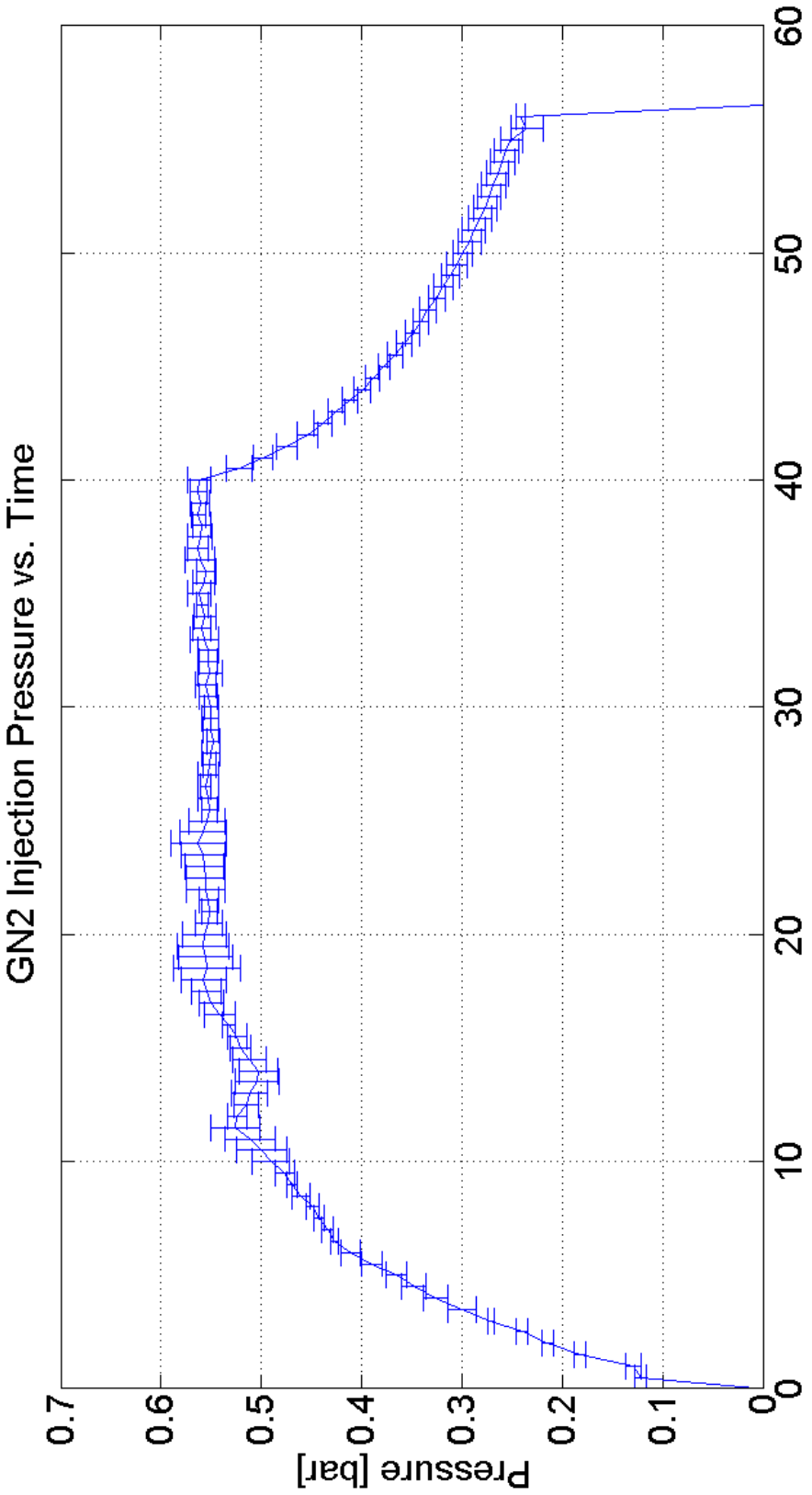

Figure 6.1. GN2 Injection Pressure vs. Time (refill=100s)

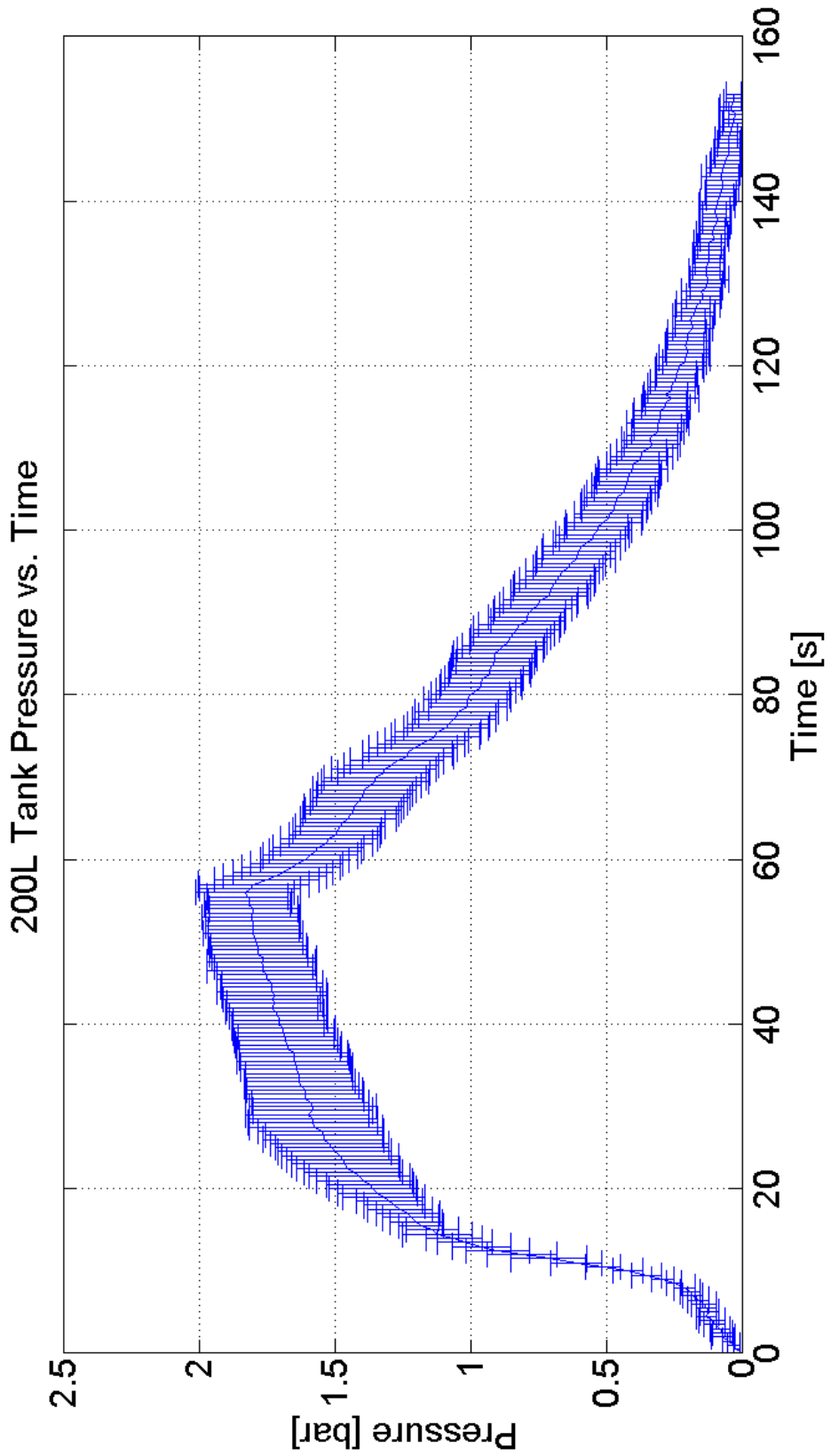

Figure 6.2. 200L Tank Pressure vs. Time (refill=100s)

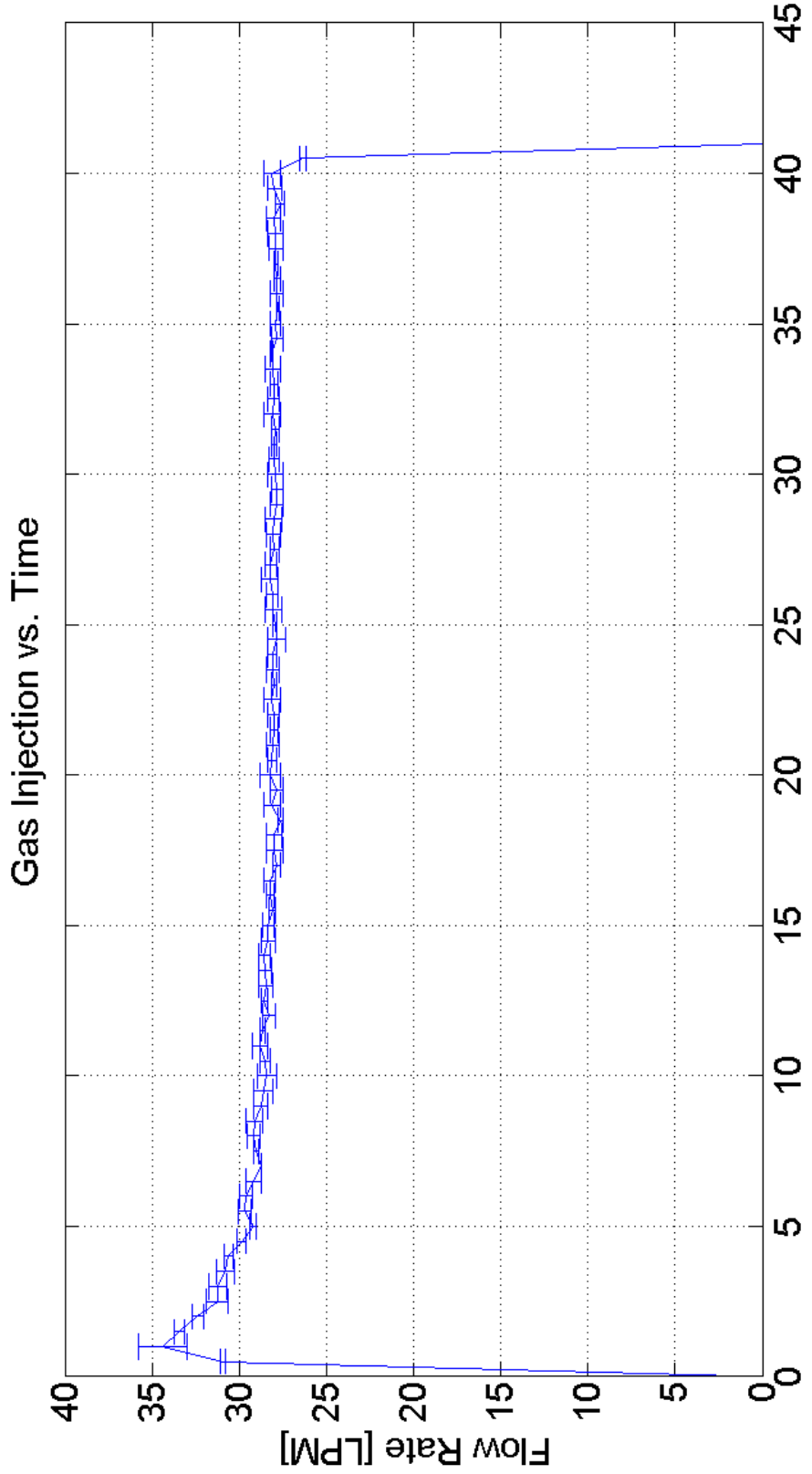

Figure 6.3. GN2 Injection Flow Rate vs. Time (refill=100s)

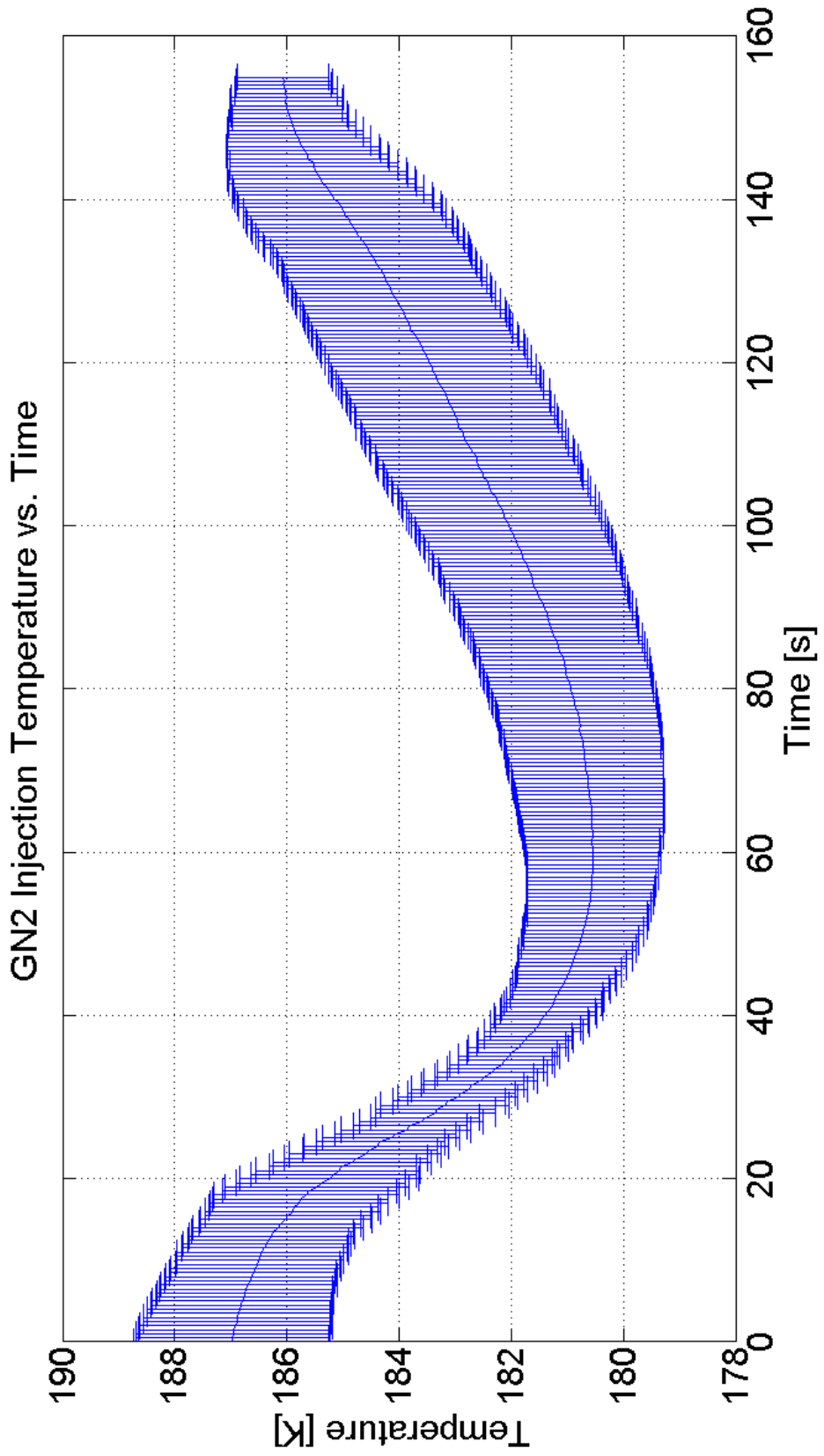

Figure 6.4. GN2 Injection Temperature vs. Time (refill=100s)

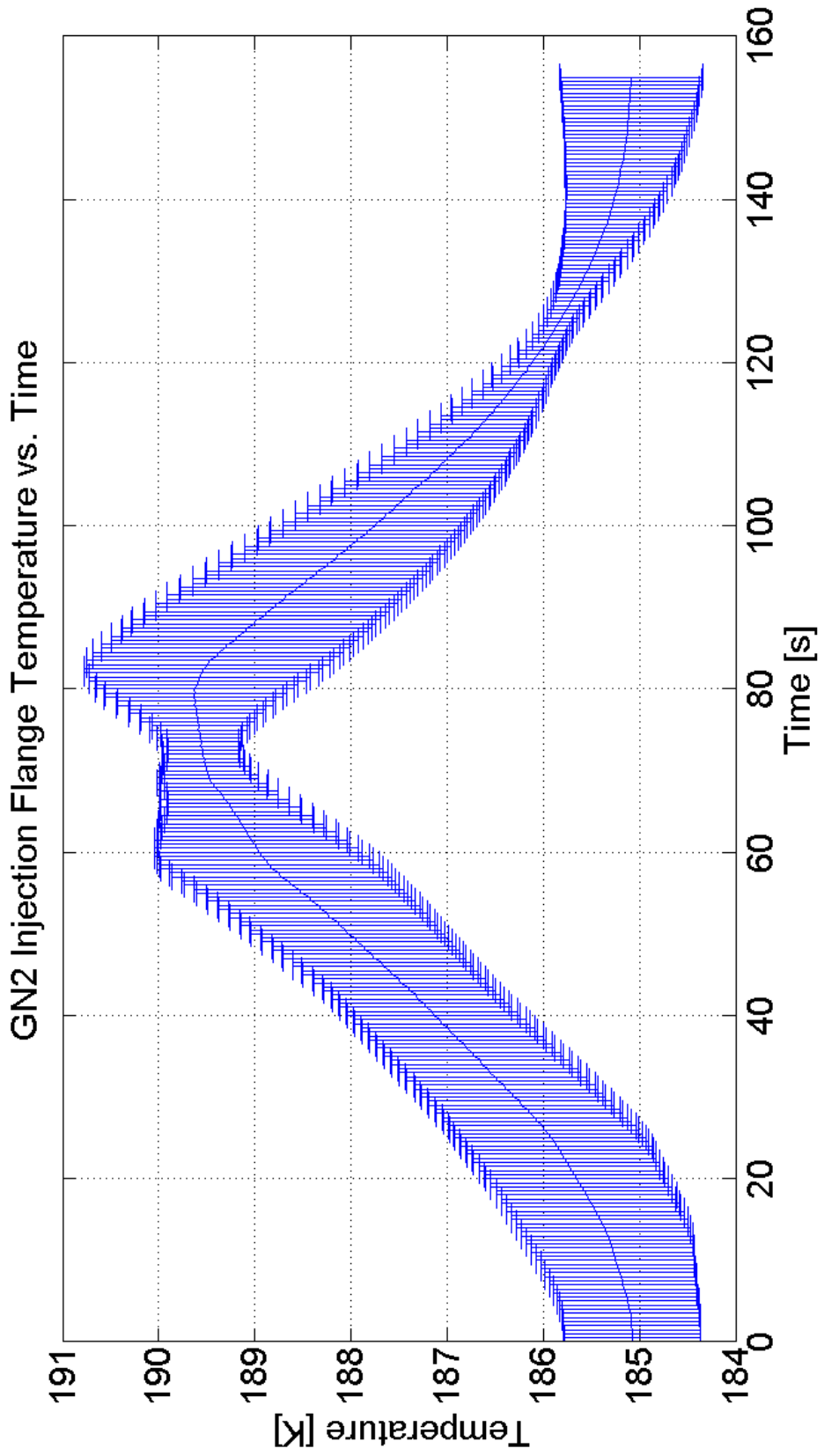

Figure 6.5. GN2 Injection Flange Temperature vs. Time (refill=100s)

Figures 6.1-6.5 shows the variation of the measured data for four different cycles. The data from four different cycles were averaged and the standard deviation between each consecutive point was found. Each of the figures above show a single cycle that which is averaged from four different cycles. Notice that the GN2 injection flow rate (Fig. 6.3) has a small standard deviation, which means the measurement is captured very well. Also, notice that in Figures 6.4 and 6.5 show a large variation in the recorded data across four cycles. This is associated with the large variation in temperature between each consecutive cycle.

In conclusion, most of the instrumentation measures the data accurately. However, due to the LN2 discharge flow rate estimation via the liquid level probe and the platinum RTD, the data collected become rough estimates. Despite, the slight discrepancies in the measurement, the cryogenic OPP pumping trends are depicted very well through the data. The error bar data (Figs. 6.1-6.5) show that the repeatability of the GN2 injection flow rate is okay. However, the temperature readings show that their is some poor reproducibility of the measurement, which is a result of the RTD being surface mounted.

6.2 Experimental versus Theoretical OPP

The *Results* Section shows evidence of the focal plate is cooling (see Sec. 5.1) and the number of cryogenic refrigerators (see Sec. 5.2). A fundamental cryogenic OPP model was derived in Section 2.3. This model with the similar pressure inputs can simulate the theoretical performance of the OPP. The GN2 injection flow rate attained in Section 5.3 are plugged directly into the theoretical model code. Recall that the primary assumptions of this model involve adiabatic drive gas, one to one volume displacement, and average properties. Table 6.1

Table 6.1. Experimental versus Ideal Pump Model Data

Refill	Efficiency [%]		Pump Work [W]		Energy Input [W]		LN2 Volume Flow Rate [LPM]	
Time [s]	Experiment	Model	Experiment	Model	Experiment	Model	Experiment	Model
60	0.13%	0.50%	0.23	1.48	258.6	294	0.33	13.3
100	0.07%	1.95%	0.46	11.88	715.1	610	0.67	27.6
120	0.03%	8.43%	0.54	112.6	1870	1335	0.75	60.4

Notice that the comparison between the experimental data and the model is compared across four different categories. The first is the overall pump efficiency, which is the ratio of the pump work to the heat input via the vaporizer. The next is the pump work, which is the product of the LN2 volumetric flow rate and the measured differential pressure. Moreover, the energy input refers to the estimated volumetric efficiency, which is simply the sum of the latent energy and the sensible energy. Finally, the LN2 volumetric flow rate refers to the measured LN2 volumetric flow rate from FT-001.

Table 6.1 shows a large deviation in the pumping efficiency. This difference is associated with a large difference in the volumetric efficiency between the experiment and the model. The model assumes a volumetric efficiency of 100%. The calculated volumetric efficiency of the experiment is simply the LN2 volumetric flow rate divided by the GN2 volumetric flow rate, which for refill time of 60s is nearly 1/40. In other words, to displace a liter of LN2, one is required to inject forty liters of GN2.

The pump work is low experimentally. Once again, this could be attributed to the poor volumetric efficiency. Notice the very low volumetric flow rate. Therefore, when that volumetric flow rate is multiplied by the corresponding differential pressure (see Table 5.7), a pump work of less than 1 W is calculated. Because of the high volumetric efficiency, the model has an increasing pump power with increasing volumetric flow rate for constant cross section tubing. This makes sense as it requires more energy to flow more LN2 through the lines than.

The next column estimates the energy input via the vaporizer. This was approximated in knowing the gage or saturation pressure of 160L CLV and the measurement taken at TI-002 (see Section 6.1 of the platinum RTD). The estimate of the heater input is slightly larger than estimated, which is a result of TI-002 being a surface measurement and not a bulk fluid temperature measurement. The notice-

able difference between the model and the experiment is strictly associated with the measurement device used in calculating the heat input via the vaporizer.

Finally, the noticeable difference between the model and the experimental flow rate is highlighted in the last column of Table 6.1. The difference is attributed to the volumetric efficiency being drastically different between the model and the experiment. This difference in the volumetric efficiency is likely associated with a partial fill of the process cylinder. This partial fill of LN2 with a constant GN2 injection time, injects gas through the transfer lines to the tube heat exchanger.

This next figure shows a modified version Figure 2.2, which shows a plot of the overall efficiency versus heater input versus GN2 injection volumetric flow rate.

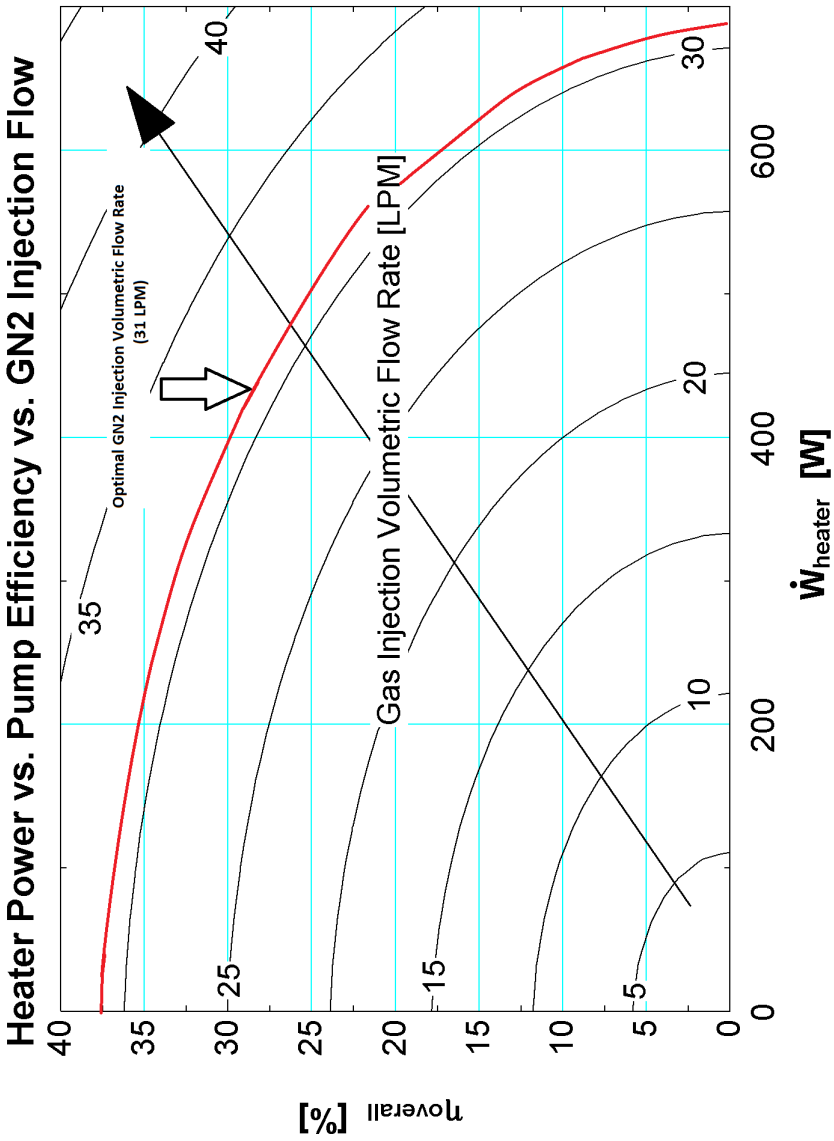

Figure 6.6. Heater Power versus Pump Efficiency versus GN2 Injection Volumetric Flow Rate

Figure 6.6 shows the modified theory. Recall from Section 5.3 that an estimated best operational point was attained, which is 31LPM. Therefore, any GN2 injection flow rate greater than 31LPM is simply excess gas that is unused. Therefore, the following theoretical figure could be modified and should ignore flow rates greater than 31LPM. From the figure above, the maximum theoretical efficiency attainable for this pump is roughly 36% given the current refilling issues of the process cylinder. In other words, LN2 discharge approaches a maximum value where the injected GN2 does not displace anymore LN2 due to the PC refilling with only 0.91L for any refill time larger than 100s. Therefore, any additional injected GN2 that enters the system is just excess gas.

In conclusion, heat transfer effects are contribute to the differences between the theoretical and experimental GN2 injection volumetric flow rates and the heater inputs. The heater input for the experiment is equivalent to the vaporizer. While the heater input in theory is equivalent to a submerged heater boiling LN2. In order to navigate to higher operational efficiencies the use of an orifice plate or flow restriction device as well adjusting the heater. Sensible heating of the GN2 contributes to a lesser GN2 volumetric flow rate due to a higher bulk fluid temperature. Heat losses of the injected GN2 contributes to higher heater power. Finally, the theory can be limited further as a result of the best operational flow rate attained from Section 5.3. Therefore, the maximum efficiency attainable by the OPP, given the current testing conditions, is only 36%.

6.3 Pumping Characteristics

The pumping characteristics of a simplex, single-acting, direct-acting pump will be applied to the OPP. The properties of the OPP that will be discusses involve the pump cycle, stroke length, and the plunger speed (see Eq. 2.12). Each of the properties will be discussed in detail below. The following table shows the calculated

parameters for the cryogenic over-pressure pump (OPP).

Table 6.2. Cryogenic Over-Pressure Pump Characteristics

Refill Time [s]	Pump Cycle Time [cycles/min]	Stroke Length [cm]	Plunger Speed [cm/min]
60	0.52	6.6	6.9
100	0.39	12.2	9.5
120	0.34	12.2	8.3

Table 6.2 shows the stroke length and the plunger speed. Notice the stroke length increases with increasing refill time. The stroke length plateaus at 100s and remains constant at 12.2cm. This plateau effect directly corresponds to the volume analysis seen in Section 5.1 Liquid Level Analysis, where the refill of the PC remains at 0.91L for any refill time greater than 100s. Recall that this fixed fill volume is associated with the an insufficient orifice. Notice that the plunger speed plateaus at 9.5 cm/min. The pump cycle time is simply the number of completed cycles per minute. Recall that a complete cycle is the sum of the discharge, delay, and refill times. The stroke length was determined by dividing the total volume during a refill (see Tab. 5.1) to the cross sectional area of the process cylinder. The dimensions of the PC used are in Section 3.5. Lastly, the plunger speed is the product of the cycle time and the stroke length as seen in Equation 2.12. Also, the plunger speed refers to the GN2/LN2 moving interface within the PC during the discharge portion of the OPP cycle.

The pump speed is significantly faster for refill time of 60s because it is a strong function of the refill time. Notice that the stroke length for refill time of 60s compared to the other refill time is nearly half. This stroke length is dependent upon the refill time, which corresponds to the LN2 volume that enters the PC. The LN2 volume that enters the PC plateaus at 0.91L and remains that way. Hence, the

stroke length remains the same for refill times of 100s and 120s. Therefore, longer refill times are associated with a larger stroke length, but remains constant for refill times greater than 100s. This plateau occurs as a result of a small orifice that restricts the flow of the solenoid valve. The plunger speed similar to the stroke length plateaus at 9.5 cm/min for refill time of 100s. The reason for this peak value is a result of the plunger speed equation being the product of the pump cycle time and the stroke length. Despite, refill times of 100s and 120s having the same stroke length, their cycle times are different.

In conclusion, the last experimental objective has been completed. The pump speed is slow as compared to other pumps. This provides evidence that the components will work less than typical reciprocating pumps. Because of the slower pump speeds, it is expected that the pump will have a longer operational time. Lastly, it is seen that the stroke length plateaus at 12.2 cm. This constant stroke length with increasing refill times greater than 100s is associated with the suction issues of LN2 during a refill.

6.4 Failure Modes of Pumps

The cryogenic over-pressure pump (OPP) has high potential in out performing centrifugal, positive displacement reciprocating, and just about any dynamic mechanical device used for pumping. Most centrifugal and positive displacement pumps are very mature technologically, but most have many moving parts. These devices evolved through improving bearings, packing, impeller, or piston designs for optimal performance. The cryogenic over-pressure pump when compared to current pumping technologies is fundamentally simple and can is expected to require little maintenance. The next paragraph briefly discusses the major components of centrifugal pumps, reciprocating pumps, and the OPP.

The cryogenic OPP, in theory, has three major components: GN2 generator,

PC, and control valves (see Sec. 2.2 for the description of the components). Therefore, the primary components of a centrifugal and reciprocating pump will be identified. Fundamentally, the centrifugal pump has an impeller and volute. The impeller is used to accelerate the fluid, which results in a low pressure within the volute. Thus, generating a differential pressure. Reciprocating pumps have a pumping chamber, piston, plunger or diaphragm, and suction and discharge nozzles.

Centrifugal pumps have impeller mounted on a drive shaft that is rotated typically by an electric motor. The shaft sits on bearings and bears the load of the impeller. Typical failures that occur with such pumps are the pump bearing that is included in the shaft seal as stated in *High Efficiency, Variable Geometry, Centrifugal pump* [5]. Additionally, the failure is observed with the DES project centrifugal pump. A shaft seal failure only exists if the motor is outside the pump casing, which is not submerged within the liquid. As for the DES centrifugal pump, a fully submerged LN2 pump, the primary mode of failure consists of cage or ball retainer wear, which is associated with shaft vibrations. The vibrations are induced from two known sources. The first is cavitation on the impeller during start-up. The second is a result of the shaft being imbalanced and results in a detrimental wobble in the shaft-bearing system. A typical maintenance schedule for the DES centrifugal pump is based on the provided recommended maintenance time of 4000hrs (5 months), which is found in the manufacturer provided pump manual. Further specifications and an engineering drawing of the Barber-Nichols pump can be found in *1.5.2.5 and 1.5.2.2.1.5 Reference Manuals (Imager Vacuum and LN2 Cooling)* under BNLNG-01B-M1.pdf [11].

A reciprocating pump mode of failure are within the packing and plunger/piston/diaphragm. These components can be seen in the following image.

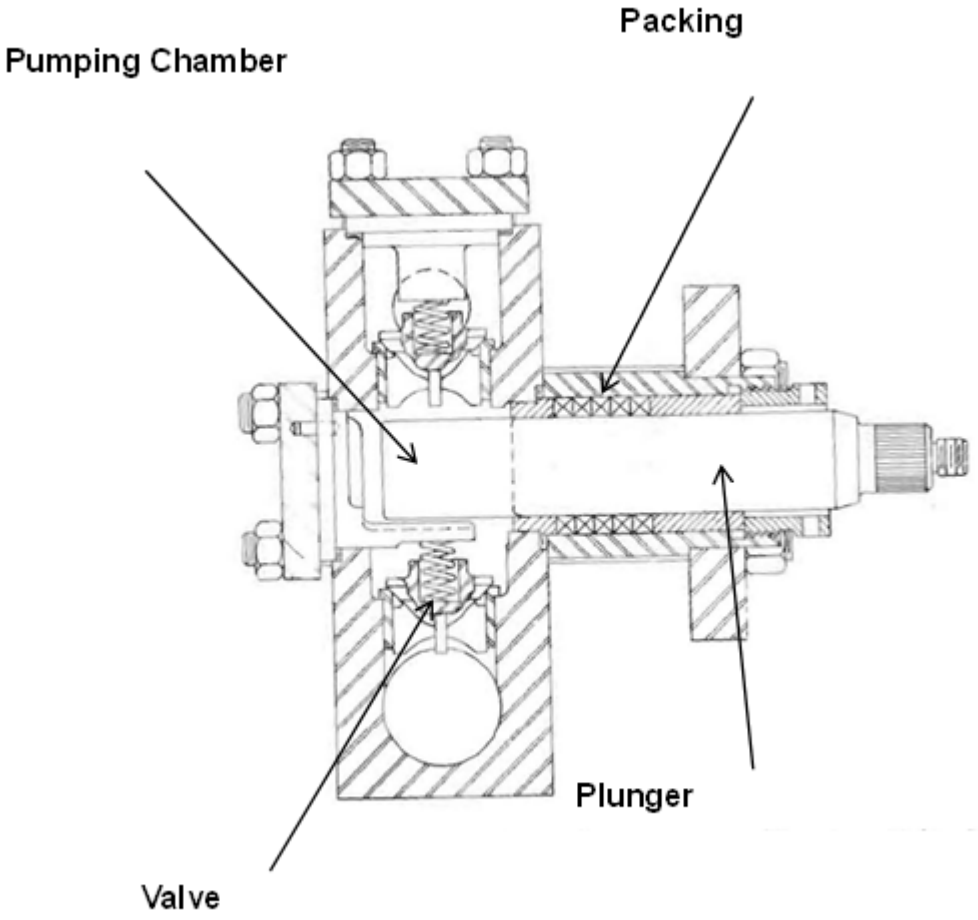

Figure 6.7. Reciprocating Pump and Components [14]

Typical failures for reciprocating pump are associated with the packing. The packing can also be seen in Figure 1.6 within the stuffing box. Notice that the stuffing box actuates the piston or plunger back and forth. An estimated packing maintenance schedule is about three months [14]. Following the packing, the plunger or piston must be replaced every six months [14]. The packing failure is associated with the chemically reactive lubrication, sufficiently applied lubrication, and the alignment of the piston or plunger. Recall that the packing allows a motor or a drive fluid to transmit its power to the process fluid. The valves of the reciprocating pumps typically must be changed every two years. Cavitation within a PD pump can result in power end of a power pump to become damaged (i.e. damaged gears or packing). Cavitation will transmit vibrations and shock to the gears and packing of power and direct-acting pumps.

Despite not having performed a reliability study of the components of the OPP, it is likely that the components can easily last for at least one year. For instance, the McMaster-Carr solenoid valves (SV-001 and SV-004) are rated to 500,000 cycles [17]. Therefore, if actuated once every minute for twenty-four hours a day seven days a week, the SV will fail after 347 days. This is rather promising. Furthermore, in eliminating the mechanical device that drives the fluid, cavitation no longer becomes an issue. This is a result of eliminating all moving parts. However, the GN2 generator becomes the component that is susceptible to premature failure. This failure can result in thermal cycling of the heater from well above 300K to as low as 77K. McMaster-Carr indicates that a cartridge heater (item #:3618K148) can last for one year before being replaced [15].

In conclusion, the cryogenic OPP is a simple design. The primary components are do not operate at high speeds. Instead, the heater component of the OPP would operate at high temperatures to generate the gas. Low maintenance cycles can be

expected from the OPP than from the reciprocating PD pumps and centrifugal pumps. In summary, the primary modes of failures for each pumping system is the packing for both reciprocating pumps and centrifugal pumps. Furthermore, bearing failures are another common means of failure for centrifugal pumps. The OPP utilizes existing valve technology and eliminates any high speed machinery; the OPP replaces it with a submerged electric heater and control valves.

6.5 Cost Comparison of an OPP vs. Centrifugal Pump for the Dark Energy Survey

A comparative cost analysis for the Barber-Nichols centrifugal pump and the cryogenic over-pressure pump is pursued. It assumes that both pumps will operate at CTIO Blanco 4m Telescope CCD cooling system. The DES project is planned for a five year survey. Thus, maintenance and repairs must be made on the CCD cooling system. Recall from Section 6.4, that the primary modes of failure for the centrifugal pump are the bearings. Also, the primary mode of failure for the OPP are the control valves and the heater in the GN2 generator.

This estimation assumes that the OPP will operate at similar pressure and temperature conditions and in a closed-loop system. This implies that a total of 5 cryogenic refrigerators are required (see Sec. 5.2 for the description behind the number of cryocoolers). Also, the OPP will operate with similar LN2 discharge and GN2 injection volumetric flow rates attained in Tables 5.1 and 5.6 for refill time of 60s. Recall, that the OPP is capable of cooling the focal plate at low volumetric flow rates. System cost, pump components, and an estimation of the work hours required for each pump will be compared. The following tables only focus on cost differences. For instance, the costs incurred by the transfer hosing, valve and instrumentation, and the telescope imager are roughly the same no matter the pump used. This assumption is based on finding an alternative pump design to the centrifugal pump

that will operate in the current CCD cooling system with some minor modifications. Lastly, all values calculated in this section are determined based on 2011-2012 prices.

The first table shows the cost of the pumping equipment. Given similar costs for the transfer hosing, telescope imager, and the valves and instrumentation. The following table shows costs that are significantly different.

Table 6.3. System Cost

System Cost						
Pump Type	Part #	Part Description	Price [$/unit]	Quantity	Final Price [$]	Total Cost [$]
Centrifugal	Pumping Resevoir	200 L Cryogenic Liquid Vessel	$ 61,800	1	$ 61,800	$ 125,000
	AL-300	Cryogenic Refrigerator System	$ 33,000	2	$ 33,000	
	BNLNG-01-000	Submersible Transfer Pump	$ 30,200	1	$ 30,200	
Over-Pressure Pump	Pumping Resevoir	200 L Cryogenic Liquid Vessel	$ 77,250	1	$ 77,250	$ 242,250
	AL-300	Cryogenic Refrigerator System	$ 33,000	5	$ 165,000	
	P-001	Over-Pressure Pump	$ 2,511	1	$ 2,511	

The table above shows the system costs, which encompasses just the 200L CLV, the number of cryogenic refrigerators, and the pumps. These three components incur the largest cost to the given CCD cooling system. This encompasses costs associated with the pumping reservoir or the 200L CLV. The prices for the centrifugal pump are known as it was the initial design. The prices for the over-pressure pump are estimates based on the costs incurred on prototype design. The over-pressure pump is composed of a process cylinder, GN2 generator, and solenoid valves. The fundamental component prices are summed and provide the value.

The largest difference between the centrifugal pump and the over-pressure pump is the cost of the cryogenic refrigerators. Notice that five cryocoolers are required. The number increases because the heat added via a 260W (see Sec. 5.4 for estimated vaporizer heat input for refill time of 60s) heater from the GN2 generator must be removed. Also, the heat load on the system must be removed as well. Another major difference is the cost of the pumping system. Notice that the over-pressure pump is significantly less in price than the centrifugal pump. This price difference is a result of the simplicity of the over-pressure pump, which encompasses inexpensive parts. The next table summarizes the parts that are needed for repairs over the entire life of the Dark Energy Survey, which is five years.

Table 6.4. Replacement Pump Components

Replacement Pump Components								
Pump Type	Part #	Part Description	Price [$/unit]		Quantity	Final Price [$]		Total Cost [$]
Centrifugal	VF-S11-2004-PM-WN	Variable Frequence Drive	$	1,030	1	$ 1,030	$	35,810
	N/A	Bearing Replacement Kit	$	1,250	20	$ 25,000		
	BNLNG-01-003	Impellar	$	2,700	1	$ 2,700		
	BNLNG-01B-015	Rotor and Stator	$	2,800	1	$ 2,800		
	BNLNG-01-001	Impellar Housing	$	880	1	$ 880		
	BNLNG-01-007B	Shaft-Rotor Assembly	$	3,400	1	$ 3,400		
Over-Pressure Pump	4710T12	Solenoid Valves	$	317	20	$ 6,340	$	10,592
	4816K124	316 SS threaded pipe (1/2")	$	24	4	$ 48		
	4816K124	Fitting Adapter	$	35	4	$ 70		
	4816K126	316 SS threaded pipe (3/4")	$	27	2	$ 27		
	2PA75	Hose Clamps	$	17	2	$ 17		
	2FGG6	316L SS Tube (4"OD)	$	115	4	$ 230		
	1RUB1	Pipe Cap 316L SS (4")	$	51	4	$ 102		
	3559K23	Cartridge Heater (10")	$	46	5	$ 228		
	N/A	Miscellaneous		N/A	N/A	$ 3,531		

Table 6.4 represents the costs incurred over the five year survey. During the five year survey the centrifugal pump will need twenty bearing replacement kits; a pump bearing replacement is completed four times a year or every 2100hrs. The reason for this is to not have a catastrophic failure, which occurs every 2800hrs. Also, the cost estimate assumes that most of the relevant components will be replaced at least once throughout the five year survey (i.e. impeller, rotor and stator, impeller housing, etc.). The Over-pressure pump is expected to have maintenance schedule of one year. Thus, a total of four cryogenic solenoid valves are needed; two for the process cylinder and two for the GN2 generator. Finally, the miscellaneous cost is added contingency. This contingency is calculated as the sum of the final prices of the replacement components divided by two.

Notice a significant difference in price between the total costs of each pump. This difference is associated with 'off the counter' replacement parts for the over-pressure pump. While the centrifugal pump requires special machined components. The largest costs incurred for both pumps are the bearing replacement kits and the solenoid valves. The parts seen in Table 6.4 are either from Barber-Nichols, McMaster-Carr, or Grainger. The part numbers for the over-pressure pump in the table above can easily be found on the suppliers website. The Barber-Nichols replacement components are found from purchase orders made at FNAL. While the parts need to be replaced, the individuals who replace them must be paid. Thus, the following table involves the costs involved in paying the workers.

Table 6.5. Repair Crew [25]

Labor							
Pump Type	Worker	[$/hr]	Work Hours	Worker Cost [$]	Total Cost [$]		
Centrifugal	Mechanical Engineer Technician	$ 27.00	800	$ 21,600	$	55,352	
	Mechanical Engineer	$ 42.19	800	$ 33,752			
Over-Pressure Pump	Mechanical Engineer Technician	$ 27.00	160	$ 4,320	$	11,070	
	Mechanical Engineer	$ 42.19	160	$ 6,750			

Table 6.5 shows the wages of a mechanical engineer technician and a mechanical engineer. Though multiple technicians and engineers may be assigned to repair the pumps, the table shows the wage for an individual technician and engineer. Also, the above estimate assumes that the number of workers are the same for both the centrifugal and over-pressure pumps. The work hours for the centrifugal pump is calculated by assuming that the repair will take place over a five day period, four times a year for five years, and for an eight hour work day. The repair hours is based upon the literature value of roughly 2800hrs between failures. Thus, a value of 2100hrs is selected as the maintenance time period to prevent any catastrophic failure. Similarly, the over-pressure pump maintenance schedule is based upon the solenoid valves guaranteed to operate for at least 500,000 cycles. Given the 500,000 cycles, the current cycle time (refill=60s, delay=15s, and discharge 40s) allows each solenoid to be turned on once every minute. Therefore, the solenoid valves are guaranteed to operate for 348 days, which is very close to a year.

Notice that the worker hours for repairing the centrifugal pump is nearly four times larger than for the over-pressure pump. This difference is associated with the estimated work hours. Because the over-pressure is estimated to have maintenance schedule of a yearly basis, the number of work hours required for the repair team is significantly less given the similar wages. The wages are determined from *Bureau of Labor Statistics* [25]. The next table shows the electrical cost associated with the electricity supplied to each of the pumps and the cryogenic refrigerators.

Table 6.6. Electrical Costs

Electrical Costs						
Pump Type	Component	Power [kW]	Hours	kWh	Cost [$]	Total Cost [$]
Centrifugal	Submersible Transfer Pump	0.22	41400	9108	$ 1,157	$ 80,024
	Cryogenic Refrigerator System	15	41400	621000	$ 78,867	
Over-Pressure Pump	Submerged Heater	0.26	43200	11232	$ 1,426	$ 207,166
	Cryogenic Refrigerator System	37.5	43200	1620000	$ 205,740	

Table 6.6 shows the number of hours in which the pump and the cryocoolers are operational. The hours of operation of the pumps and the cryocoolers are the same. This is due to the fact that both will not operate unless the other one is working. Each Cryomech AL-300 cryogenic refrigerator must be supplied 7.5kW of power to remove, at best, 316W of heat from the system. Table 6.3 shows that the centrifugal pump and current system at CTIO has two cryogenic refrigerators. When using the over-pressure pump, the number of cryocoolers increases to five. Therefore, the cryocoolers requires two and five times the electrical power for the centrifugal and over-pressure pump. Lastly, the cost of electricity is $ 0.127 kWh, which is attained from the *Bureau of Labor Statistics* [25].

The electrical costs for the over-pressure pump is over twice the electrical cost of the centrifugal. This is one of the perils of using this type of pump. The cost of the cryocooler and the electrical costs are very significant. Therefore, the number of cryocoolers limits the cost effectiveness of the CCD cooling system for both pumps. The over-pressure pump can only operate if the heat added via the GN2 generator is removed by a cryocooler bank. Lastly, a summary of the all the costs associated with the five year survey that is shown in this section can be seen in the following table.

Table 6.7. Overall Cost

Overall Cost for the Five year Survey			
Pump Type	Cost Type	Cost [$]	Overall Cost [$]
Centrifugal	Initial Costs	$ 125,000	$ 296,186
	Maintenance	$ 35,810	
	Labor	$ 55,352	
	Electricity	$ 80,024	
Over-Pressure Pump	Initial Costs	$ 242,250	$ 471,079
	Maintenance	$ 10,592	
	Labor	$ 11,070	
	Electricity	$ 207,166	

In conclusion, the initial cost of an over-pressure pump is high, which is expected. In *Reciprocating Pumps* [14], Henshaw mentions that the initial cost is typically high. The maintenance costs are typically lower for reciprocating pumps than for centrifugal pumps. Therefore, notice the difference in cost between these pumps and the costs associated with the pump components and the price it costs for workers are different. Due to the simplicity of the OPP, it inherently costs less to maintain with components and worker hours. Finally, the costs associated with electricity and the initial costs for the cryocoolers certainly incur significant costs to the system, especially to a system that has the over-pressure pump installed in it. Therefore, this section indicates that the over-pressure pump should not be installed in the system at CTIO. This is due to the excessive costs associated with the cryogenic refrigerators and the electrical costs associated with them. Also, the OPP is not optimized and requires further research and development. With further research and development of the OPP, the number of cryocoolers will likely be reduced.

CHAPTER 7

CONCLUSION

7.1 Summary of the OPP

The OPP LN2 discharge volumetric flow rates (0.330, 0.668, 0.746LPM) are lower than expected and are intermittent for operational use within the CTIO CCD cooling system. A minimum required flow rate capacity of 7.57LPM (2gpm) was expected from this pump, but was not achieved (see Tab. 2.1). Additionally, the system was tested under the quasi-closed loop CCD cooling system setup. If the system was to operate closed loop for refill time 60s, then a total of 5 cryocoolers would be required. This adds to an even higher initial cost; each cryogenic refrigerator costs about $ 33,000 each. Notice the overall cost difference seen in Table 6.7. However, experimentally it has been shown that the cryogenic OPP is capable of cooling the focal plate to 173K with lower and intermittent flow rates, which was the primary objective. Future research of the OPP can result in improved operational time of future telescopes, such as, the European Extremely Large Telescope. The more hours a telescope is in operation the more data astronomers can analyze. Moreover, scientists can utilize the telescope on a yearly basis than previously done due to a projected decrease in mean time between maintenance. In other words, the less operational time of the Blanco telescope implies that less data that will be collected, given a certain funding period.

The focal plate RTDs and the averaged flow rates of the GN2 injection line and the LN2 discharge line indicates strongly that the OPP was pumping LN2 through the transfer lines at low flow rates. Figures 5.1-5.3 graphically show that the focal plate has a warming trend due to the heaters regulating the focal plate temperature. Individual RTD temperature can be seen at temperatures below the designated set

point of the focal plate, which is 173K. Furthermore, the LN2 level data showed that the volume of the LN2 decreased during a refill (see Section 5.1 *Liquid Level*. Additionally, the volume of the tank increased slightly during a discharge of the process cylinder. The fact that the refill volume is larger than the discharge volume of the process cylinder(i.e. for refill time of 100s V_{refill}=0.495 $V_{discharge}$=0.220) clearly indicates that their is LN2 flowing through the MCCD transfer lines (see Tabs. 5.1 and 5.2).

The timing sequence, discharge, delay, and refill, are important in the OPP operation. The refill time of the PC depends upon the volume that fills the PC. The fill volume during a refill is a direct result of the size of the orifice of the solenoid valve. This effects the stroke length, which then effects the discharge time. The discharge time is the time to displace a fixed volume of LN2 out of the PC. Recall that the corrected refill time was estimated to be 35-40 seconds for all three sample times for the current OPP configuration. Therefore, the inflow volume should equal the discharge volume so that it is understand GN2 is not flowing through the line. The purpose of the delay in the experiment is to allow for system pressure to reach an equilibrium prior to the next cycle. For instance, during a closed loop operation, the delay would be eliminated entirely. This is a result of the cryocoolers work matching the heat load capacity of the system. The heat load capacity includes the heat leaks into the system as well as the heat load introduced via the CCDs.

The refill part of the OPP timing cycle is a major issue and is the result of the plateau of the fill volume occurring at refill time of 100s. Recall that the hydraulic head of the LN2 level of the tank assisted in the refilling of the PC. SV-001 to SV-004 consume 25W and SV-002 and SV-003 consume 17.5W; this heat energy is added to the system to lift the direct acting solenoid valves off of their seat. That heat energy to power the coil is conducted through the brass diaphragm to LN2. This

heat conduction into the inside of the diaphragm can result in temperatures above the saturation temperature of the LN2, which produces GN2. The production of GN2 within the orifice restricts flow of LN2 within the PC. One method to relieve this is to thermally isolate the valve diaphragm from the coil with G10, which is a common thermal insulator.

Heat transfer generally degrades performance. Also, the accuracy of the measurement system also contributes to the a lower efficiency. The worst case scenario measurement is the sum of the accuracies of each device, which is roughly 5%. For instance, the uninsulated copper piping that is routed to the GN2 injection line into the PC lowers the pumping efficiency. The efficiency is highest for refill time of 60s and lowest for refill time 120s. This is directly associated with the temperature of the GN2 injected into the PC. It is warmest with refill time of 60s (237K) and coldest with refill time 120s (138K). Recall that the lower $T_{GN2,injection}$ (TI-001) of the GN2 the higher the volumetric flow rate because the differential pressure is roughly the same across all refill times. Therefore, the $\dot{m}_{GN2,injection}$ increases with decreasing GN2 injection temperature. This correlation affects the fluid velocity, which in turn affects the heat transfer into the GN2 that is injected. The higher the flow rate the higher the heat input into the system. Thus, increasing the denominator in Equation 2.4, which is the equivalent of the heat added via the vaporizer.

The volumetric efficiency was found to be very low experimentally. The assumption made in the model is that it was 100%. Experimentally, the volumetric efficiency was nearly 2.5% for refill of 60s. The low volumetric efficiency is not only attributed to heat transfer issues, but partially filling the PC with LN2 with each consecutive stroke. The following table outlines shows the volume and mass flow rates attained experimentally.

Hypothetically, if the current pumping system were to go operational, the

Table 7.1. Volumetric Efficiency of Process Cylinder

	Discharge Flow Rates		GN2 Injection Flow Rates		
Refill Time[s]	Volumetric [LPM]	Mass [kg/min]	Volumetric [LPM]	Mass [kg/min]	Efficiency Volume
60	0.33	0.27	13.33	0.02	2.48%
100	0.67	0.54	27.57	0.06	2.42%
120	0.75	0.60	60.38	0.18	1.23%

number of cryocooler required to operate at the CTIO CCD cooling system in closed loop are 5,6, and 8 for refill times 60s, 100s, and 120s. Also, with increasing refill times the LN2 volumetric flow rates increased. Thus, given the current operation of the OPP a total of 11 process cylinders in parallel are needed to achieve the specified flow rate of 7.57LPM for the refill time of 120s. One method of working with this current setup is to connect the PCs in series with a GN2 injection line header. Also, the inlet and outlet flow rate correlations derived from the data could be used to select different flow rates lower than the best operational point of 0.6LPM of LN2 and 31LPM of GN2. If the refill volume of a single PC is increased significantly, then the number of PCs would be reduced to a lower number.

In conclusion, the cryogenic OPP does not meet the flow rate requirements of 7.57LPM (2gpm). It should not be considered as an alternate pump for the CTIO CCD cooling system. However, the OPP should be further studied for its reliability and closed loop application. The timing sequence of the OPP is important to regulate the suction and discharge flow rates so that the volume filled in the chamber is discharged. The only way of doing this is to adjust the discharge time with the refill time. This optimal timing sequence can only be solved if the refill of the PC is increased via increasing the orifice size of future valves. Furthermore, in order to increase the performance of the pump heat transfer effects must be limited and measurements must be accurate. Heat transfer affect further complicate the OPP

because it degrades its overall efficiency. Much research is required to enhance the performance of the pump.

7.2 Recommendations and Future Work

The over-pressure pump (OPP) is a device that not only could be used for cryogenic application, but for other single phase fluids. Also, it can be used where high reliability is needed. It can have much success in improving the reliability of future cooling systems. This is a result of the simplicity of the design and little moving parts. Additionally, it replaces many dynamic parts with a submerged heater. The following recommendations for the future work of the OPP should be highly considered.

The refill of the PC is an issue that can only be resolved via a new valve. A valve with the largest orifice size could only be used to take full advantage of a gravity feed refill of the PC. Because most valves are not meant to be fully submerged in a cryogen, various valves with the largest orifice size should be tested prior to being installed in future experiments. Motor operated valves should be considered. However, these valves are typically long stemmed valves that are not meant to be fully submerged in a cryogen. Therefore, the stem must be exposed to the ambient, which introduces a heat leak into the system. So a balance of the power to actuate a valve and the number of through holes in a CLV must be considered.

It is recommended that any future experimentation be done on a scale model that is installed within a vacuum chamber to eliminate conduction and convection losses. Furthermore, the setup should be wrapped in multi-layer insulation to significantly reduce radiation heat transfer. The instrumentation should be fed through insulated wire feedthrough. Scaling down future experiments of the OPP is necessary in being able to modify and adjust various components within the system. In summary, the scale model should include all three primary components. Furthermore, it should be installed in a cooling system with an adjustable heater and a appropriately

selected cryogenic refrigerator.

Once the OPP is scaled down and placed in a vacuum chamber, the variable displacement of the pump should be explored. The variable displacement capability of the OPP is simply governed by the refill time. The refill time changes the stroke length, which in turn changes the volumetric flow rate. If multiple PCs are installed, the response time to changing the flow rate dynamically should be investigated and improved upon. Variable displacement pumps allow for improved reliability and ease of adjusting the flow rate for the process.

Adding a liquid level to the process cylinders is required, to adjusting the flow rate of the OPP. Recall that their is a strong correlation between the refill time and discharge time, which is the volumetric efficiency. A liquid level probe in each PC would allow the control unit to precisely adjust the gas injection time. Also, an accurate measurement within a PC would affect the work of the cryocoolers, which can be adjusted accordingly.

In order to fully conduct the first closed loop cryogenic OPP test, a balance between the electrical input and the heat removal of the cooling system must be balance. So the cryogenic refrigerator work out must equal the heat load added (i.e. CCD heater braids) to the system plus the work input for the heater to generate the gas driving fluid. Once this balance is achieved OPP can be operational for service in almost any homogenous fluid.

A new theoretical model could be derived, which involves a control volume for each the GN2 and LN2. Pursuing a theoretical model involving the liquid and gas control volumes would allow one to understand the areas of improvement of the process cylinder. The inefficiencies, such as heat transfer, can be understood through the process cylinder or gas generator. Furthermore, the losses associated

with condensation and evaporation can be understood at the gas-liquid interface. The best approach to understanding this problem is to use the integral methods of the continuity, momentum, and energy equations.

The OPP has many applications other than for cryogenics. For instance, it can be used in replace of feedwater pumps in future power plants. In doing so, some of the heat generated to displace the slightly subcooled water can be reused to preheat liquid for the boiler. Another application is to use it to cool space satellite electronics equipment, which require highly reliable pieces of equipment. The OPP is capable of high reliability that must be proven in the future tests. It is device that simplifies most pumping systems and has must promise of revolutionizing the pumping industry if pursued further.

APPENDIX A

FLUID SELECTION FOR OPTIMAL HEAT TRANSFER IN TWO-PHASE FLOW

The current CCD cooling system uses LN2 as the process fluid. Is it the best fluid? In order to answer this question, we would investigate the properties that need to be optimized for the best heat transfer, fluid flow, and vaporization for this two-phase system. Therefore, it is important to consider the following fluid dynamic and heat transfer correlations for single phase fluid.

$$Re = \frac{\rho V D}{\mu} \tag{A.1}$$

$$Nu = \frac{hL}{k_f} \tag{A.2}$$

$$Pr = \frac{C_p \mu}{k} Pr = \frac{\upsilon}{\alpha} \tag{A.3}$$

The next set of equations deal with the condensation rate of the cryocoolers. In other words, the optimal fluid for condensing is the one which has the highest density difference and highest thermal conductivity and lowest latent heat of vaporization. The following equation is used to find the average condensation heat transfer coefficient [16].

$$h = 0.943 \cdot \left(\frac{h_{fg} \cdot g \cdot \rho_L \cdot (\rho_L - \rho_g) \cdot k_L^3}{L \cdot (T_{sat} - T_{heat,sink}) \cdot \mu_L} \right)^{1/4} \tag{A.4}$$

Finally, because the LN2 cooling system is 2-phase, it is important to understand the effects of the following heat transfer equation, which is a function of the convection number, Co, boiling number, Bo, and quality of the LN2 and GN2, x [16]. This boiling dimensionless heat transfer equation equates the ratio of the convection coefficient as a result of two-phase boiling to the liquid only heat transfer coefficient.

$$\frac{h_{fb}}{h_{lo}} = h(x, B_o, C_o) \tag{A.5}$$

$$C_o = (\frac{1-x}{x})^0.8(\frac{\rho_g}{\rho_L})^0.5 \tag{A.6}$$

$$B_o = \frac{q_w}{Gh_{fg}} \tag{A.7}$$

From analyzing these equations, one can deduce the following. Typically, when attempting to enhance heat transfer of a heat exchanger, additional surface area is added. However, the heat exchanger for the CCD cannot be modified, then we must increase $\frac{\rho_g}{\rho_L}$ ratio or the expansion ratio. Also, the latent heat of vaporization must be minimized as well. The property plots are as followed.

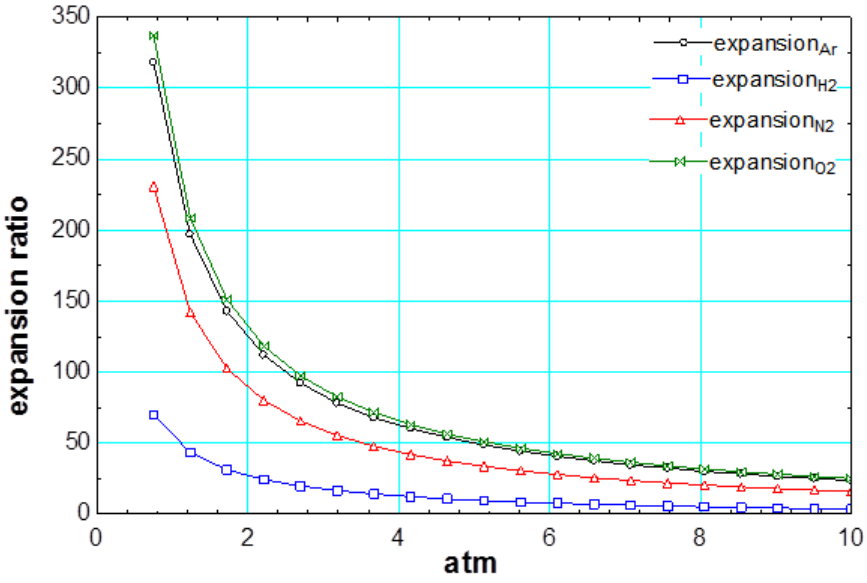

Figure A.1. Expansion Ratio versus P_{atm}

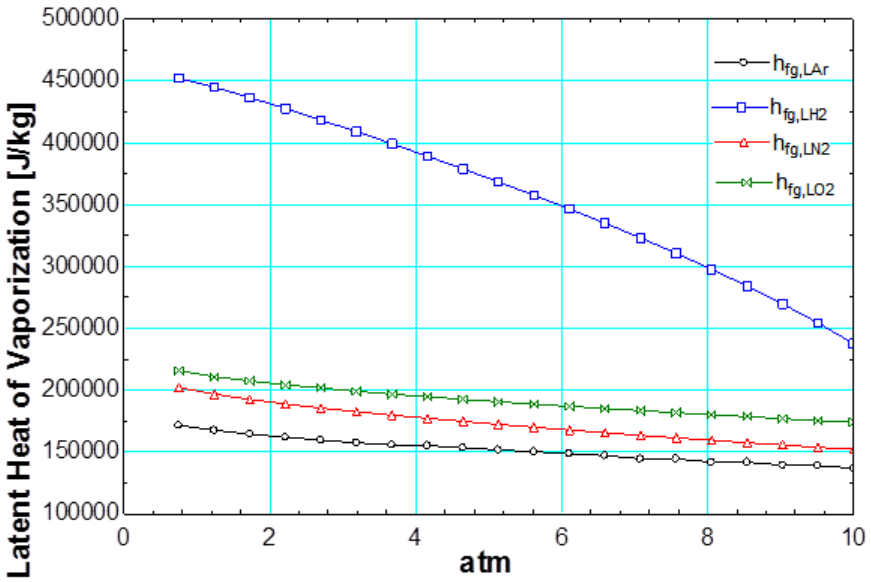

Figure A.2. Latent Heat of Vaporization versus P_{atm}

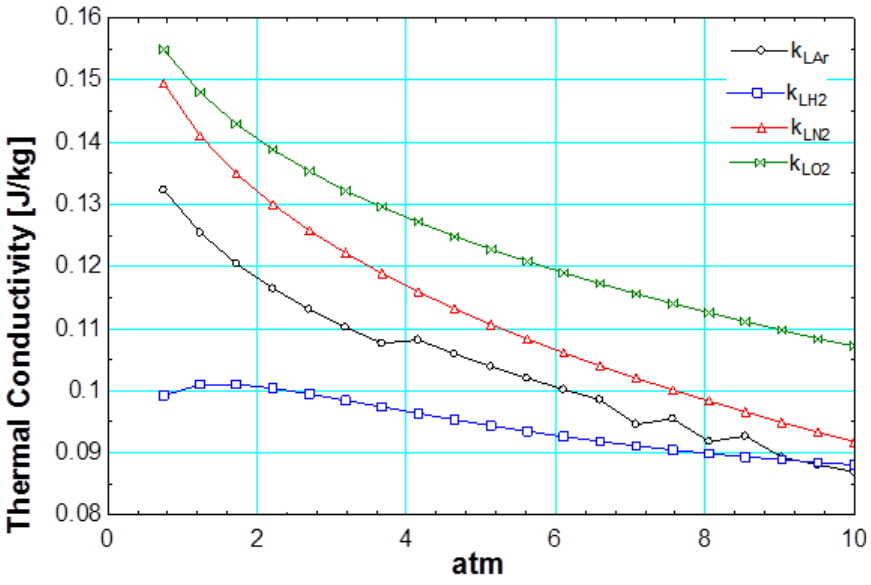

Figure A.3. Thermal Conductivity versus P_{atm}

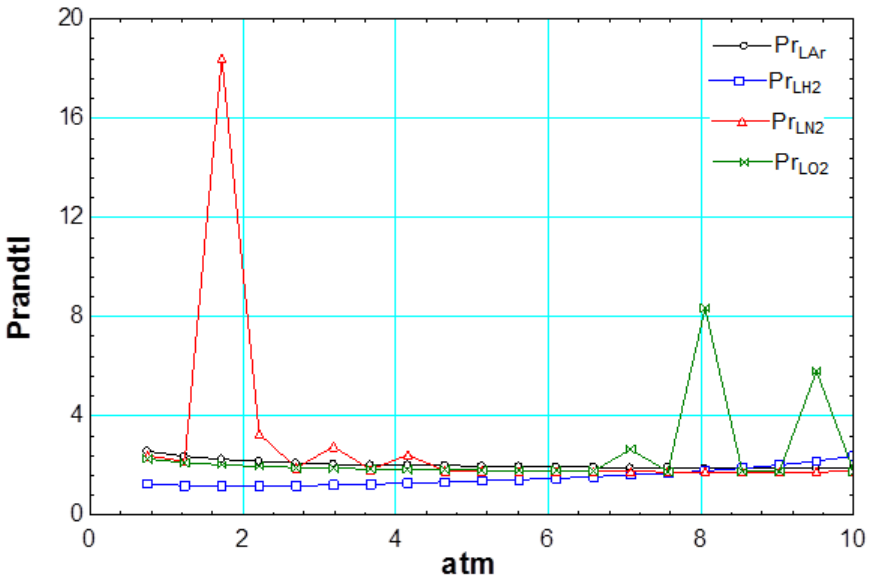

Figure A.4. Prandtl versus P_{atm}

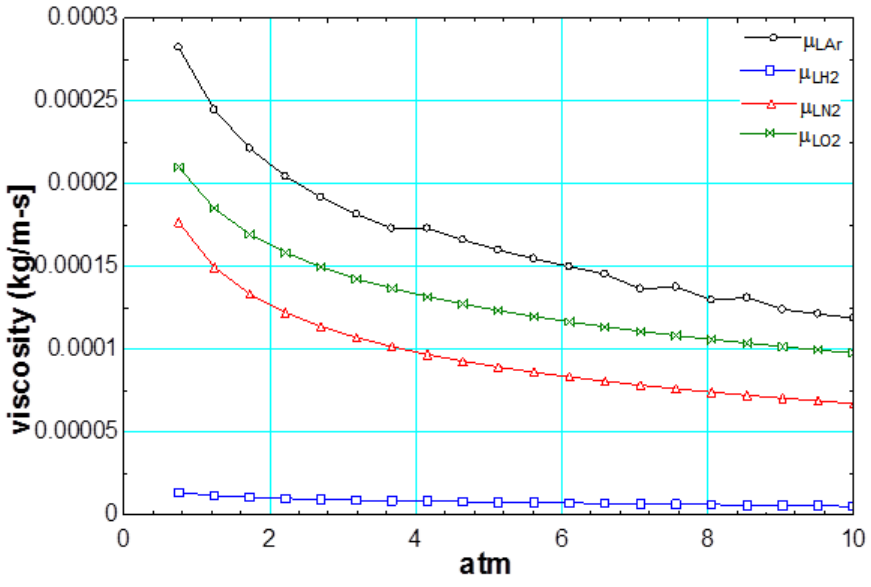

Figure A.5. Viscosity versus P_{atm}

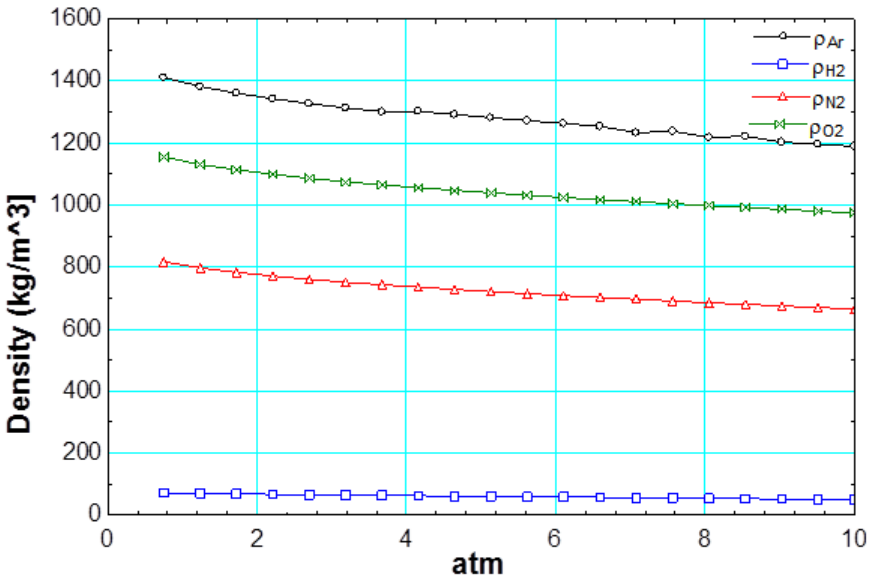

Figure A.6. Density versus P_{atm}

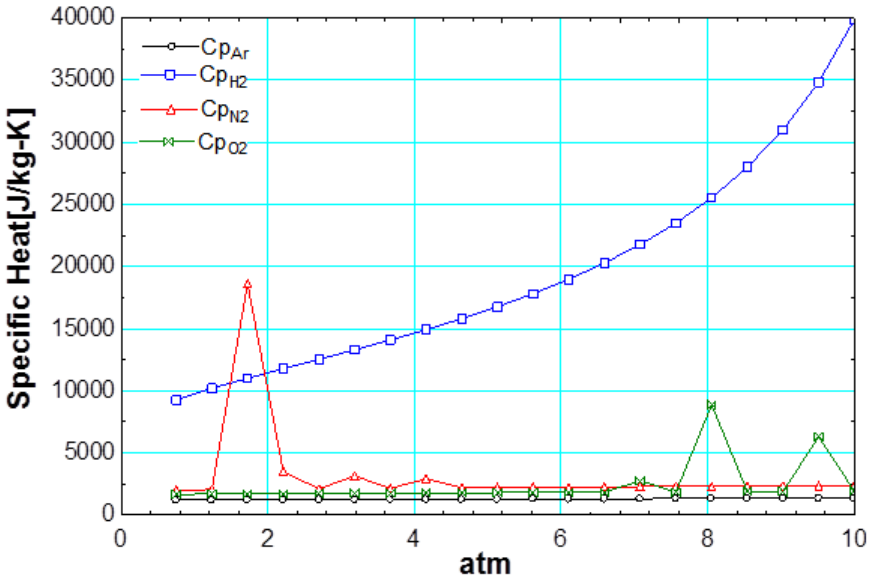

Figure A.7. Specific Heat versus P_{atm}

The following table quantifies the potential cryogenic fluids for service in the CCD cooling system. For the column *Is it Expensive?*, the answer is based upon data collected by NASA [26]. Moreover, the numerical values assigned to column C_p for each of the gases is based upon ranking the gases based upon Figure A.7 from highest to lowest (1-5).

Table A.1. Fluid Selection

Gas	Price[dollar/gallon]	Is it Expensive?	Combustible	C_p [J/(kg-K)]	Expansion Ratio	$h_{vaporization}$ [J/kg]	Total
Oxygen	2.85	yes	no	3	5	3	11
Hydrogen	0.98	no	yes	5	1	5	12
Argon	0.262	no	no	3	5	2	10
Nitrogen	0.03	no	no	3	4	1	8
Helium	0.005	no	no	N/A	N/A	0	0

The fluid best for service in the CCD cooling system is argon. Despite, the totals for oxygen and hydrogen surpassing argon values, argon is not flammable or an oxidizer. Therefore, oxygen and hydrogen are eliminated due to the danger of causing a or fueling a fire.

APPENDIX B

CTIO 4M BLANCO TELESCOPE IMAGES

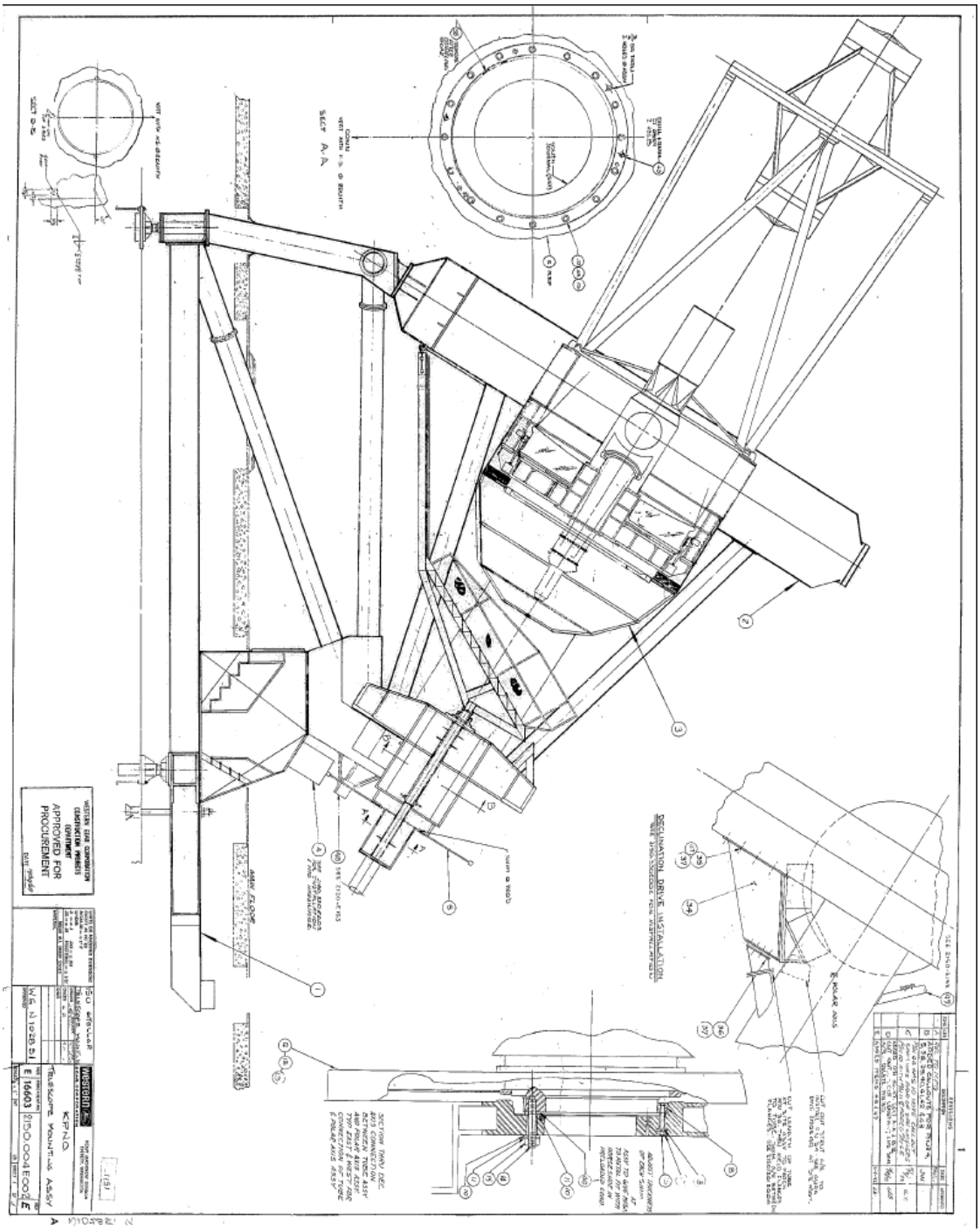

Figure B.1. Blanco 4M Telescope Side View

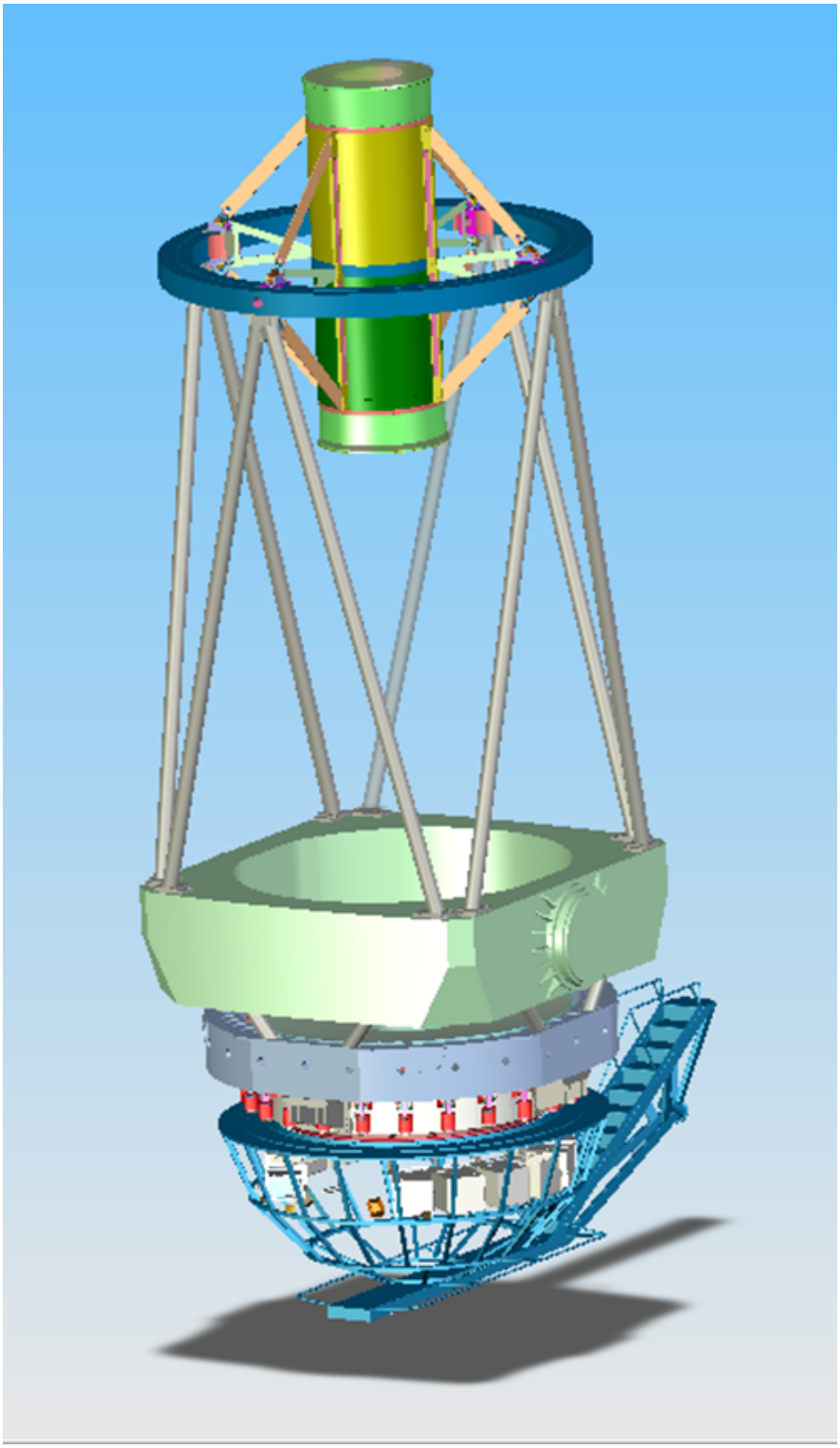

Figure B.2. Blanco 4M Telescope Three Dimensional View

APPENDIX C

VALVE AND INSTRUMENTATION LIST

REVISION Novemeber 3, 2011 - MCCDTV with Thermal Pump

Name	Fluid	Size	Description	Range / Set Point	Manufacturer	Model Number	Psig max	Signal	Excitation	Notes	PLC
6100	LN2	1/2" FNPT	Fill Try Cock, Manual valve		Rego	T9454	600			cryo-short stem valve	
6100	V	2"	Vacuum positive pressure relief on reservoir vacuum jacket	1.5 psid	Fermi	2" Parallel Plate	"atm				
6101	V	1/8" NPT	Pressure element for reading the vacuum pressure		Hastings	Type DV-6R	"atm				Input
6102	N2	4"	Heater inside reservoir	0-400 Watts	McMaster	3559K23	no diff. pres.				output
6105	V	1"	Vacuum pump out port		ACME Cryo	33-2542-02431	"atm			CVI V 1046 pump out	
6106	LN2-N2	4" tube	Pump Process Cylinder	0-100 psig	Fermi	4" SS tubing with end caps	100 psig			safety relief valve trips if overpressurized	
6200	LN2	3/4" MNPT	Fill port, trapped volume relief	-320 F to 400F	Circle Seal	K5120B-6M-150	3600			150 PSIG set point	
6202	N2	1/4" NPT	Instrument Line, Boil-Off Regulator	75-175 psig	Cash-Acme	1/4" FRM 100 psi	600			use inlet coil to warm gas before relief	
6204	LN2	1/2" FNPT	Fill Port,		Rego	T9454	600			cryo-short stem valve	
6205	LN2	1/2" FNPT	Drain Port, Manual Shutoff Valve		Rego	T9454	600			cryo-short stem valve	
6206	LN2	1/4" NPT	Drain Port, Pressure Indicator	0-200 psig	US Gage	47101	250+			2" Dial Size, use inlet coil to warm gas	
6207	LN2	1/4" NPT	Level Transmitter	0-100%	Teragon	LP7	500	4-20 mA	24 VDC		input
6209	N2	1/4" NPT	200L reservoir Pressure Indicator	0-200 psig	US Gage	47101	250+			2" Dial Size	
6210	N2		Temperature Element, Condenser Temperature	-452 to 500 deg F	Omega	SA1-RTD-B	no diff. pres	RTD		100 Ohm 3-wire RTD, surface mount	input
6211	N2		Temperature element, Top Reservoir Gas Temperature	-452 to 500 deg F	Omega	SA1-RTD-B	no diff. pres	RTD		100 Ohm 3-wire RTD, surface mount	input
6213	LN2	1 1/2" NPT	Reservoir Positive pressure main relief	150 psig	Anderson Greenwood	81BF1216-G- 150 psig	500			ASME code stamp	
6214	LN2	2" NPT	Reservoir Positive pressure 2nd main relief	165 psig	FIKE	2" SRL Flange Rupture Disk SS	165			ASME code stamp	
6215	N2	1/4" NPT	Pressure Transmitter, Vessel pressure	0-200 psia	NOSHOK	615-200-1-1-2-6	200	4-20 mA			
6216	N2	1/4" weld	Instrument Isolation Valve		Swagelok	SS-4BK-TW	1000				
6217	N2	1/2" NPT	Fill line In line Filter		Norman	Element #416G-20VM	4500				
6220	N2	1/2"FNPT	released N2 trapped volume from process cylinder	0-100 psig	Magnatrol Valve Corp.	14L32-ZCY	200			fully submerged in LN2	
6221	N2	3/8" FNPT	relief valve for trycock line	0-100psig	Circle Seal	5159-4MP 100	2400				
6223	N2	3/8" MNPT	visual pressure gage	0-200 psig	No Shock	615-2001-1-2-6	400				
6223	N2	surface mount	Gas generator input line Temperature	-452 to 500 deg F	Omega	SA1-RTD-B	no diff. pres	RTD		100 Ohm 3-wire RTD, surface mount	
6229	N2	Flare	gas Generator pressure regulator	0-100 psig	Union carbide	V9 UPE 375 580	400				
6230	N2	1/2"FNPT	Gas generator input line	0-100 psig	Magnatrol Valve Corp.	14L32-ZCY	200				
6231	N2	1 1/4" FNPT	Visual flow meter	0-6 scfm	Brooks	2500 series	100			Visual flow meter in SCFM of air	
6231	N2	1/4" MNPT to FNPT	Gas Generator trapped volume relief valve	0-140psig	Circle Seal	5120B 4MP 140	2400				
6232	N2	1/2" FNPT	check valve for GN2 supply on trycock line	0-100 psig	NIBCO	T-480	250				
6301	LN2	3/4" AN-flare	Supply line, Flow Transmitter	0.75 to 5 gpm	Sponsler	SP3/8-CB-NL-B-4	600+	4-20 mA			input
6302	LN2	1" NPT	Supply Line manual valve		McmasterGoddard	49415K34	600			-325F to 100F Long stem globe valve	
6303	LN2	1" NPT	Return Line, Manual valve near reservoir		McmasterGoddard	49415K34	600			-325F to 100F Long stem globe valve	
6304	LN2	3/4" MNPT	Return line, trapped volume relief near reservoir	-320 F to 400F	Circle Seal	K5120B-6M-150	3600			150 PSIG set point	
6305	LN2	1/4" NPT	Supply line pressure indicator near reservoir	0-200 psig	US Gage	47101	250+			2" Dial Size, use inlet coil to warm gas	
6306	LN2	3/4" MNPT	Supply line trapped volume relief near reservoir	-320 F to 400F	Circle Seal	K5120B-6M-150	3600			150 PSIG set point	
6307	LN2	1/2" FNPT	Return Line port		Rego	T9454	600			cryo-short stem valve	
6311	LN2	3/4" MNPT	Supply line trapped volume relief reservoir check valve	-320 F to 400F	Circle Seal	K5120B-6M-150	3600			150 PSIG set point	
6312	LN2	1" NPT	Check valve supply line	Swing Lift	Powell	CL#200	class 200				
6313	LN2	1/8" NPT	Differential pressure indicator, supply return	0-10PSID	Midwest Instrument	Model 125	6000			use inlet coil to warm gas before gage	
6404	N2		Supply line, Temperature indicator on Braids (QTY 10)	-452 to 500 deg F	Omega	SA1-RTD-B	no diff. pres	RTD		100 Ohm 3-wire RTD, surface mount	input
6405	LN2		Trim heater on Heat exchanger braids (QTY 10)	0-100 Watts	Lakeshore	HTR-25	external				Output
6420	V	6" conflat	Camera Vessel Ion Vacuum Pump		Varian	Vaclon_Plus_75_Ion_Pump	"atm				
6421	V	6" conflat	Camera Vessel Turbo Vacuum Pump		Alcatal	ATH 200 hybrid turbo pump	"atm				
6422	V	6" conflat	Camera Vessel Manual isolation valve, Turbo pump		MDC	302004	"atm				
6423	V	KF-40	Camera Vessel Full Range Vacuum Gage		Pfieffer	PT R26 002	"atm				
6424	V	2"	Camera Vessel Parallel plate relief		Fermi	1620-MB-106391	2 psig relief				

Figure C.1. Valve and Instrumentation List for OPP Test

APPENDIX D

NITROGEN TEMPERATURE ENTROPY DIAGRAM

One important diagram used for the pumping process as well as the system process is the temperature entropy chart. It is commonly used in designing cooling or refrigeration systems. The temperature entropy provides a start point as to how this OPP will operate. The GN2 generator will operate at a higher pressure then the tank so that it will provide the motive force necessary to discharge LN2 from the PC. Recall, that the motive force is governed by a pressure differential. Therefore, higher pressures imply higher flow rates. Thus, positive and negative effects will be discussed based on the theoretical model.

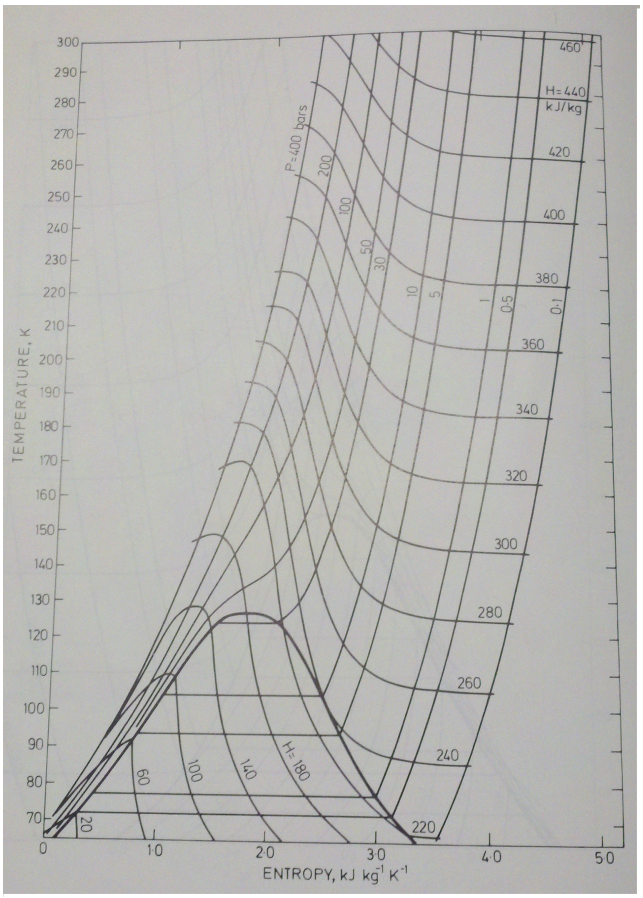

Figure D.1. Nitrogen Temperature-Entropy Diagram [20]

1. Positive Effects

   (a) High expansion ratio

i. Large expansion ratios improves the pump's ability to displace a volume of liquid nitrogen.

(b) Higher system pressure

i. Decreases the change of enthalpy, which implies that less energy is required to vaporize a volume of liquid nitrogen

i. Increases the pressure differential between the GN2 generator and 200L CLV, which is required for providing a reasonable flow rate.

2. Negative Effects

(a) Low expansion ratio

i. Small expansion ratios decreases the pump's ability to displace a volume of liquid nitrogen.

(b) Lower system pressure results in an increase of energy to vaporize a liquid volume.

i. Increases the change of enthalpy, which implies that more energy is required to vaporize a volume of liquid nitrogen.

i. Decreases the pressure differential between the GN2 generator and the 200L CLV, which lowers the supplied flow rate.

APPENDIX E

RAW DATA REFILL TIMES 60S AND 120S

The data was recorded in two types of data files. The first data file contains pressure, temperature, and flow rate measurements regarding the 200L vessel. Moreover, the second data file contains the heating data, which corresponds to focal plate RTD temperature readings, voltages, and a GN2 injection line thermocouple reading. The data recorded involves maintaining the delay before fill and gas injection constant and varying the tank refill from 60, 100, to 120 seconds. The raw data files can be found in *Lab A Over-Pressure Pump Test February Tests* [3]. The figures presented below will show the data for a refill time of 60s to 100s. Trends for pressure, temperature, and flow rate will be discussed.

The data collected for first tank refill time of sixty seconds can be seen in the following figures. The solenoid timing sequence consists of the gas injection, delay before fill, and the tank refill, which corresponds to 40, 15, and 60 seconds. This data set exhibited unusual LN2 liquid levels as well as pressure spikes. However, the initial, midpoint, and terminal points and the overall trend allows this data set to be used. Further discussion of this can be seen below.

The figure below shows the 200L CLV LN2 level versus time.

Figure E.1 shows similar trends as in Figure 4.7. Notice in Figure E.1, that a sudden spike in the liquid level occurs during a refill after the forty second discharge of the PC. This sudden surge of LN2 is associated with boiling within the transfer lines and the CCD heaters. During boiling GN2 has lesser density than LN2, but occupies a larger volume than the LN2. Therefore, the volume expansion of nearly 1:100 is being seen. In other words, 0.4L of LN2 is being generated on the transfer lines, which displaces the LN2 occupying the line. This is not associated with a faulty equipment (i.e. check valve, solenoid valve, etc.). are complete a sudden rise in the liquid level is seen. This is due to unusual boiling that occurs at the MCCD test vessel and the transfer lines. The initial, midpoint, and terminal points will only be

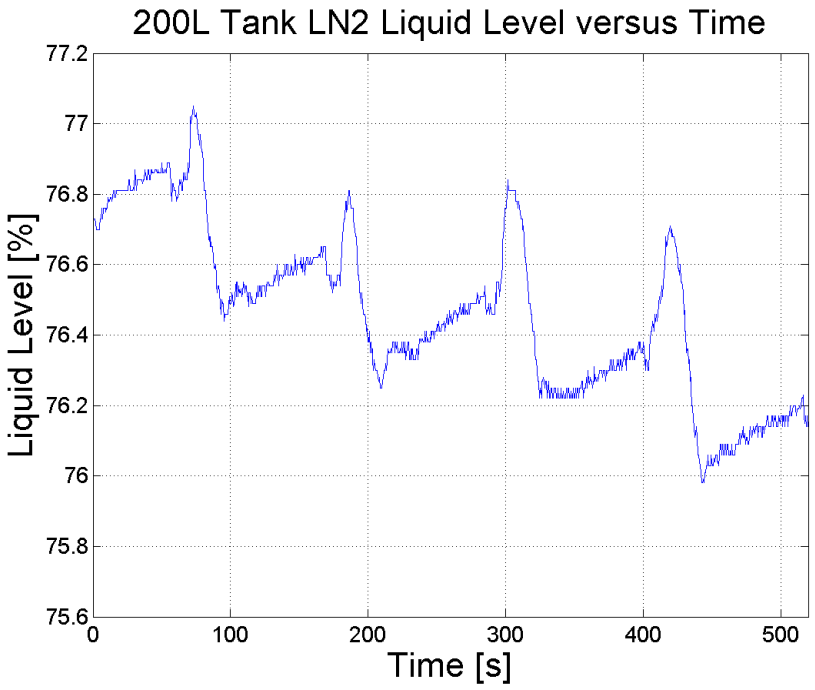

Figure E.1. 200 L Tank Liquid Level vs. Time (refill=60s)

investigated. The midpoint is simply the peak after the forty second interval.

The next figure shows the 200L CLV tank pressure versus time.

Similar to Figure E.1, Figure E.2 shows an increase in pressure during a discharge and a spike in the pressure. This again provides evidence that GN2 is generated within the transfer lines and the CCD heaters. In contrast, during a refill of the PC, the pressure within the tank decreases drastically. This trend is exhibited in refill times 100s and 120s.

The data collected for first tank refill time of one hundred twenty seconds can be seen in the following figures. The solenoid timing sequence consists of the gas injection, delay before fill, and the tank refill, which corresponds to 40, 15, and 120 seconds. For these set of figures, the trends are similar to Figures 4.7 to 4.12.

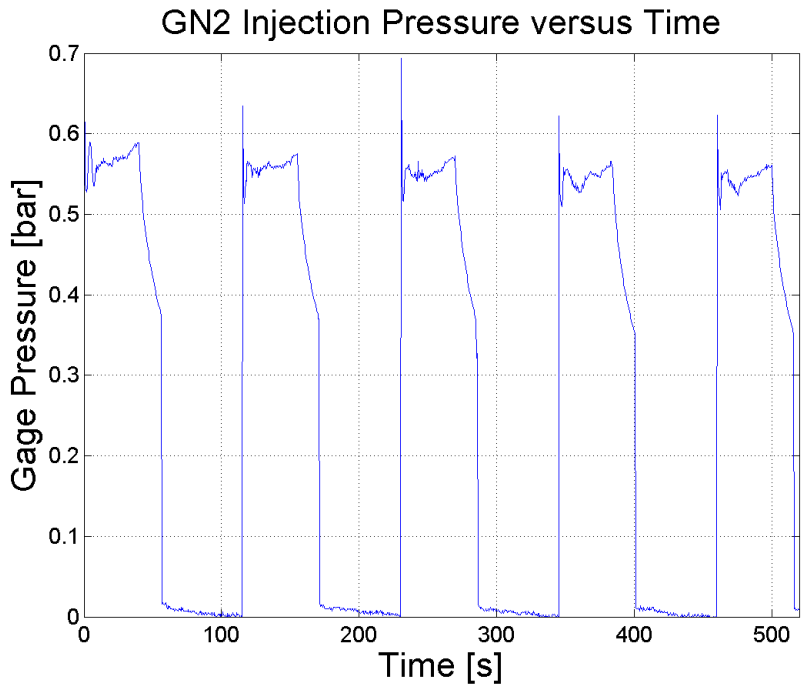

Figure E.2. GN2 Injection Pressure vs. Time (refill=60s)

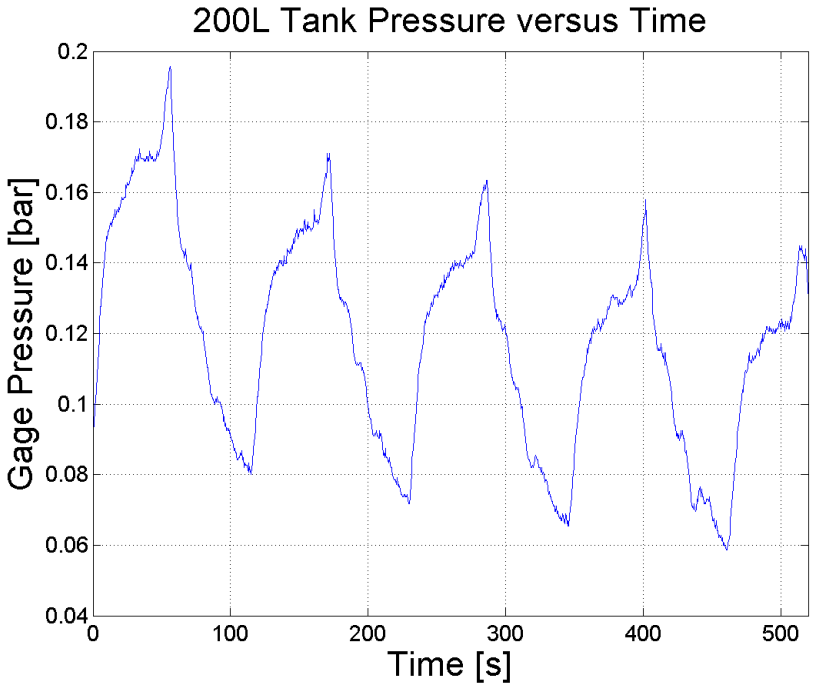

Figure E.3. 200L Tank Pressure vs. Time (refill=60s)

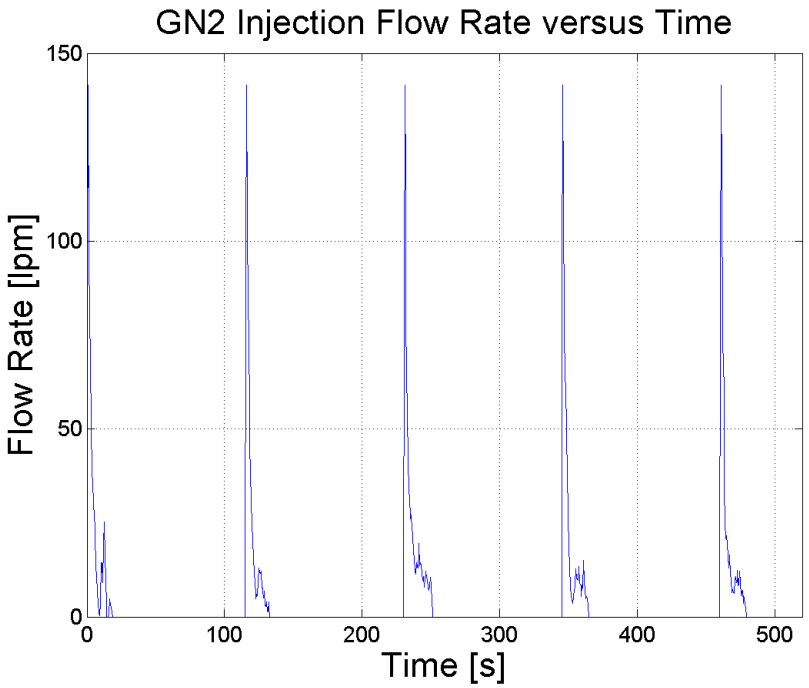

Figure E.4. GN2 Injection Flow Rate vs. Time (refill=60s)

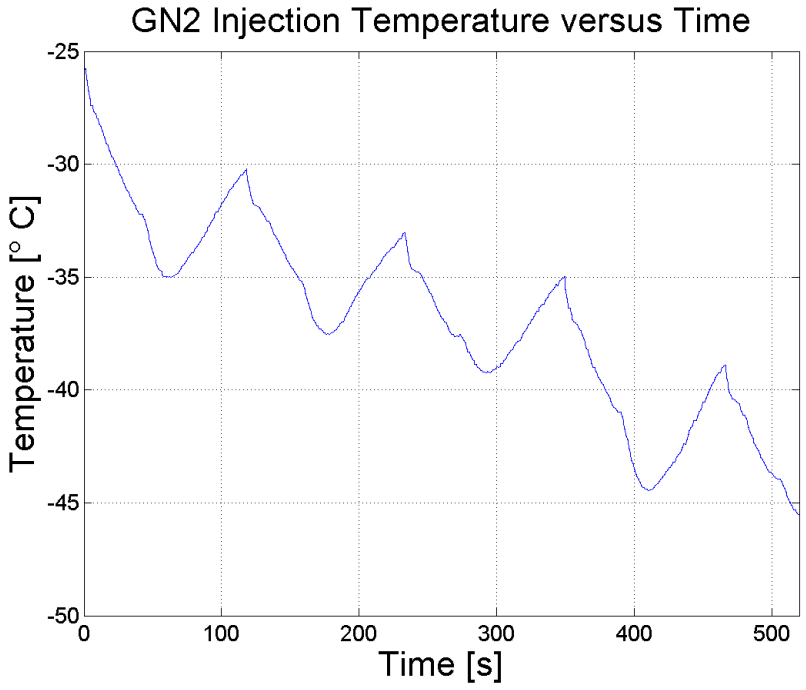

Figure E.5. GN2 Injection Temperature vs. Time (refill=60s)

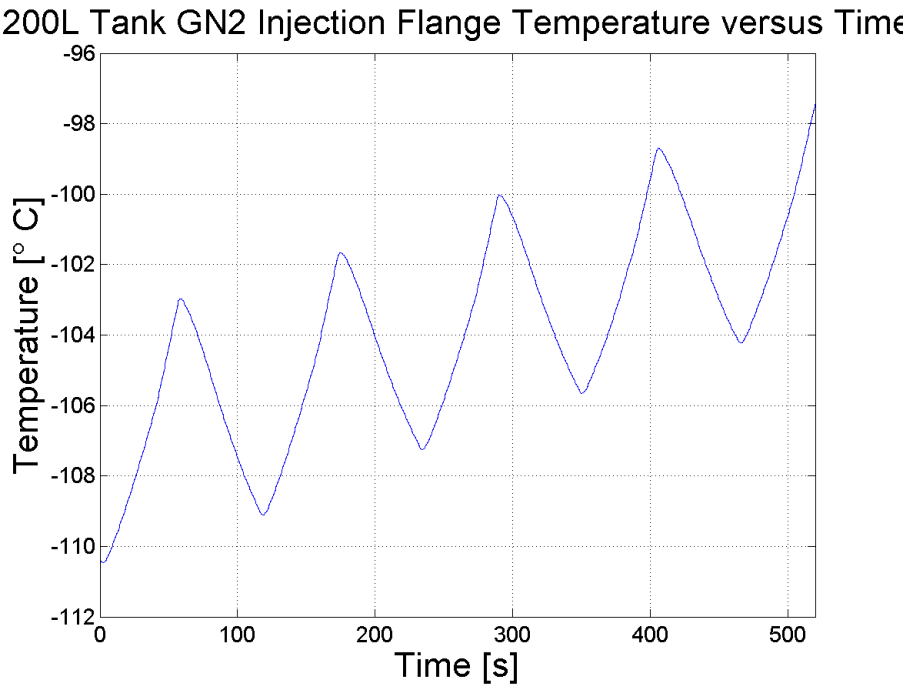

Figure E.6. 200L Tank GN2 Injection Flange Temperature vs. Time (refill60s)

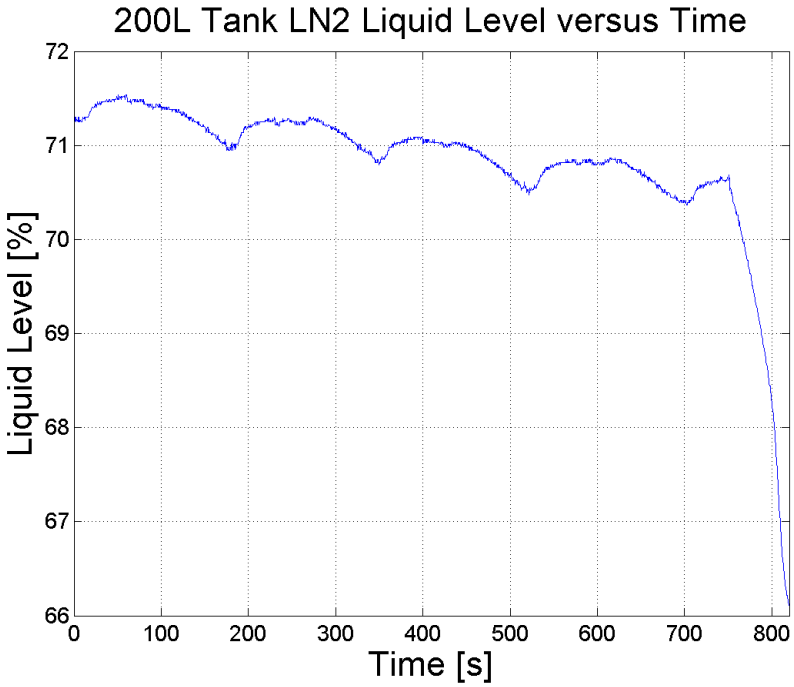

Figure E.7. 200 L Tank Liquid Level vs. Time (refill=120s)

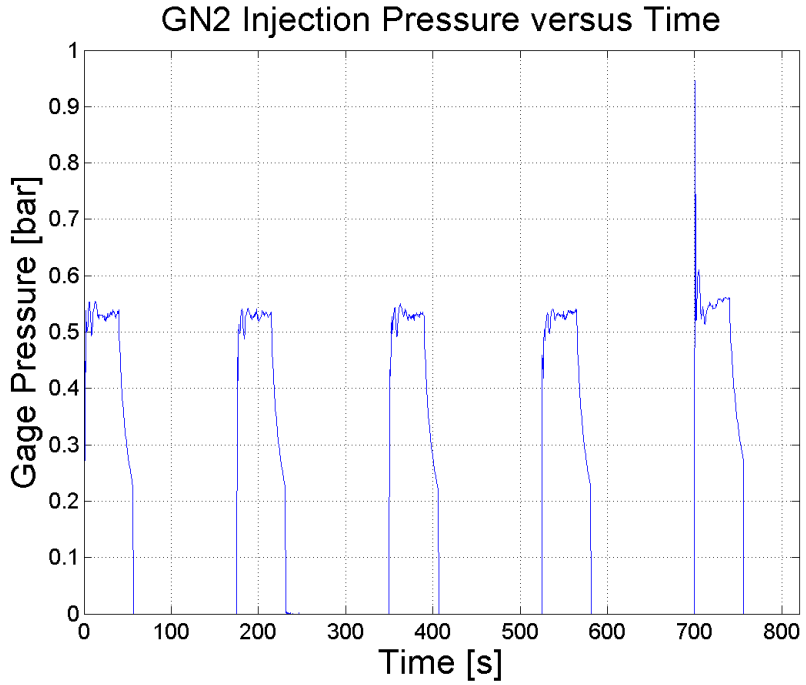

Figure E.8. GN2 Injection Pressure vs. Time (refill=120s)

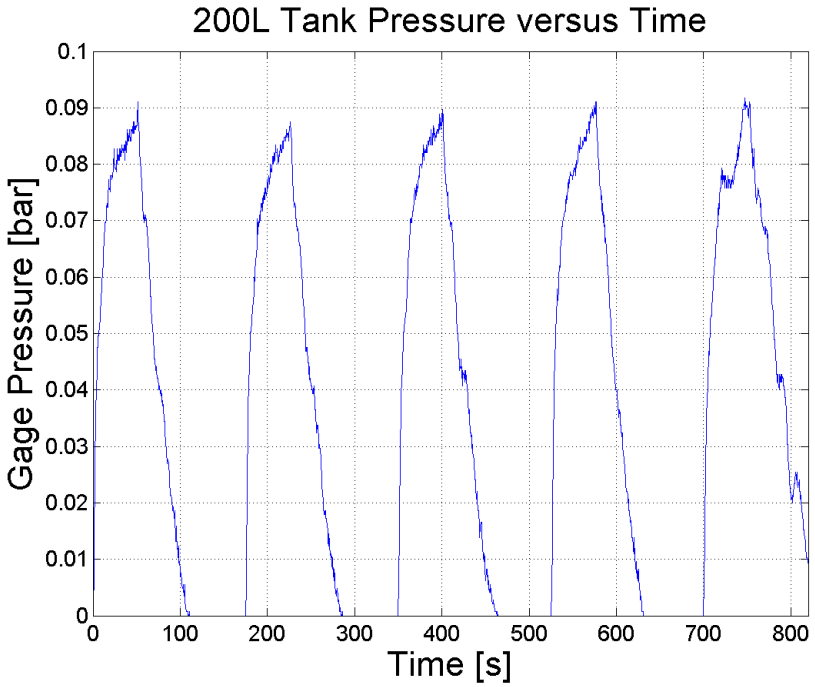

Figure E.9. 200L Tank Pressure vs. Time (refill=120s)

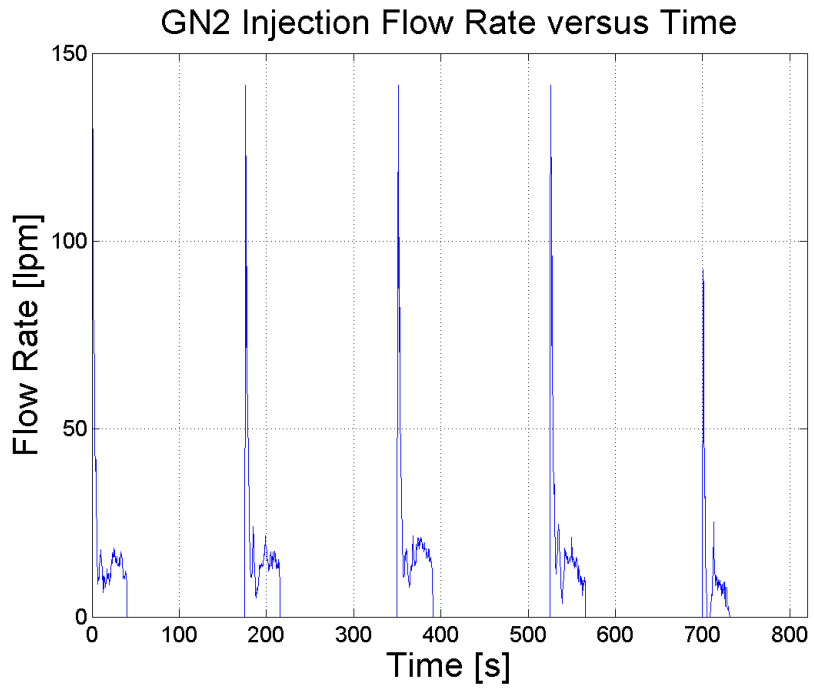

Figure E.10. GN2 Injection Flow Rate vs. Time (refill=120s)

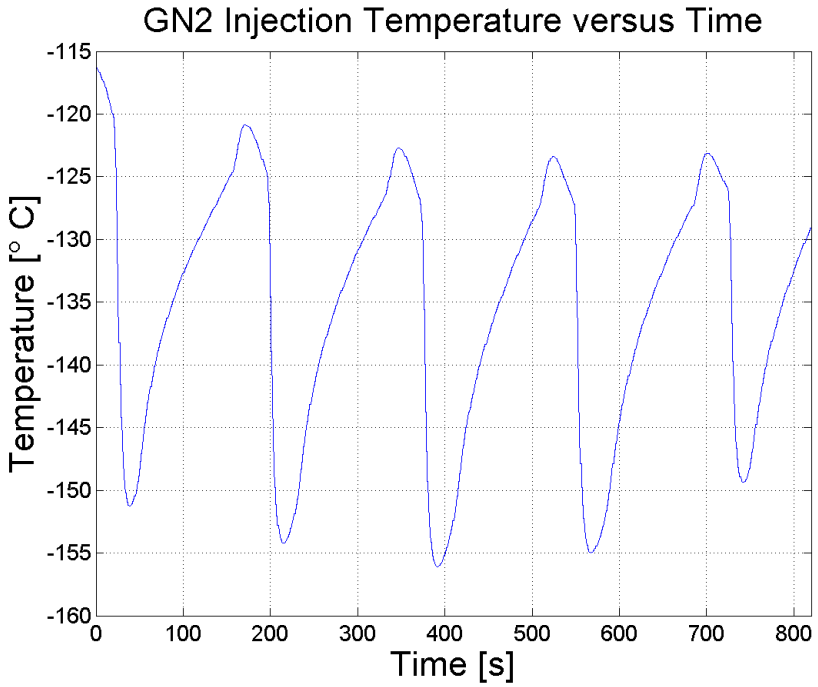

Figure E.11. GN2 Injection Temperature vs. Time (refill=120s)

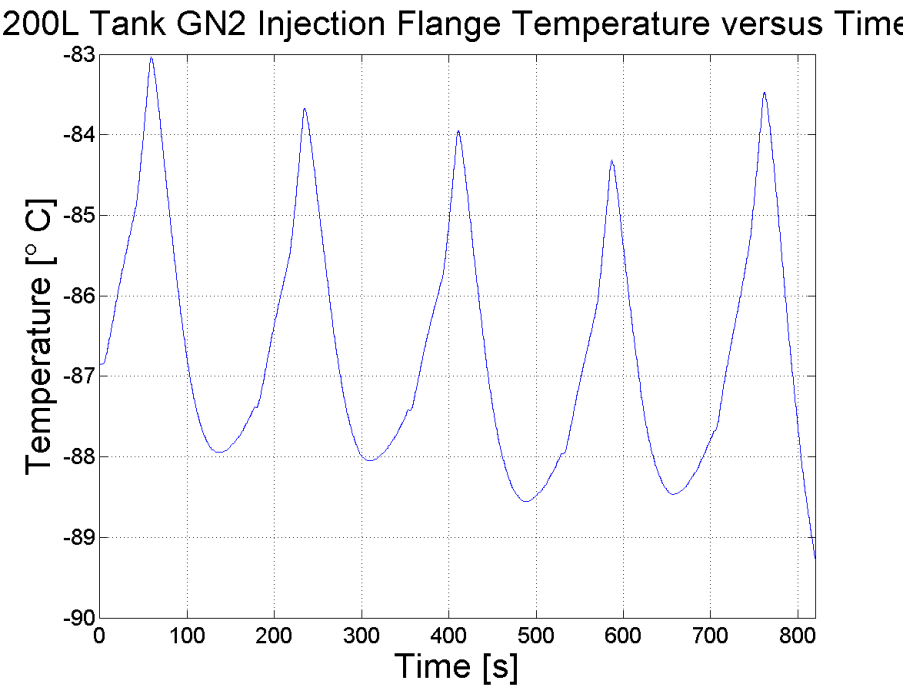

Figure E.12. 200L GN2 Injection Flange Temperature vs. Time (refill=120s)

APPENDIX F

RAW DATA: ERROR BARS

The following figures show the data with error bars for refill time of 60s.

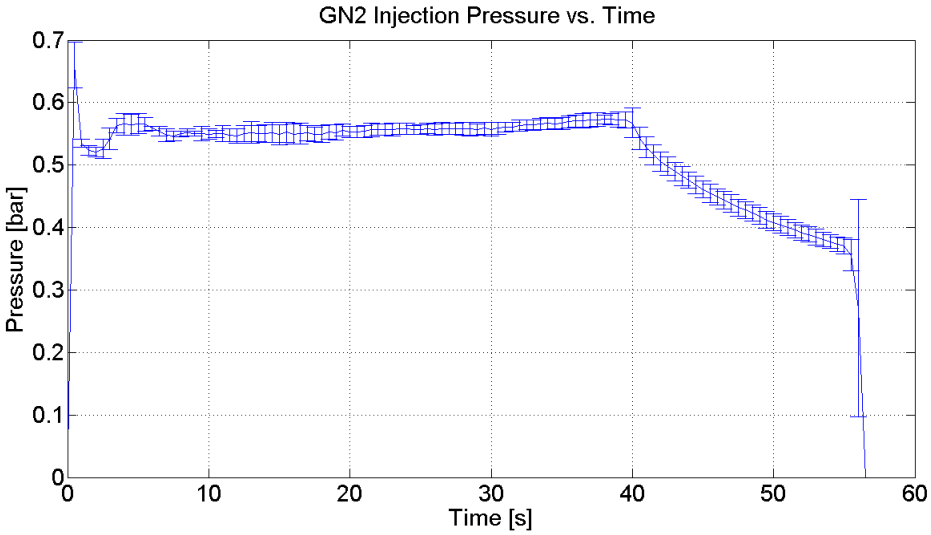

Figure F.1. GN2 Injection Pressure vs. Time (refill=60s)

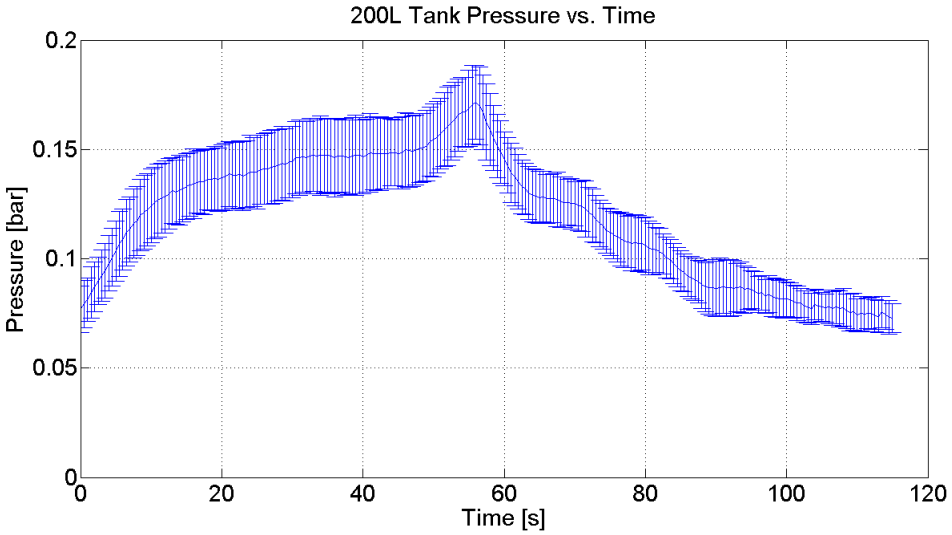

Figure F.2. 200L Tank Pressure vs. Time (refill=60s)

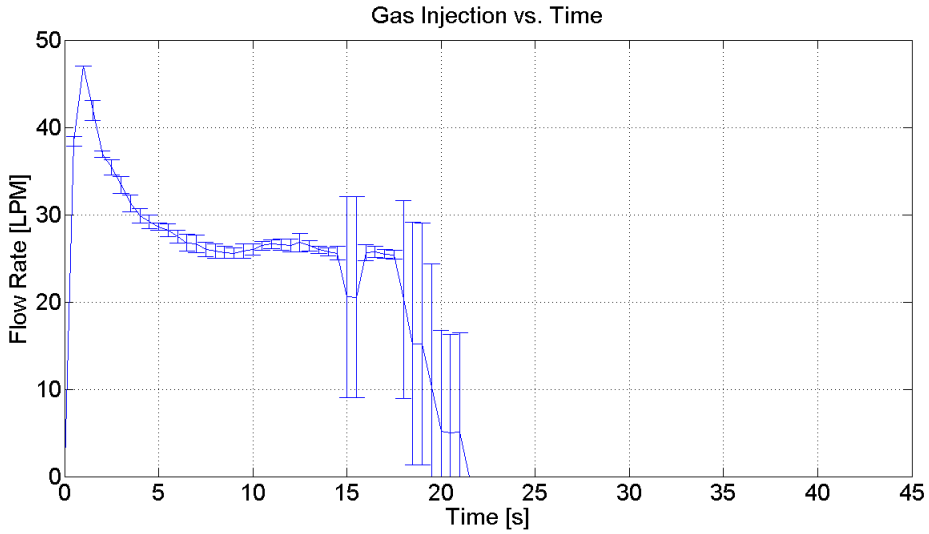

Figure F.3. GN2 Injection Flow Rate vs. Time (refill=60s)

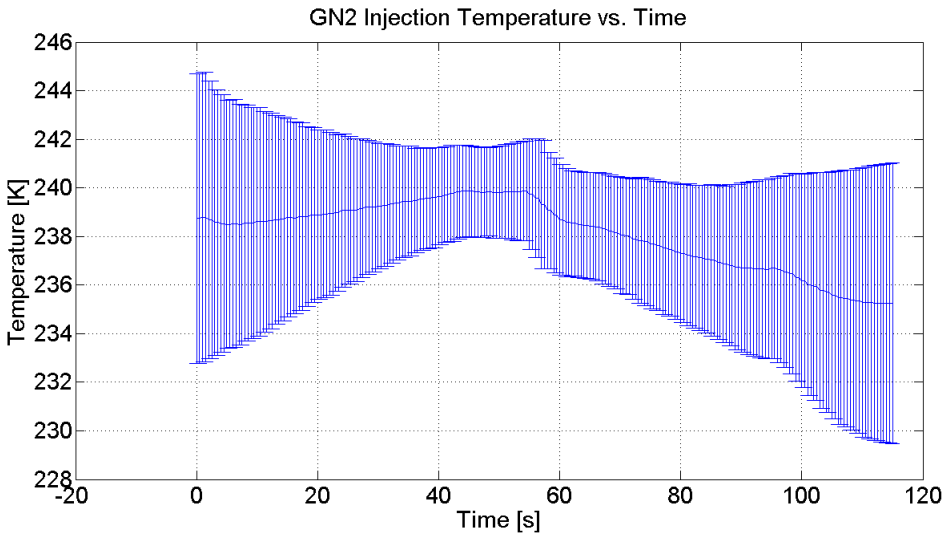

Figure F.4. GN2 Injection Temperature vs. Time (refill=60s)

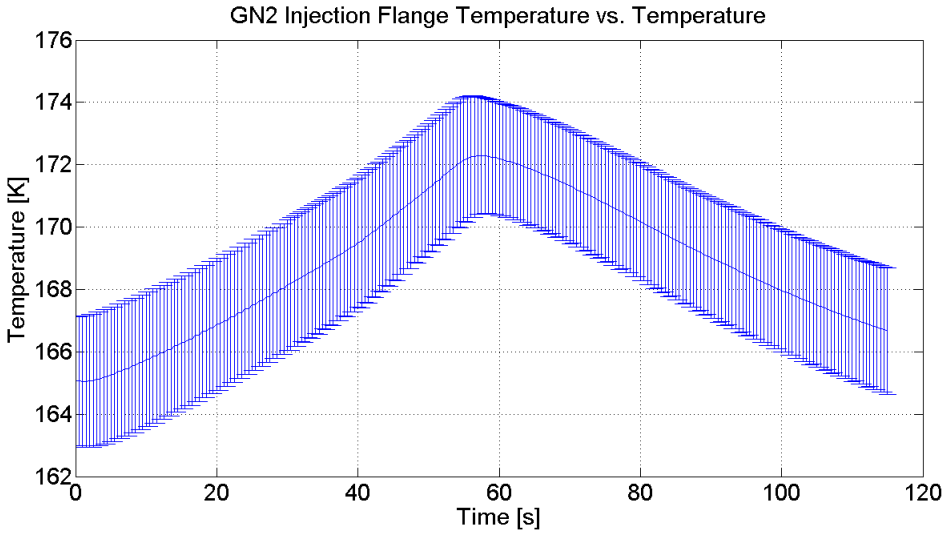

Figure F.5. GN2 Injection Flange Temperature vs. Time (refill=60s)

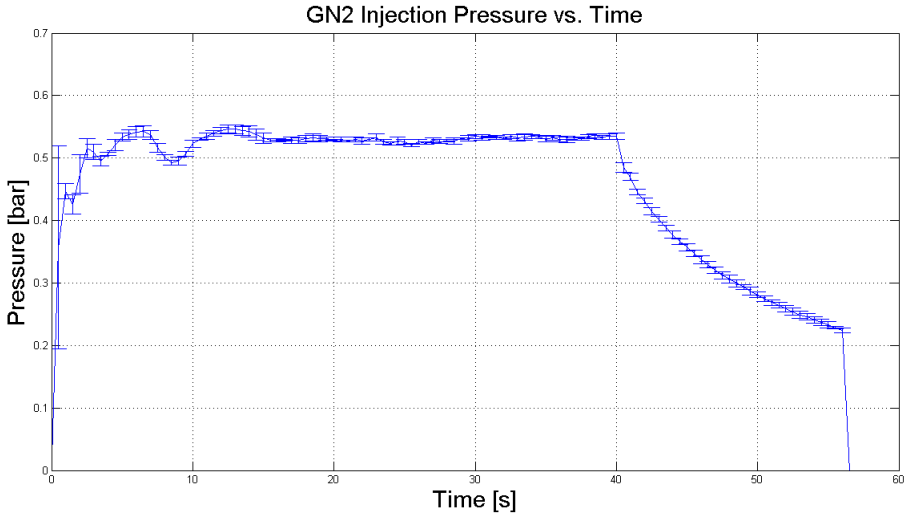

Figure F.6. GN2 Injection Pressure vs. Time (refill=120s)

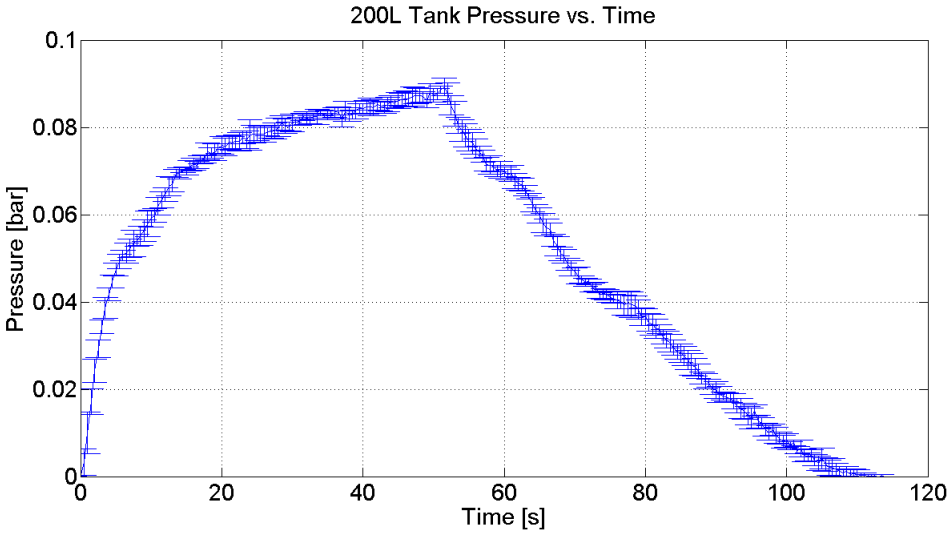

Figure F.7. 200L Tank Pressure vs. Time (refill=120s)

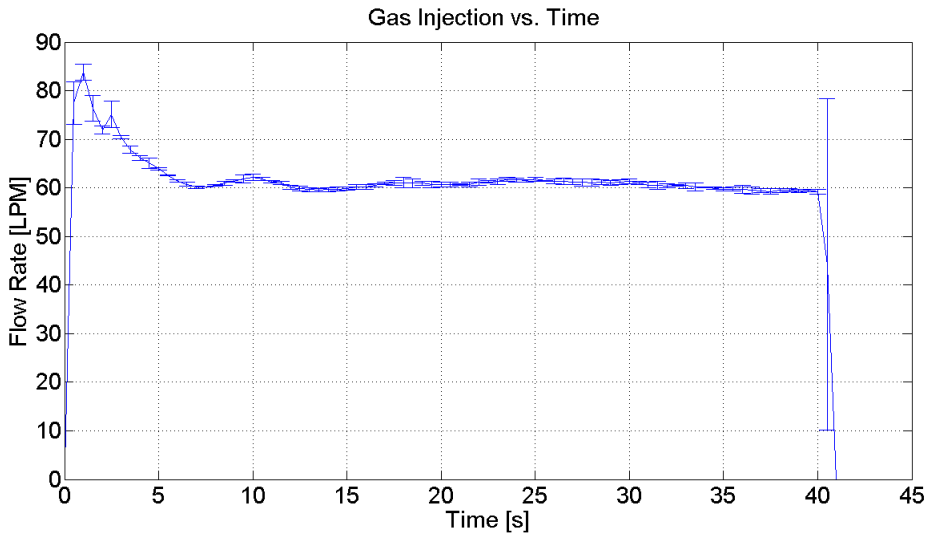

Figure F.8. GN2 Injection Flow Rate vs. Time (refill=120s)

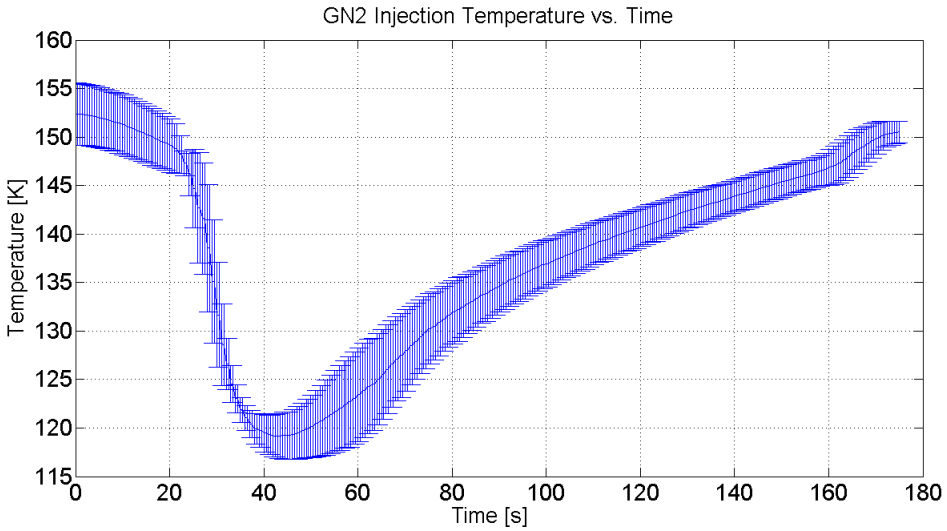

Figure F.9. GN2 Injection Temperature vs. Time (refill=120s)

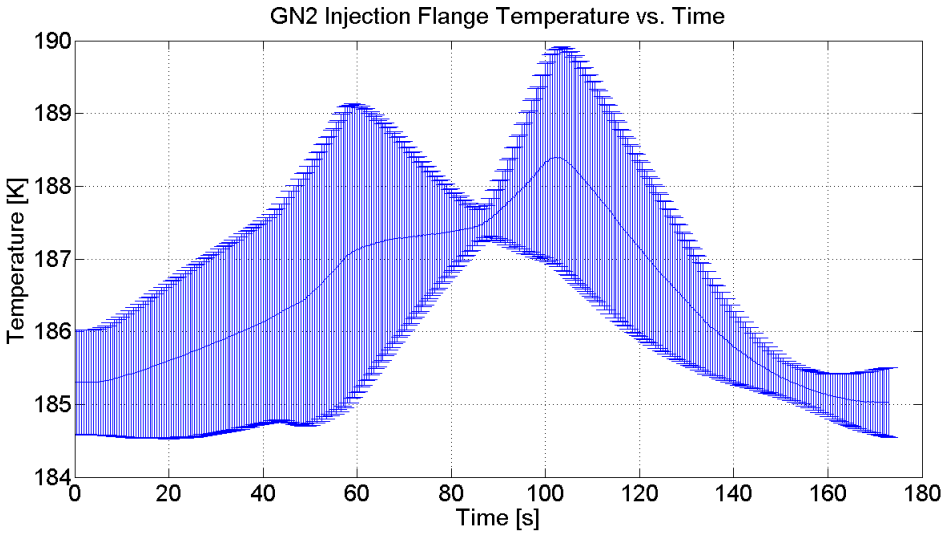

Figure F.10. GN2 Injection Flange Temperature vs. Time (refill=120s)

APPENDIX G

CORRECTED DATA FOR DATA ANALYSIS

The data manipulated in this section will be used to calculate the flow rates and thermodynamic properties. Due to improper calibration of the GN2 injection flow transmitter and the pressure transducer, the data collected on these devices must be corrected. The flow transmitter was calibrated in house [4]. The pressure transducer was reading out pressures that were off by nearly 33%. Additionally, the pressures and flow rates used in the data analysis will be averaged and shown below. The LN2 flow rate indicated via the liquid level probe within the 200L CLV needs to be corrected.

GN2 Injection Flow Calibration

The GN2 that is injected into the PC is measured by a Sponsler flow meter that is not calibrated for a flow regime of 0-5CFM. Therefore, a calibration curve was determined for similar OPP test conditions. The calibration setup, data, and curves can be found in the *Dark Energy Survey Turbine Flow Meter Calibration* [4]. There are a total of three curve fit equations, which specify flow rate in different temperature ranges. The first equation is valid for $T_{GN2,injection}$ greater than 173K.

$$\dot{V}_{correct} = (1.2193 * \dot{V}_{injection,incorrect} + 0.8681) * 28.3168466 \tag{G.1}$$

Where $\dot{V}_{injection,correct}$ is the volumetric flow rate of the GN2 injection line in liters per minute and $\dot{V}_{injection,incorrect}$ is the volumetric flow rate of the GN2 injection line in cubic feet per minute. The next equation is valid only for GN2 injection temperature of lesser than 123K.

$$\dot{V}_{correct} = (1.5821 * \dot{V}_{injection,incorrect} + 2.0104) * 28.3168466 \tag{G.2}$$

Finally, the last equation is only valid for temperatures lesser than 173K and

greater than 123K.

$$\dot{V}_{correct} = (1.5821 * \dot{V}_{injection,incorrect} + 2.0104) * 28.3168466 \tag{G.3}$$

The Equations G.1 to G.3 were used in the Matlab code that uses logic statements to select the proper equation, which is based upon the GN2 injection temperature, $T_{GN2,injection}$. The following figures display the corrected and uncorrected GN2 injection flow rate.

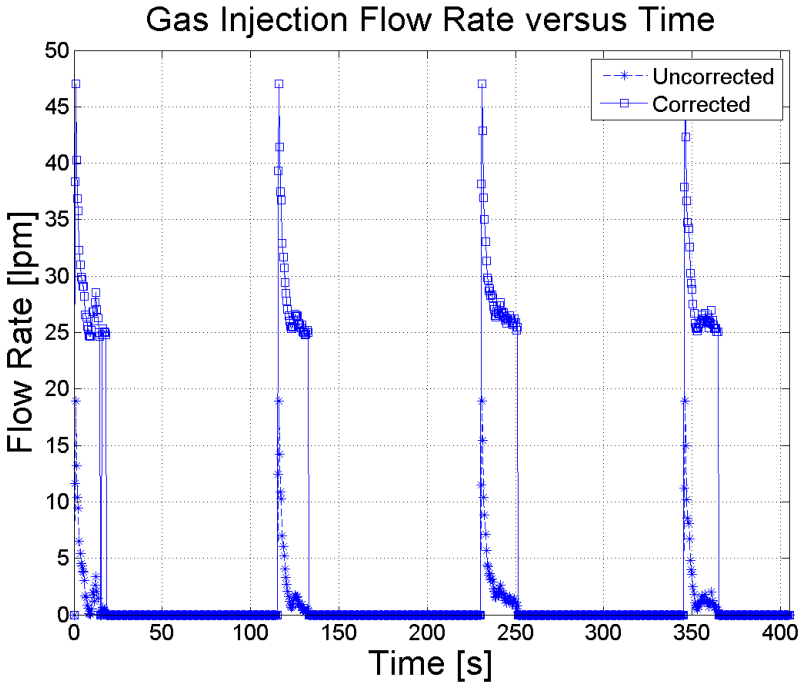

Figure G.1. Corrected and Uncorrected GN2 Injection Volumetric Flow Rate Versus Time (refill 60s)

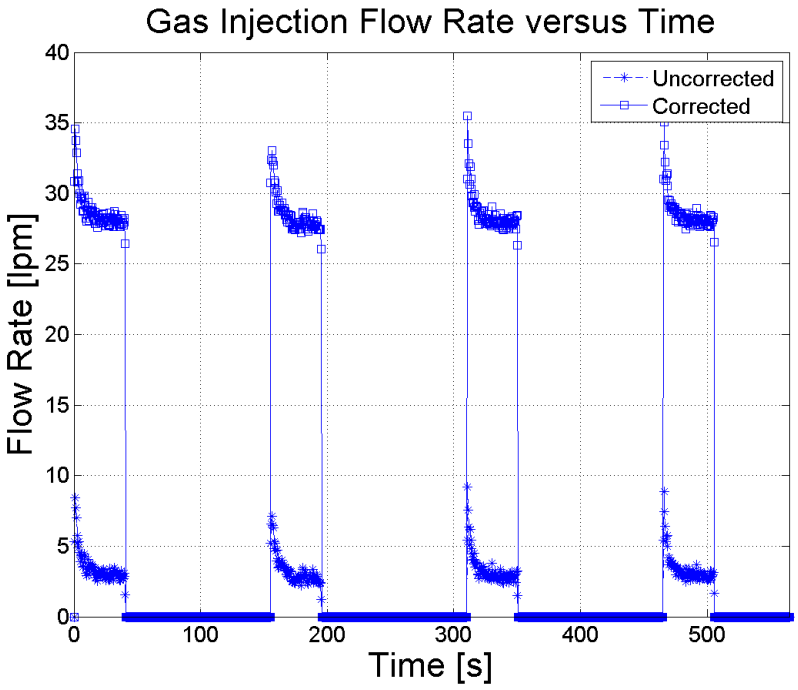

Figure G.2. Corrected and Uncorrected GN2 Injection Volumetric Flow Rate Versus Time (refill 100s)

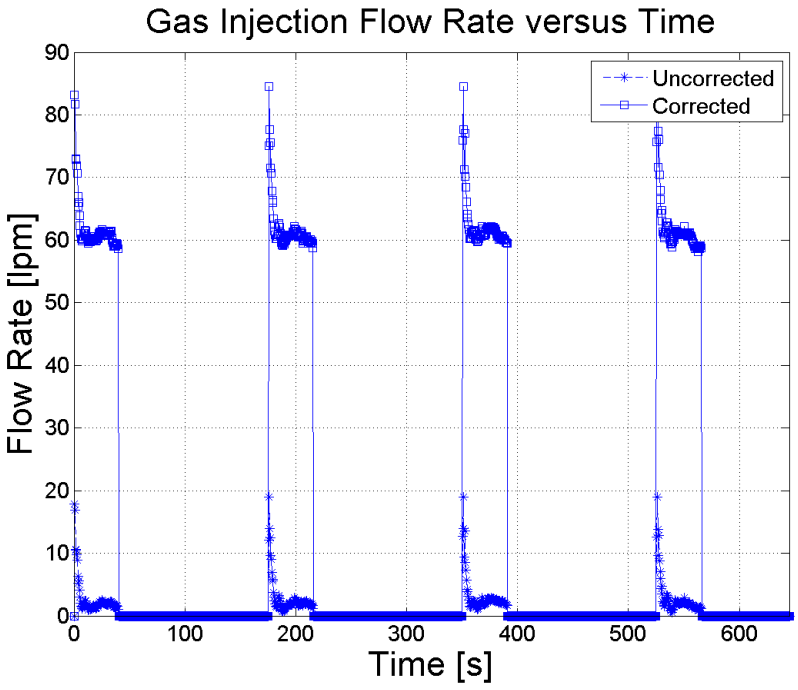

Figure G.3. Corrected and Uncorrected GN2 Injection Volumetric Flow Rate Versus Time (refill 120s)

Figure G.1 uses Equation G.2 to correct the data. The second figure,Figure G.2, uses Equation G.2 to correct the data. The third Figure G.3 uses Equation G.3 and G.2 to correct the data.

Pressure Calibration

Finally, due to an improper calibration curve input into LabView 2010, the PT-002 data must be corrected to account for this 33% offset. The following equation is utilized in correcting the raw pressure data.

$$\Delta P_{tank,correct} = \frac{2}{3} \cdot \Delta P_{tank,incorrect} \tag{G.4}$$

where $\Delta P_{tank,correct}$ is the corrected 200L CLV pressure data and $\Delta P_{tank,incorrect}$ is the incorrect pressure data. The following figures show the corrected and incorrect data for each of the refill times.

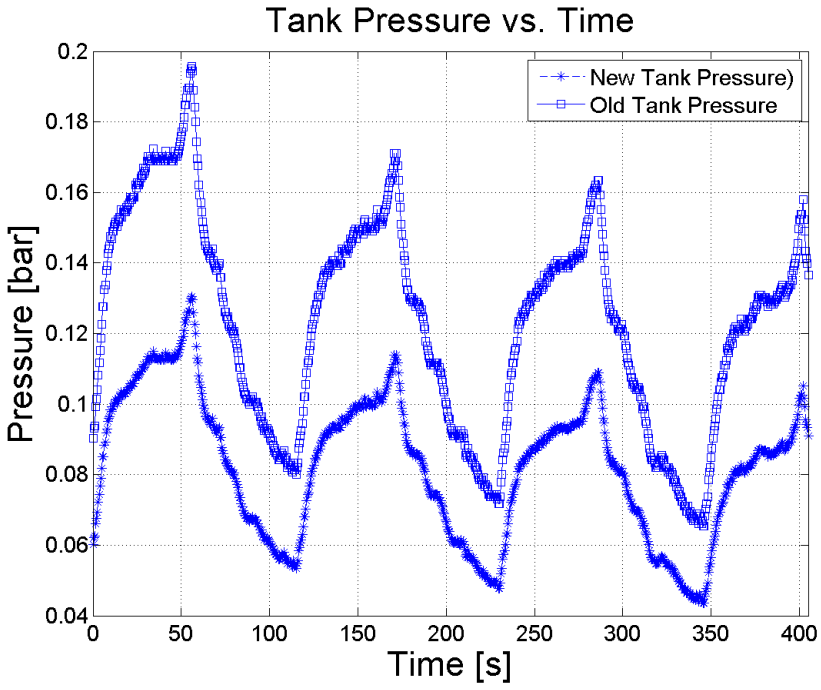

Figure G.4. Corrected and Incorrect 200L CLV Tank Pressures versus Time (refill 60s)

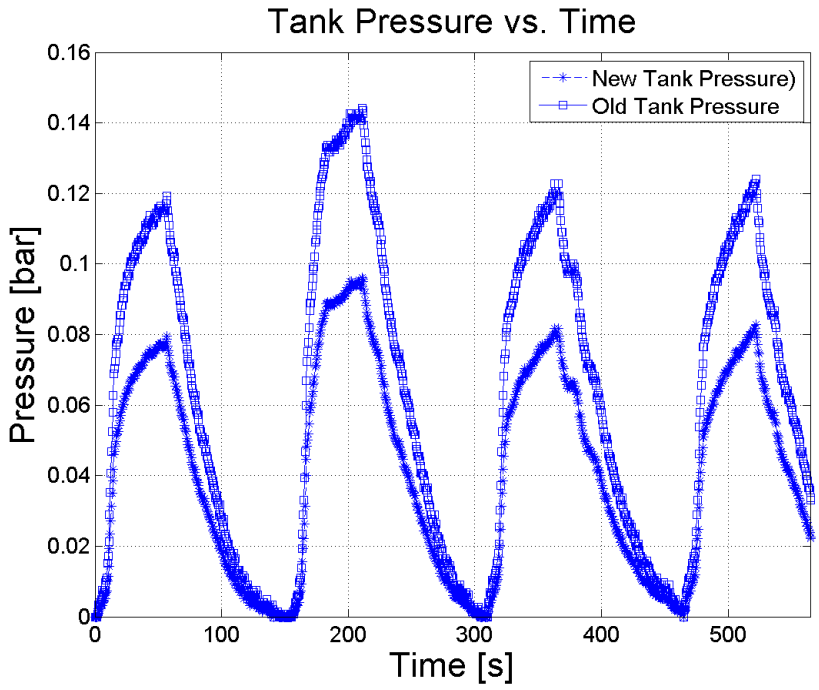

Figure G.5. Corrected and Incorrect 200L CLV Tank Pressures versus Time (refill 100s)

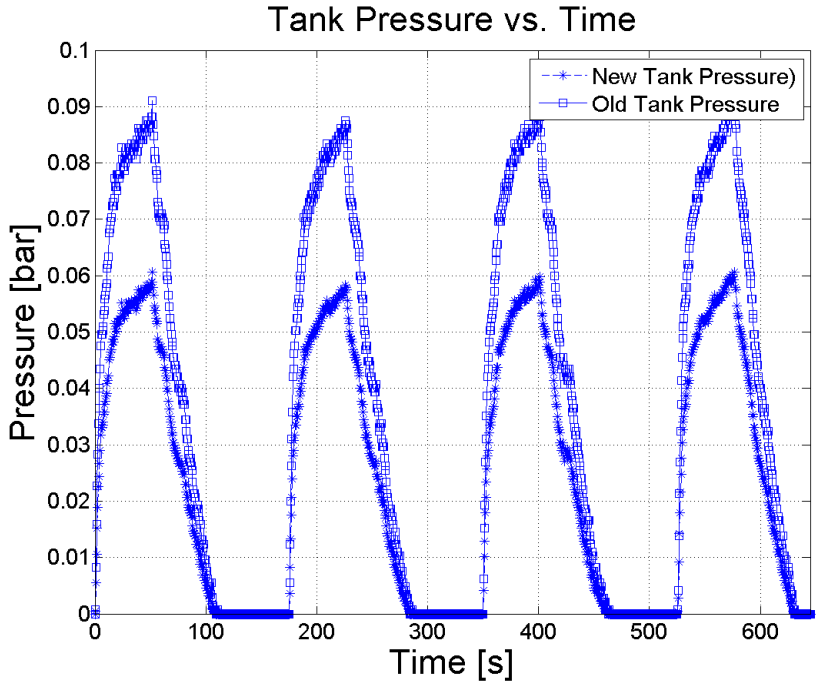

Figure G.6. Corrected and Incorrect 200L CLV Tank Pressures versus Time (refill 120s)

LN2 Discharge Flow Rate Volume Correction

The discharge flow rate of LN2 from the PC, which flows through the transfer lines to the MCCD, must be corrected. This correction is required to in order to account for the LN2 that boiled off due to heat load from the CCD heaters and the transfer line heat leaks. It is known that the saturation temperature of the tank is roughly 80-81K for all three refill times. The following equation shows the basic equation that was used to correct the data in Table 5.1.

$$\dot{Q}_{CCD} + \dot{Q}_{transfer_lines} = \dot{m}_{boil} \cdot (h_g - h_f) + \dot{m}_{boil} \cdot C_p \cdot (T_{LN2} - T_{sat}) \qquad \text{(G.5)}$$

Where $\dot{Q}_{CCD}$ is the heat input via the CCD heaters, $\dot{Q}_{transfer_lines}$ is the heat input via the 40ft of transfer lines, $\dot{m}_{boil}$ is the mass flow rate associated with boiling of LN2, $C_p\cdot$ is the specific heat of the LN2, T_{LN2} is the temperature of the LN2, and T_{sat} is the saturation temperature at the corresponding 200L CLV average pressure.

The input parameters for Equation G.5 can be seen below.

Table G.1. Corrected Volumes for LN2 Return

	Heat Input [W]				Correct
Refill Time [s]	CCD	Lines	T_LN2 [K]	P_tank [bar]	V [L]
60	144	16	78.4	1.10	0.040
100	142	16	77.9	1.06	0.040
120	111	16	77.6	1.06	0.032

The last column in Table G.1 shows the volume that should be added during the 40s discharge of the process cylinder.

BIBLIOGRAPHY

[1] Alvarez M., H. Cease. "DECam LN2 Over-Pressure Pump Process Cylinder Testing Dec. 20-22, 2011." *Dark Energy Document Database*. 6106(2011).

[2] Alvarez M. and H. Cease "DECam Over-Pressure Pump Cryo Safety Review Documentation." *Dark Energy Document Database*. 5787(2012).

[3] Alvarez M. "Lab A Over-Pressure Pump Test February Tests" *Dark Energy Document Database*. 6143 (2012).

[4] Alvarez M. "Turbine Flow Meter Calibration" *Dark Energy Document Database*. 6143 (2012).

[5] Beale C.A., M.D. Forsha, K.E. Nichols. *High Efficiency, Variable Geometry, Centrifugal Cryogenic Pump*. Cryogenic Engineering Conference, 39(1993): 925-932.

[6] Bergman T.L., D.P. Dewitt, F.P. Incopera, and A.S. Lavine. *Fundamentals of Heat and Mass Transfer* 6th ed. John Wiley and Sons Inc., 2007.

[7] Bruce R., F. Donald and T. Hisao. *Fundamentals of Fluid Mechanics* 5th ed. John Wiley and Sons Inc., 2006.

[8] Cease H., D. Depoy, G. Derylo,H.T. Diehl, J. Estrada, B. Flaugher, K. Kuk, K. Kuhlmann, A. Lathrop, K. Shultz, R.J. Reinert, R.L. Schmitt, A. Stefanik. A. Zhao. *Cooling the Dark Energy Camera CCD array using a closed-loop, two-phase liquid nitrogen system*. 2009: Fermilab Conference 10-242-PPD.

[9] Cease H. and T. Diehl. "DECam Controls-LabView Documentation V1.4142." *Dark Energy Document Database*. 5401(2012).

[10] Cease, H. Fermi National Accelerator Laboratory. (personal communications, June 04, 2012)

[11] Cease H. "1.5.2.5 and 1.5.2.2.1.5 Reference Manuals (Imager Vacuum and LN2 Cooling)." *Dark Energy Document Database*. 2667(2009).

[12] Cengel A., L. Yunus, and M.A. Boles. *Thermodynamics: An Engineering Approach*. 6th ed. Danvers, MA. 2007

[13] The Dark Energy Survey. 2012. 16 April 2012. `http://www.darkenergysurvey.org/index.shtml`

[14] Henshaw T.L. *Reciprocating Pumps*. New York, Van Nostrand Reinhold Company Inc. 1987.

[15] Jamie. McMaster-Carr, Chicago Sales. (personal communications, August 03, 2011)

[16] Lienhard J. H. IV and J.H. V. Lienhard. *A Heat Transfer Textbook*. 4th ed. Phlogston Press. 2011.

[17] Kevin. McMaster-Carr, Chicago Sales. (personal communications, August 01, 2011)

[18] Nagaraja Naidu B., R. Srinivasan, and Nathan K. Sagay. "A Modular Cryostat for Large Format and Mosaic CCDs." *Astronomical Society of India*. 29 (2001): 135-142.

[19] Review of Pumps and Water Lifting Techniques. *Food and Agriculture Organization of the United Nations*. 1986. 6 June 2011. `http://www.fao.org/docrep/010/ah810e/AH810E05.htm#5.3.1`.

[20] Russel S.B. *Cryogenic Engineering* 1959: Prepared for the Atomic Energy Commission.

[21] Schmitt R.L. "Thermodynamic and Transport Conditions in Nitrogen Circulation Loop." *Dark Energy Document Database*. 306 (2009).

[22] Schweickart R.B. and M.M. Buchko "Flexible Heat Pipes for CCD Cooling on the Advanced Camera for Surveys." *SPIE*. 3356 (1998): 292-300.

[23] Soares-Santos M. *Dark Energy Physics Expectations at DES*. XII Internation Conference on topics in Astroparticle and Underground Physics, 2011.

[24] Timmerhaus K.D. and K. Mendelssohn. *Cryogenic Engineering: Fifty Years of Progress*. Springer Science Business Media, LLC, 2007.

[25] United States. Bureau of Labor Statistics. *May 2011 State Occupational Employment and Wage Estimates*.FS-2001-09-015-KSC. 2012 March. 4 June 2012. `http://www.bls.gov/oes/current/oes_il.htm`.

[26] United States. National Aeronuatics and Space Administration. *Space Shuttle Use of Propellants and Fluids*.FS-2001-09-015-KSC. 2001 Sept. 20 June 2011. `http://www-pao.ksc.nasa.gov/kscpao/nasafact/pdf/ssp.pdf`.